The influence of mitochondrial inhibitors on zoospore and ascospore development

by

Chantel W. Swart

Submitted in fulfilment of the requirements for the degree
Philosophiae Doctor

Department of Microbial, Biochemical and Food Biotechnology
Faculty of Natural and Agricultural Sciences
University of the Free State
Bloemfontein
South Africa

Promoter: Prof. J.L.F. Kock
Co-promoters: Prof. P.W.J. van Wyk
Dr. C.H. Pohl-Albertyn

November 2010

Children's Song

We live in our own world,
A world that is too small
For you to stoop and enter
Even on hands and knees,
The adult subterfuge.
And though you probe and pry
With analytic eye,
And eavesdrop all our talk
With an amused look,
You cannot find the centre
Where we dance, where we play,
Where life is still asleep
Under the closed flower,
Under the smooth shell
Of eggs in the cupped nest
That mock the faded blue
Of your remoter heaven.

R.S. Thomas

This thesis is dedicated to:

- *My parents, M.M. and P.H.† Swart*
- *My grandparents, M.M. and C.J.† Coetzer*
- *My brother, R.E. Swart*
- *My husband to be, J.H. Pistor*

Acknowledgements

I wish to express my gratitude and appreciation to the following for their contribution to the successful completion of this study:

- ***God our Creator***, for granting me the serenity to accept the things I cannot change; courage to change the things I can and the wisdom to know the difference;

- ***Prof. J.L.F. Kock***, for being not only a role model but also a mentor; for teaching me more than just science; for his guidance; for being enthusiastic, optimistic and a true leader;

- ***Prof. P.W.J. van Wyk***, for his expertise and patience in teaching me microscopical techniques as well as always being encouraging and helpful;

- All ***co-authors*** of the different publications for their contributions, including: ***Prof. H.C. Swart***, ***Dr. E. Coetsee***, ***Mrs. W.M. Kriel*** and ***Dr. C.H. Pohl-Albertyn***;

- The financial assistance of the ***National Research Foundation (NRF)***, South Africa and the ***South African Frying Oil Initiative (SAFOI)***;

- My ***colleagues*** in the laboratory, especially ***Mrs. A. van Wyk***, for their friendship and support as well as ***Ms. B. Janecke*** from the ***Centre for Microscopy***;

- ***Mr. R. Ells***, for his true friendship and support;

- ***Mr. S.F. Collett***, for his graphical inputs, designs and encouragement;

- My fiancé, ***Mr. J.H. Pistor***, for his love, support, patience and understanding;

- My parents, ***Mrs. M.M. Swart*** and ***Mr. P.H. Swart†***, for encouraging me to reach my full potential;

- My grandparents, ***Mrs. M.M. Coetzer*** and ***Mr. C.J. Coetzer†***, for their love and support.

Contents

Chapter 1

Introduction

Chapter 2

2.1. The influence of mitochondrial inhibitors on the life cycle of ascospore producing fungi: The ascomycetous yeast *Nadsonia fulvescens*

Chapter 2 (cont.)

2.2. The influence of mitochondrial inhibitors on the life cycle of ascospore producing fungi: 3-D architecture and elemental composition of asci of *Nadsonia fulvescens*

Chapter 3

The influence of mitochondrial inhibitors on the life cycle of zoospore producing organisms: The oomycete *Phytophthora*

Chapter 4

Main Conclusions

Chapter 1

Introduction

Parts of this chapter are in the process of being submitted on invitation to the highly accredited journal: Expert Opinion on Drug Discovery.

1.1. Motivation

Fungal infections as well as fungal resistance to treatment are a continual problem that is constantly increasing. Unfortunately, research has been mostly unsuccessful to control these fungal infections (Kock et al., 2007). Fungi that are resistant towards presently used antifungals pose serious problems, especially to immuno-compromised patients. Consequently, new targets to control fungal infections are urgently needed in South Africa as well as worldwide. This study will aid in the continual screening for and uncovering of novel antifungal compounds that target novel sites, such as mitochondria. These organelles play important roles in eukaryotic cell metabolism. They are involved in a range of processes ranging from energy generation to cell signalling, cellular differentiation, cell death as well as the control of the cell cycle and cell growth (McBride et al., 2006). Any compound that affects mitochondria may therefore be of use in the control of many cell functions.

Since the late 1980s research by Kock and co-workers (Kock et al., 2007) lead to the following Acetylsalicylic acid (ASA) Antifungal Hypothesis which serves as basis for this study: (i) The asexual vegetative reproductive phase of strict aerobic respiring yeasts is more sensitive to mitochondrial inhibitors compared to yeasts with an additional fermentative pathway; (ii) the sexual reproductive phase of yeasts is more sensitive to mitochondrial inhibitors compared to the asexual vegetative growth phase; (iii) flocculation in fermentative yeasts is partially inhibited by mitochondrial inhibitors; (iv) these phenomena are attributed to mitochondrial inhibition, which in turn may be linked to the inhibition of products such as 3-hydroxy (OH) oxylipins - not necessarily indicating oxylipin function and (v) mitochondrial respiration and beta

(ß)-oxidation/fatty acid synthase type 2 (FAS II) are more pronounced during the sexual phase of yeasts compared to their asexual vegetative phase. This research therefore hypothesizes a link between mitochondrial activity, mitochondrial inhibitor sensitivity, oxylipin production and reproduction type (sexual or asexual) in respiring and fermentative yeasts. Here, increased mitochondrial inhibitor concentration leads to decreased mitochondrial activity, decreased mitochondrial oxylipin production and eventual decreased sexual reproduction followed by asexual reproduction.

This antifungal hypothesis states that mitochondria are effective targets to control fungal reproduction and should now be vigorously explored to assess its conserved status in the fungal domain. This may be done by exploring all main fungal taxa and their sensitivity towards the various mitochondrial inhibitor classes. Such a model can, as a next applied phase, be used to select specific mitochondrial inhibitors for further applied studies in combating fungal infections. Furthermore, this model may also be used as a starting point for novel physiological and molecular studies, especially to elucidate the mechanisms behind fungal pathogenicity and resistance developed against mitochondrial inhibitors used as antifungals. Due to the high incidence of fungal resistance towards known antifungals and the high number of immuno-compromised patients in South Africa as well as worldwide, the development of novel, effective and low cost antifungals will be of obvious importance.

With this as background the aim of this study became to further test the ASA Antifungal Hypothesis by including yeasts with a unique sexual cycle as well as the distantly related, fungus-like, notorious pathogen *Phytophthora*. This will not only

evaluate the general validity of this hypothesis but should also lead to novel antifungals targeting unique sites and that may be used to combat devastating diseases.

1.2. Background

Since the discovery of the oxylipin group, prostaglandins (Kock and Coetzee, 1990) in yeasts, various worldwide studies followed (Kock et al., 2007). This has lead to the discovery of other bio-active oxylipins i.e. 3-OH fatty acids (3-OH oxylipins) in various yeasts and recently in some moulds. These oxylipins were found to be associated with fungal dispersal mechanisms and also to play a role in fungal infection (Deva et al., 2000, 2001; Ncango et al., 2010). Strikingly, 3-OH oxylipins are probably produced in mitochondria via β-oxidation or FAS II implicating that mitochondrial inhibitors should have antifungal activity (Kock et al., 2007). It is therefore not surprising that a patent has been registered recently describing the use of mitochondrial inhibitors to combat yeast infection (Davis et al., 2009). As an introduction to my study, a synthesis now follows that will highlight the main events leading to the discovery of novel antifungals, targeting mitochondrial activity in yeasts and some moulds.

1.3. From oxylipins to mitochondrial inhibitors (Table 1)

Oxylipins are oxidised saturated and unsaturated fatty acids that are widely distributed in nature, for example: plants, animals and certain microbes. In 1988,

Kock and co-workers launched an extensive bioprospecting program to determine if yeasts can produce oxylipins, such as prostaglandins [Table 1, (1)]. The reason for this bioprospecting program was to find a cheaper biotechnological source for these expensive, now chemically produced autacoids that are used today to elicit several biological responses in humans and animals (Samuelsson et al., 2007). Strikingly, they found that non-steroidal anti-inflammatory drugs (NSAIDs) that selectively inhibit prostaglandin synthesis in humans also inhibit yeast growth. Consequently, this discovery was patented in 1990 (Kock and Coetzee, 1990).

In 1990, prostaglandins (Prostaglandin $F_2\alpha$ and Prostaglandin $F_2\alpha$-metabolites) were discovered in yeast using various techniques including radio-immuno assay (RIA) and gas chromatography – mass spectrometry (GC-MS) [Table 1, (2); Kock and Coetzee, 1990; Kock et al., 1991]. Kock and Coetzee (1990) also fed tritium labelled arachidonic acid (AA) to the yeast *Dipodascopsis uninucleata* in the presence of different concentrations of the NSAID, ASA. Lipid metabolites were then extracted and separated on silica gel thin layer chromatography (TLC) plates. From the results (Figure 1) it is clear that the production of mainly one metabolite was inhibited in a dose dependent manner by ASA.

With the use of various techniques including radio TLC, nuclear magnetic resonance (NMR) and GC-MS, the abovementioned ASA-sensitive metabolite was identified as 3-hydroxy eicosatetraenoic acid (3-HETE) [Figure 1; Table 1, (3); Van Dyk et al., 1991]. The year 1992 marked the uncovering of the biological importance of these 3-OH oxylipins in the release of ascospores from asci [Table 1, (4)]. It was proposed that these oxylipins probably act as lubricants to ensure effective spore release

which is essential for yeast reproduction/dispersal (Botha et al., 1992; Coetzee et al., 1992).

The first evidence, however, concerning the biological activity of 3-OH oxylipins in mammalian cells was presented by Nigam and co-workers in 1996 [Table 1, (5); Nigam et al., 1996]. It was reported that this compound affects signal transduction processes in human neutrophils and tumor cells in multiple ways, thereby rendering a biotechnological value to this compound. Later studies showed that *D. uninucleata* is capable of producing a wide variety of novel 3-OH oxylipins, including 3-OH 14:2, 3-OH 20:3 and 3-OH 20:5, when fed with different precursors (Venter et al., 1997). Furthermore, a maximum yield of 1.9 % (m/m) 3-HETE from AA was obtained by this yeast when using 200 mM AA as substrate in a novel bioprocess [Table 1, (6); Fox et al., 1997].

In 1998, Bhatt and co-workers chemically synthesized 3-OH oxylipins, which were urgently needed at the time for biological tests in mammalian as well as yeast cells [Table 1, (7); Bhatt et al., 1998]. The synthetic strategy for the production of 3-HETE involved a convergent approach coupling a chiral aldehyde with a Wittig salt. This chemically synthesized 3-HETE was then used to evoke 3-HETE specific antibodies in rabbits, which then served as primary antibodies. Together with fluorescing fluorescein isothiocyanate (FITC)-coupled secondary antibodies, the primary antibodies were used to visualize the location of 3-OH oxylipins in yeast using confocal laser scanning microscopy (CLSM). This fluorescing system will from now on be referred to as Oxytrack. In 1998, 3-OH oxylipins were mapped in *D. uninucleata*, using this Oxytrack system [Figures 2a - g; Table 1, (8); Kock et al.,

1998]. From the results it could be derived that these oxylipins are mainly associated with the sexual stage of the life cycle, i.e. ascospores (Figure 2a), gametangia (Figure 2c), ascus (Figure 2d) and released ascospores (Figure 2e).

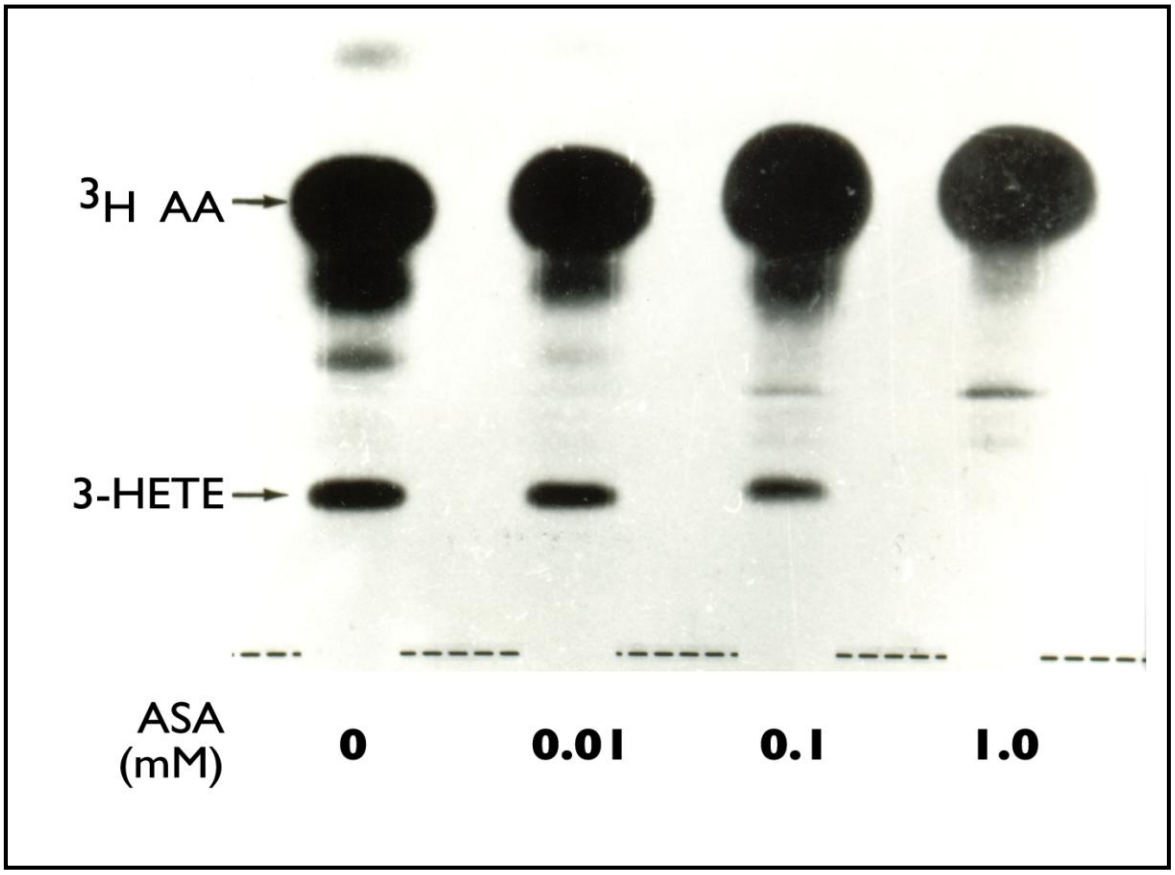

Figure 1 – Radio thin layer chromatography (TLC) plate showing various metabolites produced from tritium labelled arachidonic acid (AA) of which the formation of one, i.e. 3-hydroxy eicosatetraenoic acid (3-HETE) is mainly inhibited by acetylsalicylic acid (ASA). Taken with permission from Kock and Coetzee (1990).

The mechanics of ascospore release in *D. uninucleata* was described by Kock and co-workers in 1999 [Table 1, (9); Kock et al., 1999]. The transmission electron micrograph shown in Figure 3 of the ascospores of *D. uninucleata*, clearly shows the gear-like structures that interlock the ascospores prior to release. These gear-like

structures probably aid in ascospore release. 3-Hydroxy oxylipins were found to be present between these spores and probably act as lubricants to further aid in ascospore release.

In 2000, 3-OH oxylipins were mapped using immunogold labelling in conjunction with transmission electron microscopy (TEM) [Table 1, (10); Smith et al., 2000]. It was found that the lipid globules present in the asci of the yeast *D. uninucleata* contained 3-OH oxylipins which was probably produced in the mitochondria and then deposited in the lipid globules, thereby indicating a probable increase in mitochondrial activity associated with ascospores within asci [Table 1, (11); Smith et al., 2000].

The use of ibuprofen, an oxylipin production inhibitor, as antifungal was reported by Pina-Vaz and co-workers in 2000. In the same year ibuprofen was also reported to have anti-mitochondrial activity [Table 1, (12); Al-Nasser, 2000; Pina-Vaz et al., 2000]. Interestingly, further studies performed revealed novel oxylipins on the surface of the filamentous structures of the pathogenic yeast *Candida albicans* and was found to play a role in morphogenisis and possibly pathogenicity of this yeast [Table 1, (13); Kock et al., 2003]. Noverr and co-workers also observed ASA-sensitive oxylipins (prostaglandins) in pathogenic yeast, thereby independently confirming the discovery made by Kock and Coetzee in 1990 [Table 1, (14); Noverr et al., 2001, 2002].

Groza reported an alternative chemical synthesis route for 3-OH oxylipins in 2002 [Table 1, (15); Groza et al., 2002]. Again, this was urgently needed for further research in this field.

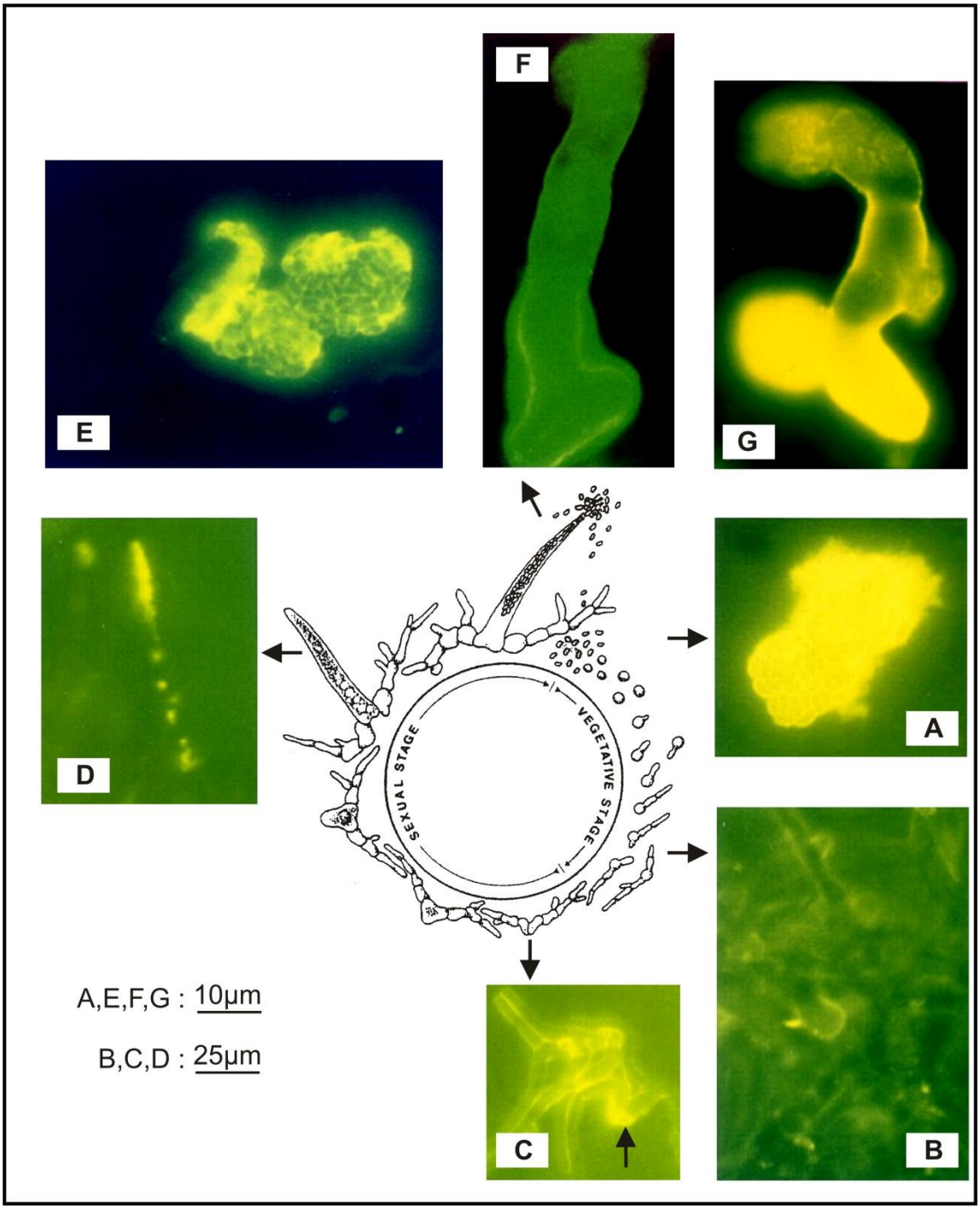

Figure 2 – Mapping of 3-hydroxy (OH) oxylipins in the yeast *Dipodascopsis uninucleata* using Oxytrack. (a) indicates released ascospores that germinate to produce hyphae (b). Hyphae/hyphal cells conjugate via gametangia (c) that give rise to an ascus (d). Ascospores (e) are released from the ascus leaving it empty (f). Ascospores inside enzyme treated wall-less asci are shown in (g). Taken with permission from Kock et al. (1998).

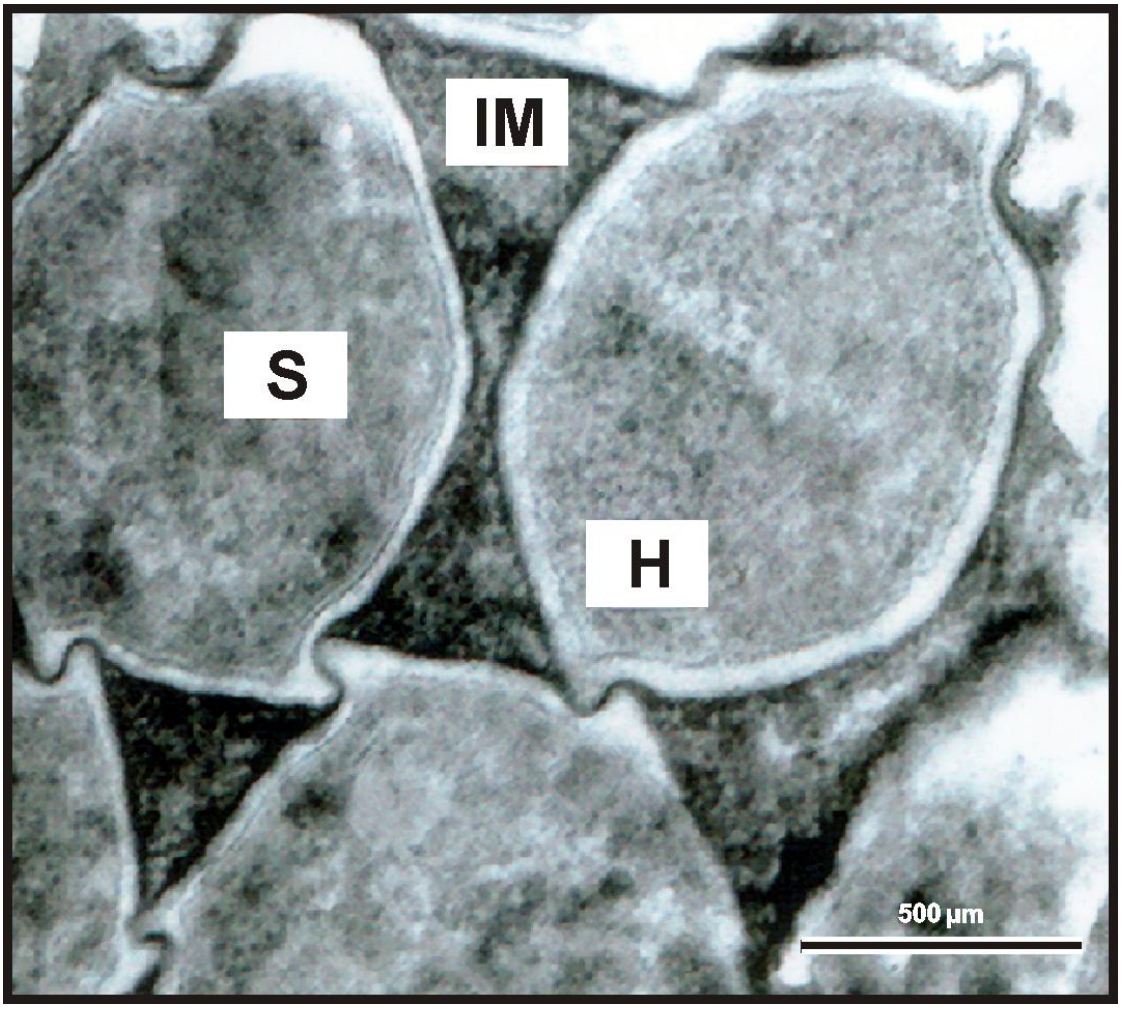

Figure 3 – Interlocking gear-like hooks observed by transmission electron microscopy (TEM) on ascospore surfaces probably aid in ascospore (S) dispersal in *Dipodascopsis uninucleata*. IM = interspore matrix, H = hooks. Taken with permission from Kock et al. (1999).

A review by Noverr and co-workers in 2003, again recognized the discovery in 1990 and confirmed the possible role of oxylipins as virulence factors. Here, various techniques including RIA and enzyme-linked-immunosorbent serologic assay (ELISA) were used to identify the prostaglandins [Table 1, (16); Noverr et al., 2003]. Groza reported yet another alternative chemical synthesis route for 3-OH oxylipins in 2004 [Table 1, (17); Groza et al., 2004] to again advance studies in this field.

Strikingly, Alem and Douglas demonstrated in 2004, that biofilms formed by *C. albicans* can be inhibited as much as 95 % by ASA. Yet, when prostaglandin E_2 was added together with ASA, the inhibitory effect of ASA was abolished. They concluded that ASA possesses potent antibiofilm activity *in vitro* and could be useful in combined therapy with conventional antifungal agents in the management of biofilm-associated *Candida* infections [Table 1, (18); Alem and Douglas, 2004]. In the same year, the application of 3-OH oxylipins in engineering was proposed by Kock and co-workers [Table 1, (19); Kock et al., 2004]. Another important discovery was made by Tsitsigiannis and co-workers, proposing that oxylipins may play a role as regulators in sexual and asexual spore formation in *Aspergillus nidulans* [Table 1, (20); Tsitsigiannis et al., 2004].

According to research performed by Alem and Douglas, prostaglandin production could indeed be a virulence factor in yeast biofilm-associated infections [Table 1, (21); Alem and Douglas, 2005] further supporting their previous studies (Alem and Douglas, 2004). Importantly, the Tsitsigiannis group provided the first genetic evidence for fungi where they characterized three *Aspergillus ppo* genes, encoding fatty acid oxygenases, similar in amino acid sequence to the mammalian cyclooxygenase (COX). This implicated Ppo activity in generating prostaglandins in fungi [Table 1, (22); Tsitsigiannis et al., 2005].

In 2005, the production of 3-OH prostaglandins by pathogenic yeasts was first described, thereby merging 3-OH oxylipin and prostaglandin research in yeast. Ciccoli and co-workers found that, during *C. albicans* infection, AA is released from the phospholipids of the infected host cell membrane [Table 1, (23); Ciccoli et al.,

2005]. *Candida albicans* then uses the released AA to produce 3-HETE, which is secreted from the yeast and converted to 3-OH prostaglandins by cyclooxygenase-2 (COX-2) in mammalian cells. They found that 3-OH prostaglandins increased inflammation in the host cell to a similar extent as normal prostaglandins. Acetylsalicylic acid then targets 3-OH prostaglandin production via β-oxidation and COX-2 respectively (Figure 4).

Further research by the Kock group indicated that 3-OH oxylipins are involved in flocculation patterns in yeast, again showing another possible function of these oxylipins [Table 1, (24)]. Studies indicated that strongly flocculating cells show both increased mitochondrial activity as well as an increase in 3-OH oxylipin production (Figure 5) when compared to weakly flocculating cells (Strauss et al., 2005). Literature also suggests that this mechanism could be a prelude to sexual reproduction in this yeast (Kock et al., 2007).

It was also shown that 3-OH oxylipins do not only have biological activity in yeast, but may have application in the field of engineering especially in the lubrication of structures for movement in micron space (Kock et al., 2006). It is proposed that 3-OH oxylipins may have similar applications as ricinoleic acid (12-OH 18:1) used in jet engines as lubricants [Table 1, (25); Kock et al., 2006].

Strikingly, Erb-Downward and Huffnagle predicted that the fungal oxylipin research field will yield practical application within the next 10 years. This suggestion was made on the basis of the many research projects that show practical applications, especially in medicine [Table 1, (26); Erb-Downward and Huffnagle, 2006].

In 2007, the presence of prostaglandins was again confirmed in the pathogenic yeast, *C. albicans* as well as observed in another pathogenic yeast *Cryptococcus neoformans*. This was done by using GC-MS analysis which again indicated the wide distribution of these oxylipins in the fungal domain [Table 1, (27); Erb-Downward and Noverr, 2007].

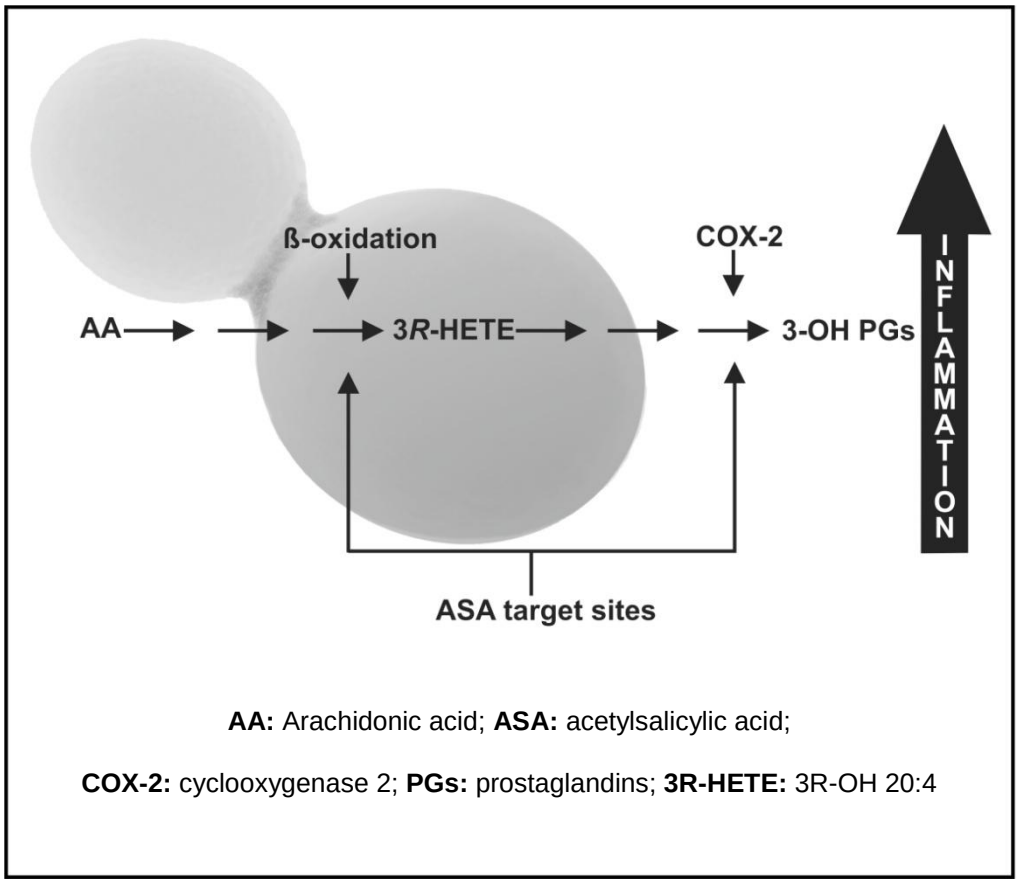

Figure 4 – During *Candida albicans* infection, arachidonic acid (AA) is released from the phospholipids of the infected host cell membrane. *Candida albicans* can use AA to produce 3-hydroxy eicosatetraenoic acid (3-HETE), which is then excreted from the yeast and converted to 3-hydroxy (OH) prostaglandins by cyclooxygenase-2 (COX-2) in mammalian cells. These 3-OH prostaglandins in turn increase inflammation in the host cell. Acetylsalicylic acid (ASA) probably targets beta (β)-oxidation as well as the COX-2 system. Taken with permission from Strauss (2005).

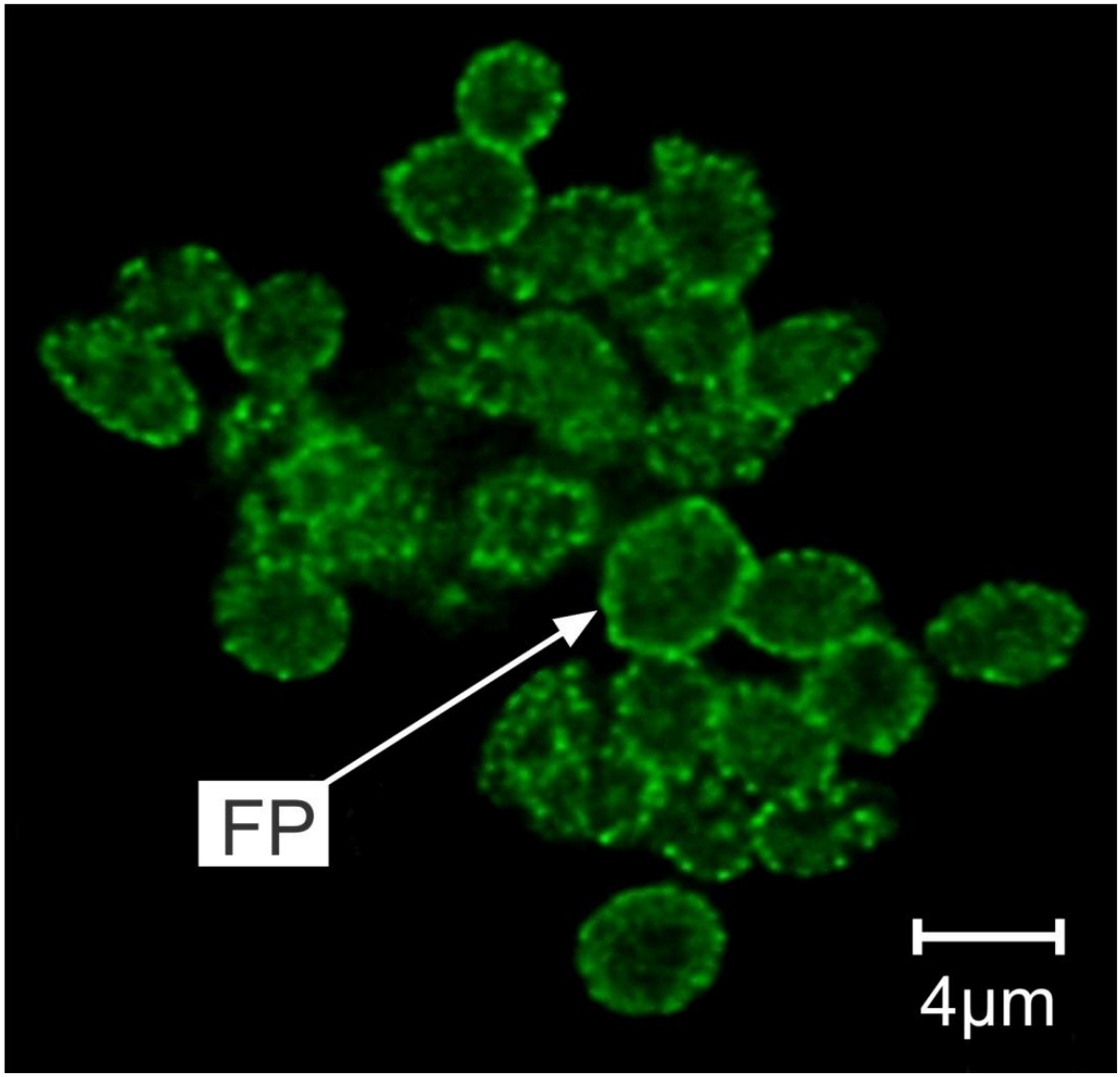

Figure 5 – A confocal laser scanning micrograph indicating increased 3-hydroxy (OH) oxylipins (FP = fluorescing protuberances) associated with strongly flocculating yeast cells (as indicated by the green fluorescence). Taken with permission from Strauss et al. (2005).

The use of the Oxytrack system (where primary antibodies specific for 3-OH oxylipins, coupled to secondary FITC-coupled antibodies are used to determine the location of 3-OH oxylipins in yeast) as a method to specifically detect sexual reproduction in yeasts was reported in 2007. This method is based on the principle

that 3-OH oxylipins accumulate in sexual structures, such as asci due to increased activity in mitochondria. Therefore, this can be used as a system to track sexual reproduction structures in yeasts [Table 1, (28); Kock et al., 2007]. From the vast number of studies performed up till this point, an ASA Antifungal Hypothesis was established [Table 1, (29); Kock et al., 2007] indicating a link between yeast reproduction (sexual and asexual), oxylipin production, mitochondrial activity and ASA sensitivity. In this hypothesis yeasts can be divided into two groups (Figure 6), namely those that can only aerobically respire and those that can aerobically respire and also ferment. It was observed that as the ASA concentration increases, the mitochondrial activity and 3-OH oxylipin production decrease in both groups. Also, the yeasts that can only aerobically respire were found to be more sensitive to ASA than yeasts that can also ferment. Studies indicated that the sexual stages in both groups are more sensitive to ASA than the asexual stages and that the accumulation of 3-OH oxylipins as well as mitochondrial activity decreases from the sexual to the asexual stage.

Further studies indicated the importance of oxylipins in endovanilloid and pain pharmacology, thereby indicating that oxylipin research was also applicable to human physiology and not only yeasts [Table 1, (30); Starowicz et al., 2007]. Based on previous studies, a Mitotrack system was developed in 2008, where an increase in mitochondrial membrane potential ($\Delta\psi_m$) was determined using the fluorescing dye, Rhodamine 123 (Rh123), which stains mitochondria with increased activity, selectively. This is attributed to the highly specific attraction of this cationic, lipophilic, fluorescing dye to the relatively high negative electric potential across the mitochondrial membrane in living cells (Johnson et al., 1980). Green fluorescence

obtained when using this dye indicates a high mitochondrial $\Delta\psi_m$ (collected at 450 nm). Using this method, it was confirmed by Swart and co-workers that an increase in mitochondrial activity is associated with the sexual stages in yeast reproduction [Figure 7; Table 1, (31); Swart et al., 2008]. This was to be expected since an increase in energy production is probably needed for ascosporogenesis.

All of these studies aided in the development of an anti-mitochondrial yeast bio-assay in 2009 (Kock et al., 2009), capable of screening mitochondrial inhibitors. Here, anti-mitochondrial refers to any process where mitochondrial function is directly or indirectly inhibited [Table 1, (32); Kock et al., 2009]. These bio-assays were mainly based on studies performed on *Eremothecium ashbyii* as indicator organism and enables the screening of novel compounds for anti-mitochondrial, antifungal activity. This bio-assay, when fully developed, will enable the rapid screening of various novel compounds for anti-mitochondrial, antifungal and possibly anticancer activity.

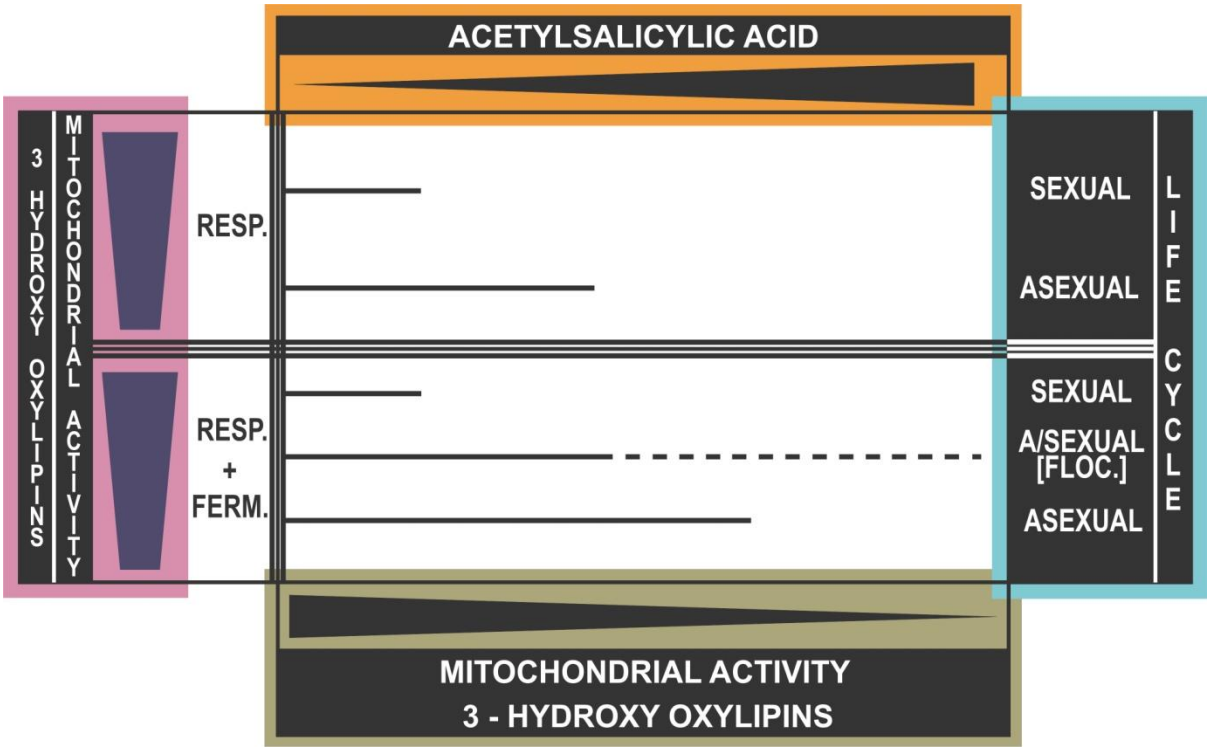

Figure 6 – A schematic representation of the Acetylsalicylic acid (ASA) Antifungal Hypothesis that suggests a possible link between 3-hydroxy (OH) oxylipin production, mitochondrial activity and ASA sensitivity. X-axis, top: increase in ASA concentration from left to right. X-axis, bottom: decrease in mitochondrial activity and 3-OH oxylipin levels from left to right. Y-axis, left: decrease in mitochondrial activity and 3-OH oxylipin levels from sexual reproductive to asexual growth phases in both strictly aerobic yeast (RESP.) and yeasts with both aerobic and fermentative pathways (RESP. + FERM.). Y-axis, right: different phases of yeast life cycles, i.e. sexual, asexual as well as asexual/sexual flocculation (FLOC.). Middle block: response surface showing the relative sensitivities of different yeast phases towards increasing levels of ASA. Taken with permission from Kock et al. (2007).

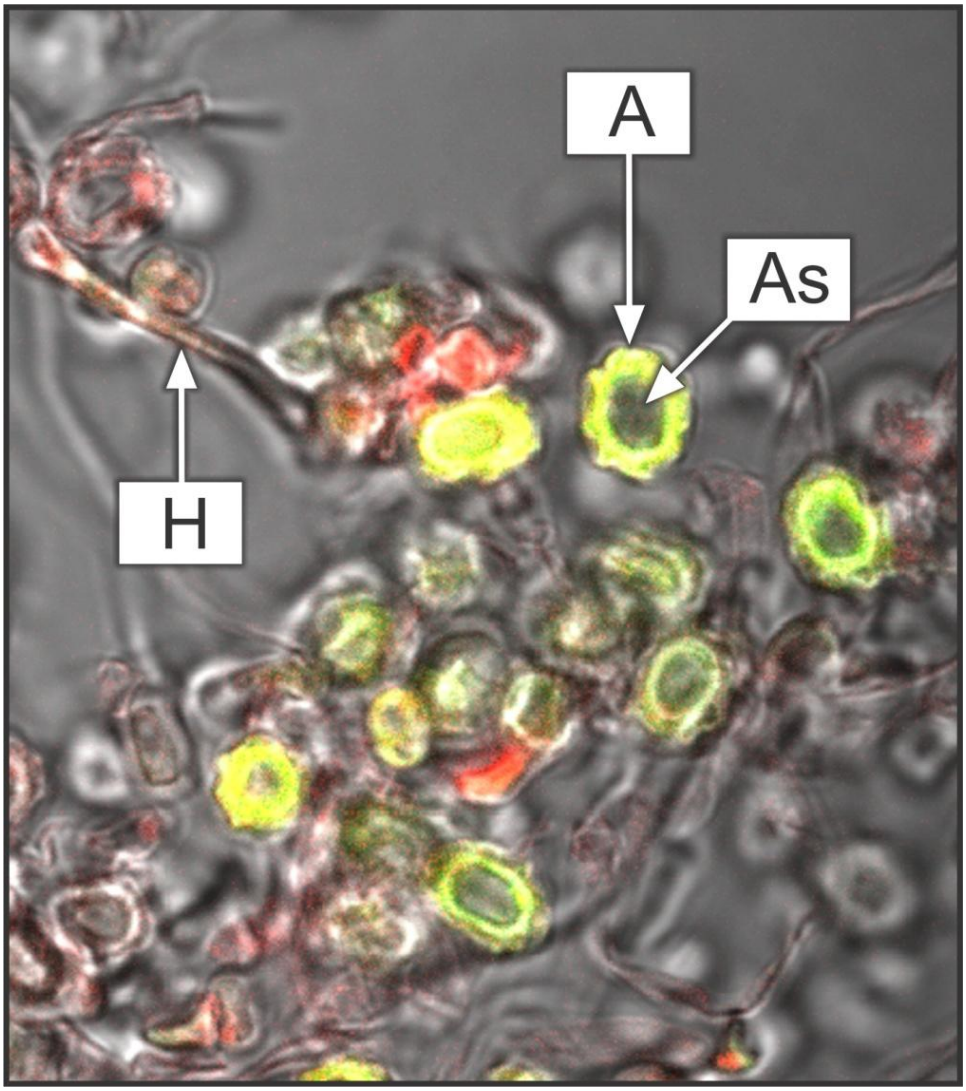

Figure 7 – A confocal laser scanning micrograph indicating an increase in mitochondrial membrane potential ($\Delta\psi_m$) associated with the sexual stage [asci, (A)] of *Galactomyces reessii* (as can be seen by the yellow-green fluorescence). The surrounding vegetative cells showed a low mitochondrial $\Delta\psi_m$. Taken with permission from Swart et al. (2008). H = hyphae; As = ascospore.

Finally this research has now lead to the registration of a patent by the Kock group, describing the use of NSAIDs as anti-mitochondrial antifungals [Table 1, (33); Davis et al., 2009]. Will this application confirm the prediction made by Erb-Downward and Huffnagle in 2006 [Table 1,(26); Erb-Downward and Huffnagle, 2006]? Here,

NSAIDs at very low concentrations are used to affect a dual action, i.e. anti-inflammatory as well as antifungal, thereby targeting mitochondria and the inflammation-causing COX enzyme pathway in humans and mammals.

1.4. Concluding Remarks

Since the discovery of ASA-sensitive oxylipins in yeast (Kock and Coetzee, 1990), this field of research has expanded significantly. A highlight is the proposal of the ASA Antifungal Hypothesis (Kock et al., 2007) linking yeast sexual reproduction, mitochondrial activity as well as sensitivity towards ASA. This hypothesis has recently been extended to also include more anti-mitochondrial compounds as well as the mould *Aspergillus* and moulds of the Mucorales (Leeuw et al., 2009; Ncango et al., 2010). Here, fruiting dispersal structures characterised by active cell proliferation such as structures with active conidia development in *Aspergillus* and sporangia of *Mucor* also showed increased mitochondrial activity (similar to yeast sexual phases) and again increased sensitivity towards mitochondrial inhibitors. This hypothesis (renamed as the Anti-mitochondrial Antifungal Hypothesis) now suggests that mitochondrial inhibitors may be used as novel antifungals targeting mitochondrial activity and therefore dispersal structures of a wide array of fungi and fungi-like organisms. This is important since fungi have become resistant to many antifungal drugs due to extensive exposure making treatment ineffective. It is therefore not surprising that a patent has been registered recently aimed at the treatment of *Candida* infections with anti-mitochondrial drugs [Table 1, (33); Davis et al., 2009].

It is now important to further test the general validity of this hypothesis by including fungi with complex life cycles as well as distantly related pathogenic fungus-like organisms. In addition, more mitochondrial inhibitors should be tested for their ability to specifically inhibit structures of dispersal that may also be responsible for infection.

1.5. Purpose of Research

With this as background, the purpose of this study became to:

1. Evaluate the general validity of the Anti-mitochondrial Antifungal Hypothesis by:
   1.1 Including the yeast *Nadsonia fulvescens* which is characterized by a unique sexual life cycle (Chapter 2).
   1.2 Assessing if the distantly related fungus-like oomycete and notorious plant pathogen, *Phytophthora*, also fits this hypothesis (Chapter 3).
2. Further develop and validate the bio-assay using *N. fulvescens* as indicator organism to screen for various compounds exhibiting anti-mitochondrial, antifungal activity (Chapter 2; 2.1., 2.1.6., Chapter 4; 4.2., 4.3.).

Please note: The chapters to follow are presented in the format depicted by the journal of submission. As a result repetition of some information could not be avoided.

1.6. References

Alem MAS, Douglas LJ (2004). Effects of aspirin and other non-steroidal anti-inflammatory drugs on biofilms and planktonic cells of *Candida albicans*. Antimicrob. Agents Chemother. 48(1): 41 – 47.

Alem MAS, Douglas LJ (2005). Prostaglandin production during growth of *Candida albicans* biofilms. J. Med. Microbiol. 54: 1001 – 1005.

Al-Nasser IA (2000). Ibuprofen-induced liver mitochondrial permeability transition. Toxicol. Lett. 111(3): 213 – 218.

Bhatt RK, Falck JR, Nigam S (1998). Enantiospecific total synthesis of a novel arachidonic acid metabolite 3-hydroxy eicosatetraenoic acid. Tetrahedron Lett. 39: 249 – 252.

Botha A, Kock JLF, Coetzee DJ, Van der Linde NA, Van Dyk MS (1992). The influence of NSAIDs on the life cycle of *Dipodascopsis*. Syst. Appl. Microbiol. 15: 155 – 160.

Ciccoli R, Sahi S, Singh S, Prakash H, Zafiriou M, Ishdorj G, Kock JLF, Nigam S (2005). Oxygenation by cyclooxygenase-2 (COX-2) of 3-hydroxyeicosatetraenoic acid (3-HETE), a fungal mimetic of arachidonic acid, produces a cascade of novel bioactive 3-hydroxy-eicosanoids. Biochem. J. 390: 737 – 747.

Coetzee DJ, Kock JLF, Botha A, Van Dyk MS, Smit EJ, Botes PJ, Augustyn OPH (1992). Yeast Eicosanoids II. The distribution of arachidonic acid metabolites in the life cycle of *Dipodascopsis uninucleata*. Syst. Appl. Microbiol. 15: 311 – 318.

Davis HJ, Sebolai OM, Kock JLF, Lotter AP (2009). Use of non-steroidal anti-inflammatory drugs in the treatment of opportunistic infections. Patent Applied No. 2009/06259.

Deva R, Ciccoli R, Schewe T, Kock JLF, Nigam S (2000). Arachidonic acid stimulates cell growth and forms a novel oxygenated metabolite in *Candida albicans*. Biochim. Biophys. Acta 1486: 299 – 311.

Deva R, Ciccoli R, Kock JLF, Nigam S (2001). Involvement of aspirin-sensitive oxylipins in vulvovaginal candidiasis. FEMS Microbiol. Lett. 198: 37 – 43.

Erb-Downward JR, Huffnagle GB (2006). Role of oxylipins and other lipid mediators in fungal pathogenesis. Future Microbiol. 192: 219 – 227.

Erb-Downward JR, Noverr MC (2007). Characterization of prostaglandin E_2 production by *Candida albicans*. Infect. Immun. 75: 3498 – 3505.

Fox S, Ratledge RC, Friend J (1997). Optimisation of 3-hydroxyeicosanoid biosynthesis by the yeast *Dipodascopsis uninucleata*. Biotechnol. Lett. 19: 155 – 158.

Groza NV, Ivanov IV, Romanov SG, Myagkova GI, Nigam S (2002). A novel synthesis of 3(*R*)-HETE, 3(*R*)HTDE and enzymatic synthesis of 3(*R*), 15(*S*)-DiHETE. Tetrahedron 58: 9859 – 9863.

Groza NV, Ivanov IV, Romanov SG, Shevchenko VP, Myasoedov NF, Nigam S, Myagkova GI (2004). Synthesis of tritium labelled 3(*R*)-HETE and 3(*R*), 18(*R*/*S*)-DiHETE through a common synthetic route. J. Labelled Compd. Radiopharm. 47: 11 – 17.

Johnson LV, Walsh ML, Chen LB (1980). Localization of mitochondria in living cells with Rhodamine 123. PNAS 77: 990 – 994.

Kock JLF, Coetzee DJ (1990). Regulation of growth and metabolism of fungi, particularly yeasts. SA Preliminary Patent no. 90/4397.

Kock JLF, Coetzee DJ, Van Dyk MS, Truscott M, Cloete FC, Van Wyk V, Augustyn OPH (1991). Evidence for pharmacologically active prostaglandins in yeasts. S. Afr. J. Sci. 87: 73 – 76.

Kock JLF, Venter P, Linke D, Schewe T, Nigam S (1998). Biological dynamics and distribution of 3-hydroxy fatty acids in the yeast *Dipodascopsis uninucleata* as investigated by immunofluorescence microscopy. Evidence for a putative regulatory role in the sexual reproductive cycle. FEBS Lett. 472: 345 – 348.

Kock JLF, Van Wyk PWJ, Venter P, Smith DP, Viljoen BC, Nigam S (1999). An acetylsalicylic acid sensitive aggregation phenomenon in *Dipodascopsis uninucleata*. Antonie Leeuwenhoek 75: 261 – 266.

Kock JLF, Strauss CJ, Pohl CH, Nigam S (2003). Invited review: The distribution of 3-hydroxy oxylipins in fungi. Prostaglandins Other Lipid Mediat. 71: 85 – 96.

Kock JLF, Strauss CJ, Pretorius EE, Pohl CH, Bareetseng AS, Botes PJ, Van Wyk PWJ, Schoombie W, Nigam S (2004). Revealing yeast spore movement in confined spaces. S. Afr. J. Sci. 100: 237 – 243.

Kock JLF, Strauss CJ, Pohl CH, Van Wyk PWJ, Botes PJ (2006). Yeast Biomechanics. Proceedings: III European Conference on Computational Mechanics Solids, Structures and Coupled Problems in Engineering. Lisbon, Portugal, 5 – 8 June 2006, Eds. CA Mota Soares et al. pp. 725. ISBN – 10 1-4020-4994-3.

Kock JLF, Sebolai OM, Pohl CH, Van Wyk PWJ, Lodolo EJ (2007). Oxylipin studies expose aspirin as antifungal. FEMS Yeast Res. 7: 1207 – 1217.

Kock JLF, Swart CW, Ncango DM, Kock JL Jr, Munnik IA, Maartens MM, Pohl CH, Van Wyk PWJ (2009). Development of a yeast bio-assay to screen anti-mitochondrial drugs. Curr. Drug Disc. Technol. 6(3): 186 – 191.

Leeuw NJ, Swart CW, Ncango DM, Kriel WM, Pohl CH, Van Wyk PWJ, Kock JL (2009). Anti-inflammatory drugs selectively target sporangium development in *Mucor*. Can. J. Microbiol. 55(12): 1392 – 1396.

McBride HM, Neuspiel M, Wasiak S (2006). “Mitochondria: more than just a powerhouse”. Curr. Biol. 16(14): R551 – R560.

Ncango DM, Swart CW, Pohl CH, Van Wyk PWJ, Kock JLF (2010). Mitochondrion activity and dispersal of *Aspergillus fumigatus* and *Rhizopus oryzae*. Afr. J. Microbiol. Res. 4(9): 830 – 835.

Nigam S, Sravan Kumar G, Kock JLF (1996). Biological effects of 3-HETE, a novel compound of the yeast *Dipodascopsis uninucleata*, on mammalian cells. Prostaglandins Leukot. Essent. Fatty Acids 55: 39.

Noverr MC, Phare SM, Toews GB, Coffey MJ, Huffnagle JB (2001). Pathogenic yeasts *Cryptococcus neoformans* and *Candida albicans* produce immunomodulatory prostaglandins. Infect. Immun. 69(5): 2957 – 2963.

Noverr MC, Toews GB, Huffnagle JB (2002). Production of prostaglandins and leukotrines by pathogenic fungi. Infect. Immun. 70(1): 400 – 402.

Noverr MC, Erb-Downward JR, Huffnagle GB (2003). Production of eicosanoids and other oxylipins by pathogenic eukaryotic microbes. Clin. Microbiol. Rev. 16(3): 517 – 533.

Pina-Vaz C, Sansonetty F, Rodrigues AG, Martinez-De-Oliveira J, Fonseca AF, Mardh P (2000). Antifungal activity of ibuprofen alone and in combination with fluconazole against *Candida* species. J. Med. Microbiol. 49: 831 – 840.

Samuelsson B, Morgenstern R, Jakobsson P (2007). Membrane Prostaglandin E synthase-1: A novel therapeutic agent. Pharmacol. Rev. 59: 207 – 224.

Smith DP, Kock JLF, Van Wyk PWJ, Venter P, Coetzee DJ, Van Heerden E, Linke D, Nigam S (2000). The occurrence of 3-hydroxy-oxylipins in the ascomycetous yeast family Lipomycetaceae. S. Afr. J. Sci. 96: 247 – 249.

Starowicz K, Nigam S, Di Marzo V (2007). Biochemistry and pharmacology of endovanilloids. Pharmacol. Ther. 114(1): 13 – 33.

Strauss CJ (2005). The role of lipids in the flocculation of *Saccharomyces cerevisiae*. PhD Thesis, University of the Free State, South Africa.

Strauss CJ, Kock JLF, Van Wyk PWJ, Lodolo EJ, Pohl CH, Botes PJ (2005). Bioactive oxylipins in *Saccharomyces cerevisiae*. J. Instit. Brewing 111(3): 304 – 308.

Swart CW, Van Wyk PWJ, Pohl CH, Kock JLF (2008). Variation in yeast mitochondrial activity associated with asci. Can. J. Microbiol. 54(7): 532 – 536.

Tsitsigiannis DI, Kowieski TM, Zarnowski R, Keller NP (2004). Endogenous lipogenic regulators of spore balance in *Aspergillus nidulans*. Eukaryot. Cell 3(6): 1398 – 1411.

Tsitsigiannis DI, Bok J, Andes D, Fog Nielsen K, Frisvad JC, Keller NP (2005). *Aspergillus* cyclooxygenase-like enzymes are associated with prostaglandin production and virulence. Infect. Immun. 73(8): 4548 – 4559.

Van Dyk MS, Kock JLF, Coetzee DJ, Augustyn OPH, Nigam S (1991). Isolation of a novel arachidonic acid metabolite 3-hydroxy-5, 8, 11, 14-eicosatetraenoic acid (3-HETE) from the yeast *Dipodascopsis uninucleata*. FEBS Lett. 283: 195 – 198.

Venter P, Kock JLF, Sravan Kumar G, Botha A, Coetzee DJ, Botes PJ, Bhatt RK, Falck JR, Schewe T, Nigam S (1997). Production of 3*R*-hydroxy-polyenoic fatty acids by the yeast *Dipodascopsis uninucleata*. Lipids 32(12): 1277 – 1283.

Table 1: Highlights – Oxylipin Research

Year	Highlight	Main Ref.
(1) 1988	Bioprospecting for prostaglandins Non-steroidal anti-inflammatory drugs (NSAIDs) as antifungals – patent	Kock and Coetzee, 1990
(2) 1990	Discovery of prostaglandins in yeast	Kock and Coetzee, 1990
(3) 1991	Discovery of acetylsalicylic acid (ASA) sensitive 3-hydroxy (OH) oxylipins	Van Dyk et al., 1991
(4) 1992	Biological effects of 3-hydroxy (OH) oxylipins in yeast	Botha et al., 1992; Coetzee et al., 1992
(5) 1996	Biological effects of 3-hydroxy (OH) oxylipins in mammalian cells	Nigam et al., 1996
(6) 1997	Discovery of novel 3-hydroxy (OH) oxylipins Biosynthesis of 3-hydroxy eicosatetraenoic acid (3-HETE)	Fox et al., 1997
(7) 1998	Chemical synthesis of 3-hydroxy (OH) oxylipins	Bhatt et al., 1998
(8) 1998	Mapping of 3-hydroxy (OH) oxylipins in *Dipodascopsis uninucleata*	Kock et al., 1998
(9) 1999	Mechanics of ascospore release in *Dipodascopsis uninucleata* Function of oxylipin-lubricants	Kock et al., 1999
(10) 2000	Mapping of oxylipin-lubricants with gold labelled Transmission electron microscopy (TEM)	Smith et al., 2000
(11) 2000	3-hydroxy (OH) oxylipins in asci	Smith et al., 2000
(12) 2000	Ibuprofen: anti-mitochondrial antifungal	Al-Nasser, 2000 Pina-Vaz et al., 2000
(13) 2000 – 2003	3-hydroxy (OH) oxylipins discovered in pathogenic yeast	Kock et al., 2003
(14) 2001 – 2002	Confirmation of Kock's discovery of prostaglandins in yeast	Noverr et al., 2001, 2002
(15) 2002	Alternative chemical synthesis route of 3-hydroxy (OH) oxylipins	Groza et al., 2002
(16) 2003	Oxylipins widely distributed in yeasts Possible role as virulence factors	Noverr et al., 2003
(17) 2004	Alternative chemical synthesis route for 3-hydroxy (OH) oxylipins	Groza et al., 2004

(18) 2004	Acetylsalicylic acid (ASA) and prostaglandins influence pathogenic yeast biofilms	Alem and Douglas, 2004
(19) 2004	Mechanical function of 3-hydroxy (OH) oxylipins in yeast spore release	Kock et al., 2004
(20) 2004	Oxylipins control mitospore and meiospore ontogeny	Tsitsigiannis et al., 2004
(21) 2005	Prostaglandins in pathogenic yeasts	Alem and Douglas, 2005
(22) 2005	First genetic evidence of prostaglandin production by fungi	Tsitsigiannis et al., 2005
(23) 2005	Merging 3-hydroxy (OH) oxylipin and prostaglandin research in yeast Discovery of 3-(OH) prostaglandins	Ciccoli et al., 2005
(24) 2005	3-hydroxy (OH) oxylipins and yeast flocculation	Strauss et al., 2005
(25) 2006	3-hydroxy (OH) oxylipins introduced to field of engineering	Kock et al., 2006
(26) 2006	Prediction: Practical application of fungal oxylipins in next 10 years	Erb-Downward and Huffnagle, 2006
(27) 2007	Prostaglandins in pathogenic yeasts	Erb-Downward and Noverr, 2007
(28) 2007	Oxylipin probes to expose sexual reproduction in yeasts (Oxytrack)	Kock et al., 2007
(29) 2007	Acetylsalicylic acid (ASA) Antifungal Hypothesis	Kock et al., 2007
(30) 2007	Endovanilloid and pain pharmacology	Starowicz et al., 2007
(31) 2008	Mitotrack (Rhodamine 123) probes for asci	Swart et al., 2008
(32) 2009	Practical application: yeast bio-assay to screen anti-mitochondrials	Kock et al., 2009
(33) 2009	Non-steroidal anti-inflammatory drug (NSAID) used as anti-mitochondrial antifungals – patent	Davis et al., 2009

Chapter 2

2.1. The influence of mitochondrial inhibitors on the life cycle of ascospore producing fungi: The ascomycetous yeast *Nadsonia fulvescens*

Parts published in: AJMR Vol. 4(16), pp. 1727 – 1732, 18 August 2010, Variation in mitochondrial activity over the life cycle of *Nadsonia fulvescens*. (ISI-accredited scientific journal)

Abstract

The yeast *Nadsonia fulvescens* is characterized by a unique life cycle giving rise to a parent cell with two attached buds – one of the buds eventually develop into the ascus with one to two spiny ascospores. Here the parent cell with both attached buds can be considered the sexual phase with the parent cell playing a pivotal role in zygote formation and movement. Upon formation of the brown coloured asci (after 6 – 8 days of cultivation), most ascus-attached parent cells with first bud were still intact, containing cytoplasm and increased mitochondrial activity. When anti-mitochondrial compounds were added to young (i.e. 6 – 8 day old) cultures of this yeast, the mitochondrial activity was inhibited in the parent cell with attached bud followed by the formation of less asci with ascospores (many not fully developed or malformed and white coloured giving rise to white colonies). We conclude that sufficient mitochondrial activity in the parent cell and first bud is necessary to produce enough energy for the formation of a proper ascus with brown coloured ascospore(s).

Key words: asci, ascospore, life cycle, mitochondria, mitochondrial inhibitors, *Nadsonia fulvescens*.

2.1.1. Introduction

Increased mitochondrial activity in sexual cells, and not in asexual cells, seems to be a conserved characteristic in ascomycetous yeasts (Kock et al., 2007; Ncango et al., 2008). The only exception thus far noted was Zy*gosaccharomyces*. In this case both sexual and asexual reproductive structures are characterised by low mitochondrial activity. This is explained by the strong fermentative metabolism of this yeast probably yielding enough energy for ascus and ascospore formation (Swart et al., 2008).

In this study, variation in mitochondrial activity over the unique life cycle of *Nadsonia fulvescens* was investigated. This yeast performs heterogamic conjugation between the parent cell and the first bud, followed by the movement of the zygote to a second bud on the opposite end of the parent cell. The latter is then delimited by a septum and becomes the ascus containing ascospore(s) (Lodder and Kreger-van Rij, 1952; Kurtzman and Fell, 1998). Consequently, the parent cell with both buds is involved in sexual reproduction and can be regarded as the sexual phase.

2.1.2. Materials and Methods

2.1.2.1. Strain used and cultivation

In this study *N. fulvescens* UOFS Y-0705 was obtained from the yeast culture collection of the University of the Free State in Bloemfontein (South Africa). This

yeast was grown on yeast-malt (YM) agar (Wickerham, 1951) at 22 ºC, for up to 15 days while sporulation was followed, using a light microscope (Axioplan, Zeiss, Göttingen, Germany) coupled to a Colourview Soft Digital Imaging System (Münster, Germany). Consequently, 6 – 8 day old cells (forming brown colonies) were then subjected to the following experimental procedures:

2.1.2.2. Mapping of 3-hydroxy (OH) oxylipins

The presence and distribution of 3-hydroxy (OH) oxylipins in this yeast was mapped according to Kock et al. (1998) using above sporulating yeast cells. In short, cells were treated with a primary antibody specific for 3-OH oxylipins, washed with phosphate buffered saline (PBS; Oxoid, Hampshire, England) and further treated with a primary antibody-specific fluorescein isothiocyanate (FITC)-conjugated secondary antibody (Jackson Immunoresearch Laboratories, USA). Cells were washed again with PBS to remove the unbound secondary antibodies and then fixed on a microscope slide and viewed using a Nikon TE 2000 (Japan), confocal laser scanning microscope (CLSM).

2.1.2.3. Mapping of mitochondria

Since 3-OH oxylipins in yeasts are produced by beta (β)-oxidation in mitochondria (Kock et al., 2007), it was decided to map the distribution of these organelles in vegetative and sexual cells. Consequently, above sporulating cells were treated with a primary monoclonal antibody (Genway Biotech Inc., San Diego, USA) specific for mitochondria (30 µL for 1 h in the dark at room temperature). Cells were then washed with PBS to remove unbound antibodies and further treated with a FITC-

conjugated secondary antibody (Jackson Immunoresearch Laboratories, USA), specific for the primary antibody, (30 µL for 1 h in the dark at room temperature). Cells were washed again with PBS to remove the unbound secondary antibodies. Staining was executed in 2 mL plastic tubes in order to maintain cell structure. After washing, the cells were fixed in Dabco (Sigma-Aldrich, USA) on a microscope slide and viewed using a Nikon TE 2000, CLSM.

2.1.2.4. Bio-assay preparation

Cells from 6 – 8 day old cultures were scraped from YM agar plates and suspended in sterile distilled water (dH_2O). Two hundred µL of this suspension was then spread out on soft agar plates (containing 0.5 % m/v agar) to form a homogenous lawn. A well was then constructed in the middle of the plate (0.5 cm in diameter and depth) and 46 µL of the mitochondrial inhibitors that is aspirin (acetylsalicylic acid; ASA; Sigma, Steinheim, Germany), benzoic acid (The British Drug Houses Ltd., Poole, England), ibuprofen (Sigma-Aldrich, Steinheim, Germany) and salicylic acid (The British Drug Houses Ltd., Poole, England), all at a concentration of 8 % m/v ethanol (dissolved in 96 % ethanol; ethanol obtained from Merck, Gauteng, South Africa) were added to each well respectively. Similar experiments were performed where only 96 % ethanol was added to the plates as control to study the effect of ethanol. Fluconazole was tested using an E-test strip (Davies Diagnostics, South Africa) containing various concentrations of fluconazole (0.016 – 256 µg/mL). Plates were incubated at 22 ºC for 6 – 8 days and viewed for formation of inhibition zones as well as white (asexual) and brown (asexual and sexual) zones. All plates are referred to as bio-assay plates.

2.1.2.5. Identification and analysis of 3-hydroxy (OH) oxylipins

In order to identify the 3-OH oxylipins observed microscopically and to determine if anti-mitochondrial compounds inhibit these oxylipins, cells from the white and brown zones of 6 – 8 day old ibuprofen treated bio-assays respectively were used for analysis. This experiment was performed as described by Van Heerden et al. (2005). In short, after scraping cells from respective zones, they were suspended in 100 mL dH_2O and the pH decreased to 3.8 with 3 % formic acid (Merck, Darmstadt, Germany). Next, oxylipins were extracted and then dissolved in 2x volumes of ethyl acetate (Merck, Darmstadt, Germany). After the organic and water phases had separated, the organic phase was evaporated with N_2 gas (AFROX, Bloemfontein, South Africa). This was followed by derivatizing (methylating and silylating) extracts which were finally dissolved in 400 µL chloroform:hexane (4:1) (Merck, Darmstadt, Germany). All experiments were performed in at least duplicate. Derivatized samples from the white and brown zones respectively were injected into a Finnigan Trace GC Ultra gas chromatograph (Thermo Electron Corporation, San Jose, Calif., USA) with a HP5 (60 m x 0.32 mm diameter) fused silica capillary column (0.1 µm coating thickness) coupled to a Finnigan Trace DSQ MS (Thermo Electron Corporation, San Jose, Calif., USA). The carrier gas was helium at 1.0 mL/min. The initial oven temperature of 110 ºC was maintained for 2 min then increased to a final temperature of 280 ºC at a rate of 5 ºC/min. The gas chromatography – mass spectrometer (GC-MS) was auto-tuned for an *m/z* of 50 - 400. One µL of the sample was injected into the GC-MS at a split ratio of 1:50 at an inlet temperature of 230 ºC (Venter et al., 1997).

2.1.2.6. Transmission Electron Microscopy (TEM)

Yeast material scraped from white and brown zones of 6 – 8 day old ibuprofen treated bio-assays respectively were chemically fixed with 0.1 M (pH 7) sodium phosphate-buffered glutardialdehyde (3 % v/v) for 3 h and then for 1.5 h in similarly buffered osmium tetroxide (0.5 % v/v) (Van Wyk and Wingfield, 1991). These fixed cells were then embedded in epoxy resin and polymerized at 70 ºC for 8 h (Spurr, 1969). An LKB III Ultratome was used to cut 60 nm sections with glass knives. Uranyl acetate (6 % m/v; saturated) (Merck, Darmstadt, Germany) was used to stain these sections for 10 min, followed by lead citrate (Merck) (Reynolds, 1963) for 10 min. The preparation was viewed with a Philips CM 100 transmission electron microscope (TEM) (Eindhoven, The Netherlands).

2.1.2.7. Determination of mitochondrial membrane potential ($\Delta\psi_m$)

In order to assess the influence of anti-mitochondrial compounds on mitochondrial activity, yeast cells were collected from the white and brown zones of 6 – 8 day old ibuprofen treated bio-assays respectively and then washed with PBS in a 2 mL plastic tube to get rid of agar and debris. Next, cells were treated with Rhodamine 123 (Rh123; 31 µL per sample), a mitochondrial stain (Molecular Probes, Invitrogen Detection Technologies, Eugene, Oregon, USA), for 1 h in the dark at room temperature. Cells were washed again with PBS to remove excess stain and fixed on microscope slides in Dabco (Sigma-Aldrich, USA). Finally, cells were viewed with a CLSM and the relative intensity of the fluorescence of the cells from the different zones, determined.

2.1.2.8. Quantitative measurement of metabolic state

Cells (equal weight) of *N. fulvescens* were scraped from each of the above 6 – 8 day old anti-mitochondrial drug treated (i.e. ASA, benzoic acid, ibuprofen and salicylic acid) bio-assay plates (white and brown zones) respectively and suspended in sterile PBS solution. One hundred µL of the cell suspension was added to a 96-well flat bottom polystyrene microtiter plate (Corning Incorporated, NY, USA). Fifty µL of menadione (Fluka, USA; 1 mM in acetone) was added to 2.5 mL XTT [0.5 g XTT (Sigma Chemicals, St. Louis, Mo., USA) in 1 L Ringer's lactate solution] and transferred to the cell suspension. The mixture was incubated in the dark for 3 h at 37 ºC. After incubation the formazan product was spectrophotometrically measured in terms of optical density at 492 nm using a Labsystems iEMS reader (Thermo BioAnalysis, Helsinki, Finland).

2.1.2.9. Oxygen inhibition studies

Mitochondrial activity in cells of *N. fulvescens* was inhibited by limiting oxygen availability. Cells were scraped from 6 – 8 day old, YM agar grown plates and suspended in sterilized dH_2O. A homogenous lawn was then spread out onto YM agar plates containing 1.6 % (m/v) agar. Plates were placed in an anoxic jar. An Anaerocult A System (Merck, Darmstadt, Germany) was used to create an anoxic environment within the anoxic jar. Anaerotest Test Strips (Merck, Darmstadt, Germany) were placed in the jar, confirming the anoxic atmosphere. The jar was incubated for 6 – 8 days at 22 ºC. As the control, the corresponding agar plates were placed next to the jar in the incubator (oxic conditions) and incubated for the same period.

2.1.3. Results and Discussion

When the yeast *N. fulvescens* was cultivated for up to 15 days as described, its whole unique life cycle could be observed. After conjugation between the parent cell and the first bud, the zygote moves into a second bud formed at the opposite end of the parent cell. This second bud is then delimited by a septum and becomes the ascus. The parent cell with both attached buds can therefore be considered as the sexual phase with the parent cell playing a pivotal role in zygote formation and movement. Usually one, rarely two spherical, brownish, spiny to warty ascospores were formed within the ascus giving rise to brown coloured colonies. Upon formation of the brown coloured asci (within 6 – 8 days of cultivation at 22 ºC), most parent cells (> 98%) with attached first bud were still intact and contained cytoplasm. A small number of older parent cells with first bud already released their content. As the ascus grew older (in general more than 10 days of cultivation at 22 ºC), most parent cells (> 98%) as well as the attached first bud released their content and appeared to be empty. Consequently, it was decided to study mitochondrial activity and inhibition only in intact 6 – 8 day old cultures.

Immunofluorescence studies (Figure 1) show that mitochondrially produced 3-OH oxylipins are associated mainly with the parent cell where zygote formation occurs (Figure 1a) and decrease in concentration as the ascus grows older and the parent cell with first bud release their content (Figures 1b and c). This is usually abundantly observed in cultures grown for more than 10 days at 22 ºC. Strikingly, in Figure 1(b) the ascus contained significantly lower levels of oxylipins when compared to the parent cell. [Rotating 3-dimensional (3-D) images of Figures 1a and c are available

on the CD at the back of this thesis]. Depletion of oxylipins is as expected, in accordance with the loss of mitochondria (Figure 1d) from the parent cell when asci grow older. Using GC-MS (Figure 2), only one type of 3-OH oxylipin (i.e. 3-OH 12:3; retention time = 22.63 min; Figure 2a) produced by *N. fulvescens* could be observed. The base peak at *m/*z = 175 (Figure 2b) depicts a hydroxyl group at carbon 3 as counted from the carboxyl group (Kock et al., 2007).These results fit the ASA Antifungal Hypothesis proposed by Kock and co-workers in 2007. According to the hypothesis, the sexual phase should contain increased amounts of one or more 3-OH oxylipins which is an indication of increased mitochondrial activity probably necessary for ascospore formation in *N. fulvescens*. Interestingly, 3-OH oxylipins are probably produced in parental cells with attached first bud during zygote formation. Is it possible that mitochondrial activity increases upon zygote formation as a prelude to probably high energy requiring ascosporogenesis? Is this a conserved characteristic in fungi?

The influence of different mitochondrial inhibitors dissolved in ethanol was tested on the life cycle of *N. fulvescens* using a bio-assay based on the agar diffusion test method. Similar results were obtained for all mitochondrial inhibitors tested compared to that found for ibuprofen (Figure 3a). At relatively high concentrations (that is close to origin of well) ASA, benzoic acid, ibuprofen and salicylic acid, inhibited growth followed by a white zone where selective inhibition of the sexual stage was observed (Figure 3a). In this zone, underdeveloped white coloured ascospores were observed microscopically. When ethanol alone (control) was added, only a small inhibition zone and brown zone were visible and no white zone (that is no selective inhibition of the sexual phase) (Figure 3b). Finally a brown zone

containing normal cells with mature asci and amber coloured ascospores was observed microscopically on the periphery of the bio-assay plate after the addition of the different mitochondrial inhibitors. Microscopy studies of the brown zones observed in both cases (that is in the presence of anti-mitochondrials and ethanol alone) were similar to the brown coloured cultures observed on similar agar plates without addition of anti-mitochondrials or ethanol. Similar results (formation of white and brown zones) were obtained when E-test strips containing the antifungal fluconazole was added to the bio-assay (Figure 3c). It is interesting to note that small white “petit” colonies with underdeveloped ascospores developed in the inhibition zone (Figure 3d). Is this a resistance mechanism developed by this fermentative yeast to overcome the anti-mitochondrial function (Kontoyiannis, 2000) of this antifungal? The respiration function of these resistant colonies and possible mutations should now be further studied.

After observing cell cultures from the different zones macroscopically and microscopically, the next step was to study their ultrastructure (Figures 4a - d). Ibuprofen treated cells from the brown zone (after 6 – 8 days of cultivation) showed normal development with the formation of young primordial smooth ascospores and lipid globules between parent cell and second bud that eventually give rise to mature asci containing usually one ascospore with hair-like protuberances (Kurtzman and Fell, 1998; Figures 4a and b). Mostly mature asci with intact parent cells i.e. filled with cytoplasm, was observed, although in the minority of cases some empty parental cells with mature asci was visible (Figure 4b). Cells from the white zone showed asci with underdeveloped small ascospores and no hair-like outgrowths or lipid globules as described above (Figures 4c and d).

Next we determined the mitochondrial activity in 6 – 8 day old ibuprofen treated bio-assays by staining cells with Rh123, a cationic lipophilic dye that assesses transmembrane potential ($\Delta\psi_m$). This was performed on equal amounts of cells from both the white and brown zones respectively (Johnson et al., 1980; Swart et al., 2008). Cells from the brown zone showed significantly ($p < 0.001$) increased fluorescence (relative intensity = 4050 +/- 85; n = 10) compared to similar cells in the white zone (relative intensity = 2810 +/- 752; n = 10) as collected at 450 nm. This indicates increased mitochondrial activity in these cells present in the brown zone which is probably needed for proper ascospore formation. Likewise, no evidence of mitochondrially produced 3-OH fatty acids were found in cells in the white zone using GC-MS thereby further showing a decreased mitochondrial activity (that is β-oxidation) in this zone.

Mitochondrial activity was also determined by measuring mitochondrial dehydrogenase activity (Kuhn et al., 2003) in 6 – 8 day old cells present in the white and brown zones, respectively, using the XTT-assay. These zones were obtained by the addition of the various anti-mitochondrial drugs to the bio-assay as previously described. Results indicate that anti-mitochondrial drugs inhibit mitochondrial activity (measured at 492 nm) significantly ($p < 0.001$; n = 8) that is ASA: white zone 1.4 +/- 0.24, brown zone 2.42 +/- 0.08; Benzoic acid: white zone 0.88 +/- 0.08, brown zone 2.58 +/- 0.12; Ibuprofen: white zone 0.99 +/- 0.33, brown zone 2.39 +/- 0.35; Salicylic acid: white zone 0.80 +/-0.12, brown zone 2.17 +/- 0.14.

Finally, the effect of anti-mitochondrial compounds was compared to the effect of oxygen limitation conditions on sporulation. As expected, anoxic conditions, which

are known to also inhibit mitochondrial function, yielded white colonies (inhibit sporulation) compared to brown colonies (with normal sporulation) observed under oxic conditions (results not shown).

To conclude, this study shows evidence that sufficient mitochondrial activity associated with the parent cell and first bud before sporulation is needed for normal ascospore formation. In *N. fulvescens*, mitochondria seem not to be involved inside the ascus in ascospore formation. Here the parent cell and first bud (where zygote formation takes place) is characterised by increased mitochondrial activity. Is zygote formation triggered by increased mitochondrial activity or *vice versa*? The use of *N. fulvescens* as indicator to select compounds with anti-mitochondrial antifungal properties should now be assessed and compared to the *Eremothecium* bio-assay protocol (Kock et al., 2009). *Nadsonia fulvescens* is regarded as a yeast with both respiring and fermentative capability (showing the Pasteur Effect). According to literature, the asexual and sexual reproductive phases of yeasts with and without the "Pasteur Effect", are both inhibited by anti-mitochondrial drugs (Kock et al., 2007). Here, yeasts that can respire and ferment were more resistant (regarding growth and ascus formation) to anti-mitochondrial compounds compared to strict respiring yeasts. This may be ascribed to the production of sufficient energy needed for asexual as well as sexual growth through an alternative anaerobic glycolytic fermentative pathway where mitochondria are less involved (Kock et al., 2007). It is interesting to note that the respiring and fermentative *Zygosaccharomyces baillii* may produce mature asci even under anoxic conditions (Swart et al., 2008). In future the influence of anti-mitochondrial drugs on mutants of *Nadsonia* which are strictly aerobic should be investigated.

2.1.4. Acknowledgements

The South African National Research Foundation (NRF) Blue Skies Research Programme (BS2008092300002) is acknowledged for financial support as well as A.S. Bareetseng for preparing the TEM micrograph in Figure 4b.

2.1.5. References

Browne GS, Nelson C, Nguyen T, Ellis BA, Day RO, Williams KM (1999). Stereoselective and substrate dependent inhibition of hepatic mitochondrial β-oxidation and oxidative phosphorylation by the non-steroidal anti-inflammatory drugs ibuprofen, flurbiprofen and ketorolac. Biochem. Pharmacol. 7: 837 – 844.

Byczkowski JZ, Korolkiewicz KZ (1976). Inhibition of monoamide oxidase activity by phenacetin and salicylamide. Pharmacol. Res. Commun. 5: 477 – 483.

Han YH, Kim SH, Park WH (2008). Antimycin A as a mitochondrial electron transport inhibitor prevents the growth of human lung cancer A549 cells. Oncol. Rep. 20(3): 689 – 693.

Higgins ES, Friend WH, Rogers KS (1978). Depression by ethionine of phosphorylating oxidation in hepatic mitochondria. Experientia 34(5): 578 – 579.

Johnson LV, Walsh ML, Chen LB (1980). Localization of mitochondria in living cells with Rhodamine 123. PNAS 77: 990 – 994.

Kock JLF, Venter P, Linke D, Schewe T, Nigam S (1998). Biological dynamics and distribution of 3-hydroxy fatty acids in the yeast *Dipodascopsis uninucleata* as investigated by immunofluorescence microscopy. Evidence for a putative regulatory role in the sexual reproductive cycle. FEBS Lett. 472: 345 – 348.

Kock JLF, Sebolai OM, Pohl CH, Van Wyk PWJ, Lodolo EJ (2007). Oxylipin studies expose aspirin as antifungal. FEMS Yeast Res. 7: 1207 – 1217.

Kock JLF, Swart CW, Ncango DM, Kock JLF Jr., Munnik IA, Maartens MMJ, Pohl CH, Van Wyk PWJ (2009). Development of a yeast bio-assay to screen anti-mitochondrial drugs. Curr. Drug Disc. Technol. 6: 186 – 191.

Kontoyiannis DP (2000). Modulation of fluconazole sensitivity by the interaction of mitochondria and Erg3p in *Saccharomyces cerevisiae*. J. Antimicrobial Chemother. 46: 191 – 197.

Krause MM, Brand MD, Krauss S, Meisel C, Vergin H, Burmester GR, Buttgereit F (2003). Non-steroidal anti-inflammatory drugs and a selective cyclooxygenase 2 inhibitor uncouple mitochondria in intact cells. Arthritis Rheum. 48(5): 1438 – 1444.

Kuhn DM, Balkis M, Chandra J, Mukherjee PK, Ghannoum MA (2003). Uses and limitations of the XTT assay in studies of *Candida* growth and metabolism. J. Clin. Microbiol. 41(1): 506 – 508.

Kurtzman CP, Fell JW (1998). Definition, classification and nomenclature of the yeast. In Kurtzman and Fell (eds) The yeasts – a taxonomic study, 4th ed, Elsevier Science Publication BV, Amsterdam, The Netherlands.

Lageweg W, Wanders RJA (1993). Studies on the effect of fenoprofen on activation and oxidation of long chain and very long chain fatty acids in hepatocytes and subcellular fractions from rat liver. Biochem. Pharmacol. 1: 79 – 85.

Lal N, Kumar J, Erdahl WE, Pfeiffer DR, Gadd ME, Graff G, Yanni JM (2009). Differential effects of non-steroidal anti-inflammatory drugs on mitochondrial dysfunction during oxidative stress. Arch. Biochem. Biophys. 490: 1 – 8.

Lodder J, Kreger-van Rij NJW (1952). The yeast – a taxonomic study. North-Holland Publishing Co., Amsterdam, The Netherlands.

McDougall P, Markham A, Cameron I, Sweetman AJ (1983). The mechanism of inhibition of mitochondrial oxidative phosphorylation by the non-steroidal anti-inflammatory agent diflunisal. Biochem. Pharmacol. 17: 2595 – 2598.

Ncango DM, Swart CW, Goldblatt ME, Pohl CH, Van Wyk PWJ, Botes PJ, Kock JLF (2008). Oxylipin and mitochondrion probes to track yeast sexual cells. Can. J. Microbiol. 54(6): 450 – 455.

Norman C, Howell KA, Millar AH, Whelan JM, Day DA (2004). Salicylic acid is an uncoupler and inhibitor of mitochondrial electron transport. Plant Physiol. 134: 492 – 501.

Oyagbemi AA, Saba AB, Azeez OI (2010). Capsaicin: a novel chemopreventive molecule and its underlying molecular mechanisms of action. Indian J. Cancer 47(1): 53 – 58.

Reynolds ES (1963). The use of lead citrate at high pH as an electron opaque stain in electron microscopy. J. Cell. Biol. 17: 208 – 212.

Rodriguez RJ, Acosta D (1996). Inhibition of mitochondrial function in isolated rat liver mitochondria by azole antifungals. J. Biochem. Toxicol. 11(3): 127 – 131.

Somasundaram S, Sigthorsson G, Simpson RJ, Watts J, Jacob M, Tavares IA, Rafi S, Roseth A, Foster R, Price AB, Wrigglesworth JM, Bjarnason I (2000). Uncoupling of intestinal mitochondrial oxidative phosphorylation and inhibition of cyclooxygenase are required for the development of NSAID-enteropathy in the rat. Aliment. Pharmacol. Ther. 14: 639 – 650.

Spurr AR (1969). A low viscosity epoxy resin embedding medium for electron microscopy. J. Ultrastruct. Res. 26: 1 – 43.

Swart CW, Van Wyk PWJ, Pohl CH, Kock JLF (2008). Variation in yeast mitochondrial activity associated with asci. Can. J. Microbiol. 54(7): 532 – 536.

Van Heerden A, Kock JLF, Botes PJ, Pohl CH, Strauss CJ, Van Wyk PWJ, Nigam S (2005). Ascospore release from bottle-shaped asci in *Dipodascus albidus*. FEMS Yeast Res. 5: 1185 – 1190.

Van Wyk PWJ, Wingfield MJ (1991). Ascospore ultrastructure and development of *Ophiostoma cucullatum*. Mycologia 83: 698 – 707.

Venter P, Kock JLF, Sravan KG, Botha A, Coetzee DJ, Botes PJ, Bhatt RK, Falck JR, Schewe T, Nigam S (1997). Production of 3*R*-hydroxy-polyenoic fatty acids by the yeast *Dipodascopsis uninucleata.* Lipids 32(12): 1277 – 1283.

Wickerham LJ (1951). Taxonomy of yeasts. Technical Bulletin No. 1029. US Department of Agriculture. Washington D.C., USA.

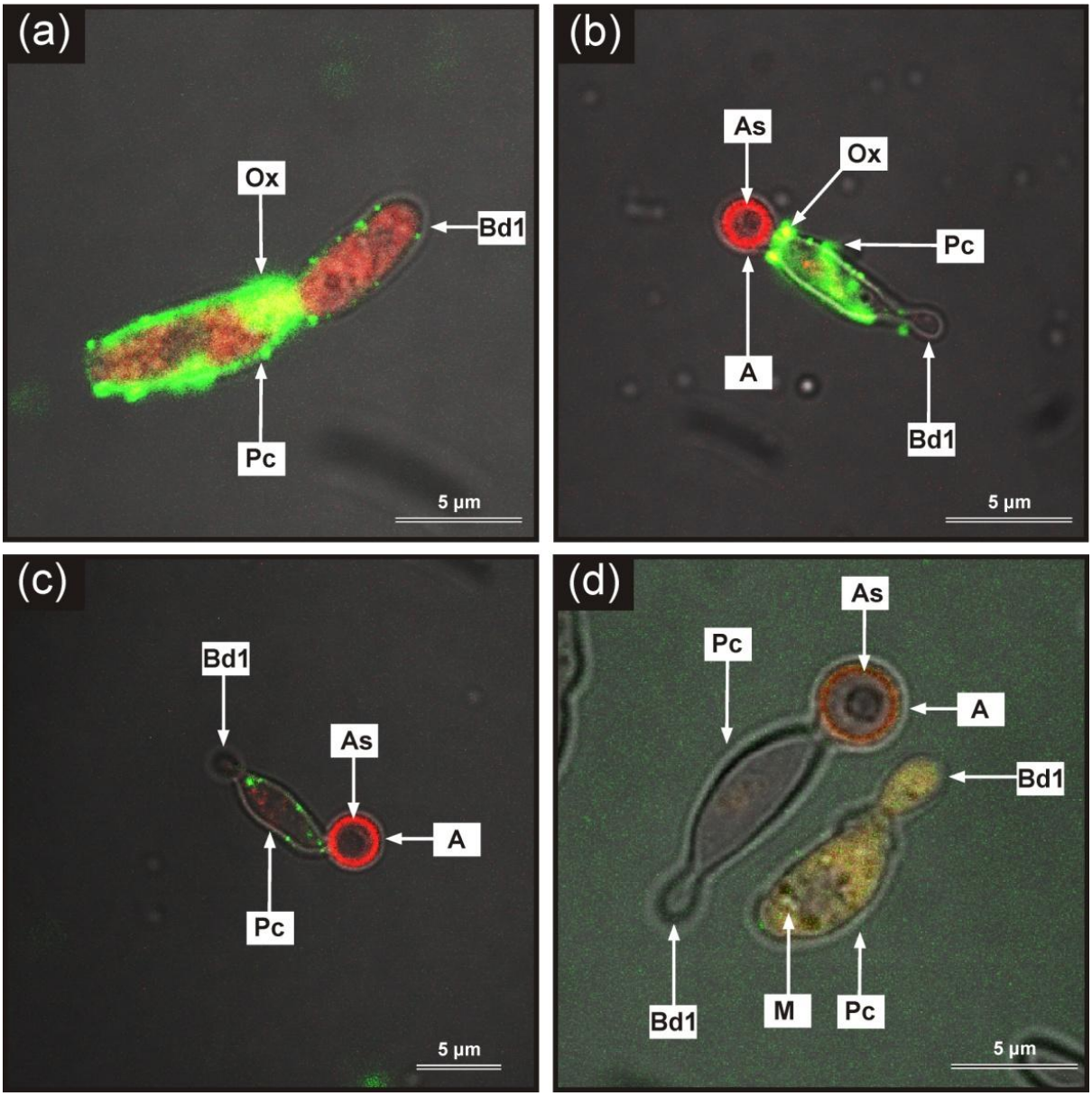

Figure 1 – Confocal laser scanning micrographs of cells in different developmental stages towards ascus (A) formation. Cells were probed with fluorescing antibodies specific for oxylipins (Ox) and mitochondria (M). Oxylipins are observed in the parent cell (Pc) with first attached bud (Bd 1) (a) and parent cell attached to both first bud and ascus (b). Oxylipins are depleted in parent cell after further development (c). Monoclonal antibody probes indicate a higher mitochondrion concentration in the parent cell and first bud compared to old mature ascus, attached to empty parent cell with attached first bud (d). As = ascospore.

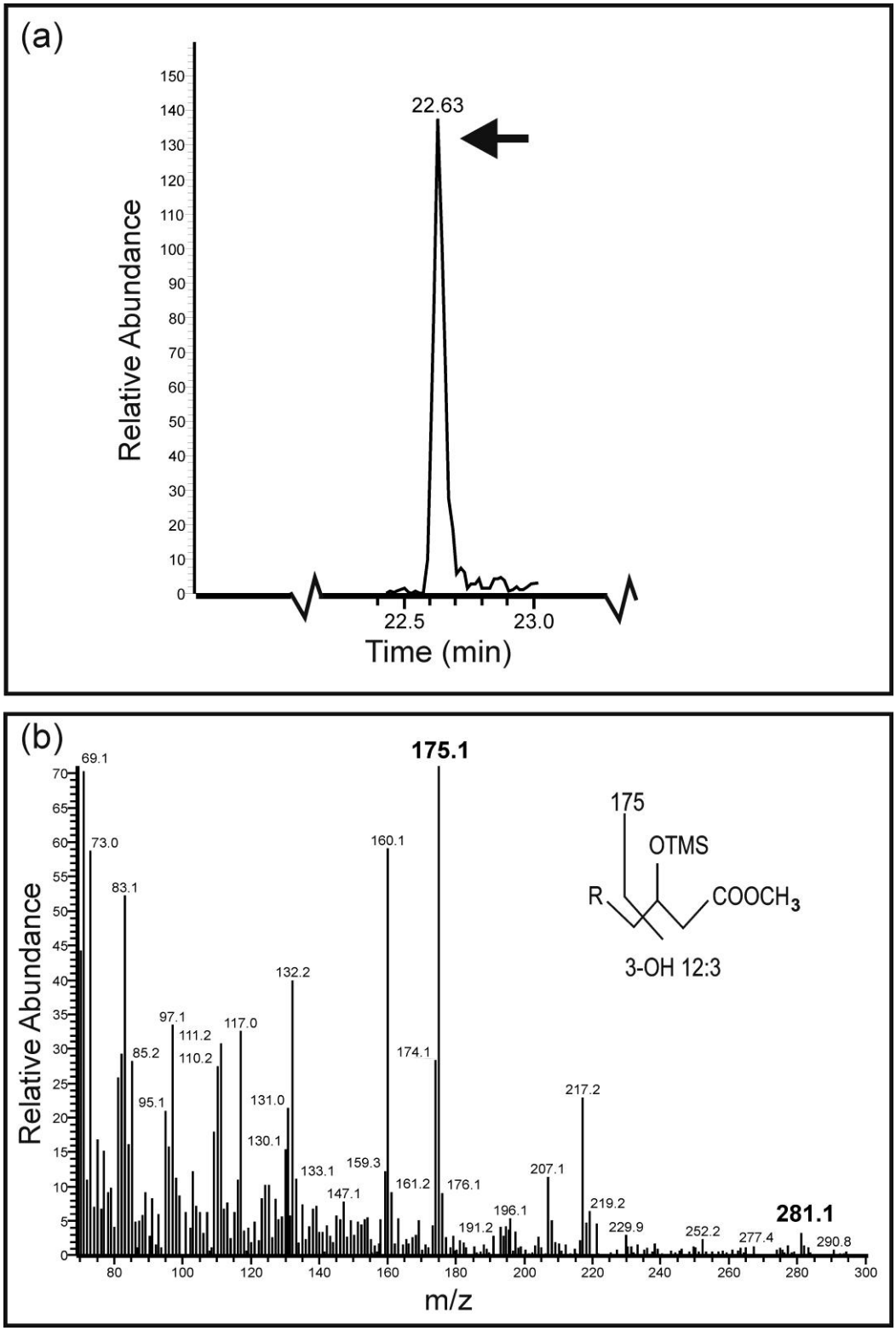

Figure 2 – Gas chromatography – mass spectrometry (GC-MS) profiles showing the total ion chromatogram (a) and mass spectrum (b) of 3-hydroxy (OH) 12:3 found in the yeast *Nadsonia fulvescens* producing brown asci mainly attached to intact parent cells.

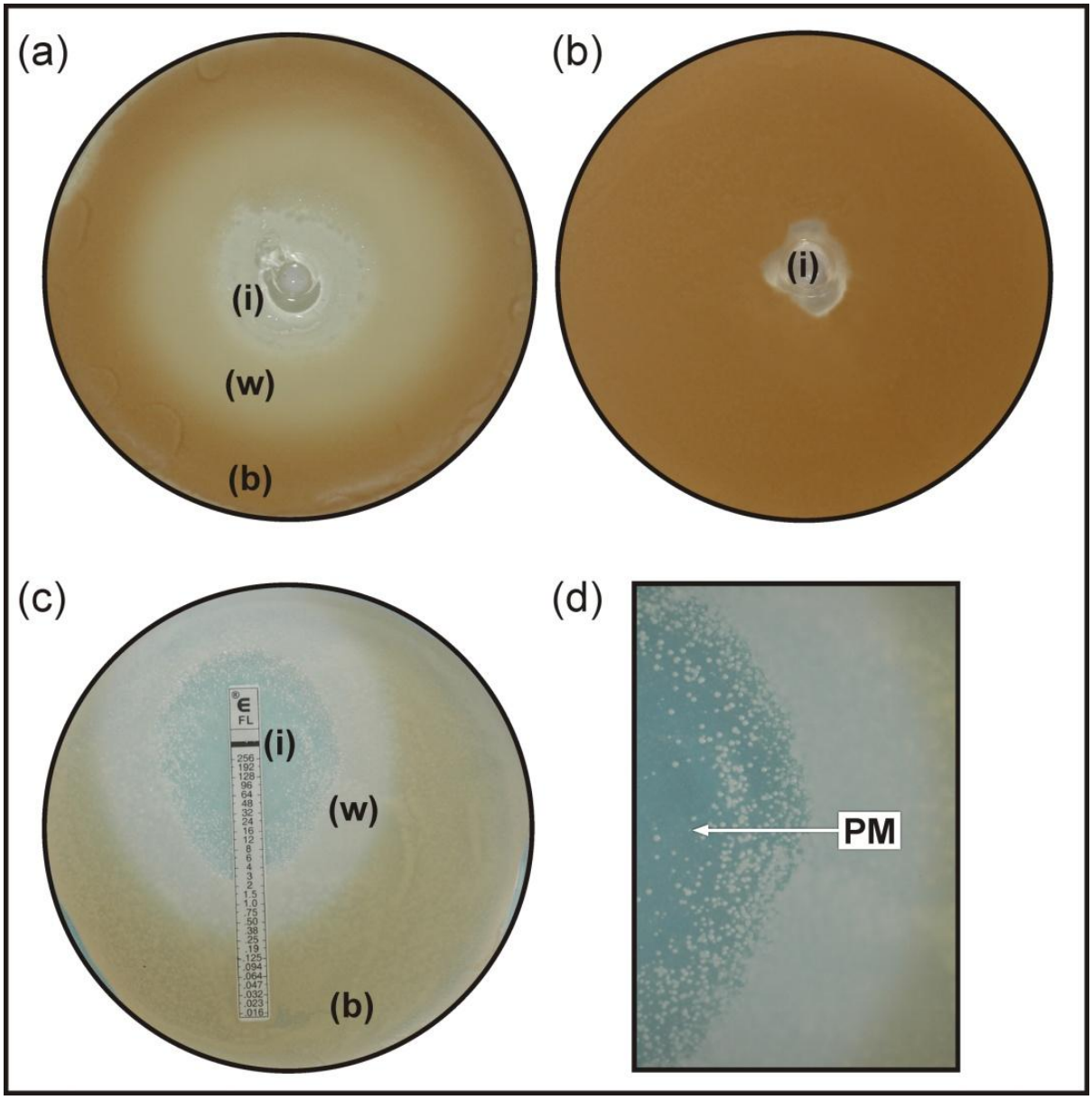

Figure 3 – Photograph of a *Nadsonia fulvescens* bio-assay treated with ibuprofen (a) indicating the inhibition zone (*i*), the white zone (*w*) as well as a brown zone (*b*). Ethanol control is shown in (b) containing only a small inhibition zone (*i*). Fluconazole E-test strips were also tested using *N. fulvescens* as indicator yeast (c) showing an inhibition zone (*i*), white zone (*w*) and brown zone (*b*). Petite mutants (PM) are formed in the inhibition zone (d).

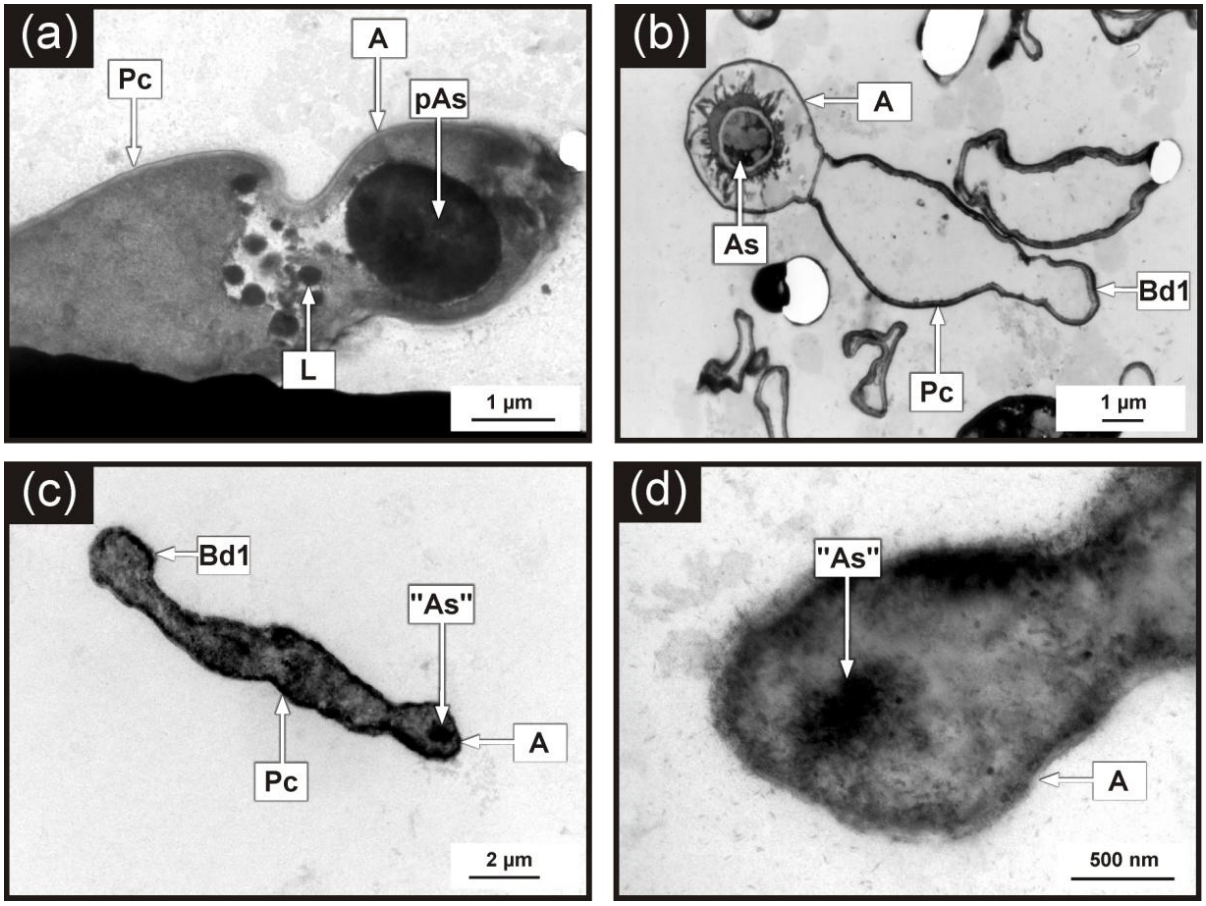

Figure 4 – Transmission electron micrographs showing ibuprofen treated cells obtained from the brown as well as white zones. Cells obtained from the brown zone (a, b) indicate lipid (L) globules concentrated around the neck of the second bud cell (A) where a young (primordial) ascospore (pAs) is being produced (a). A scarce older mature ascus (A) with a mature ascospore (As) could also be observed in the cells obtained from the brown zone (b). Cells obtained from the white zone (c, d) only show small, immature ascospores (“As”). Bd 1 = first attached bud; Pc = parent cell.

2.1.6. Supplementary Information

The bio-assay developed with the yeast *N. fulvescens* as indicator organism (described in 2.1.2.4.), could be applied as a first screen for anti-mitochondrial, antifungal drugs. To evaluate the efficacy of the bio-assay, various compounds were tested (Table 1). Some of these compounds are known in literature to have anti-mitochondrial activity (Byczkowski and Korolkiewicz, 1976; Higgins et al., 1978; McDougall et al., 1983; Lageweg and Wanders, 1993; Rodriguez and Acosta, 1996; Browne et al., 1999; Somasundaram et al., 2000; Krause et al., 2003; Norman et al., 2004; Kock et al., 2007; Han et al., 2008; Lal et al., 2009; Oyagbemi et al., 2010). These all selectively inhibited the sexual phase (mature amber coloured ascospore formation). Further studies should now be done on these drugs to determine their possible effect on mitochondria. More antifungals should also be tested to expand the current database.

Interestingly, most of the anti-inflammatory compounds tested showed anti-mitochondrial activity with the exception of Phenylbutazone and Sulfinpyrazone. For the antimalaria drugs, chloroquine tested negative, but Quinine tested positive for anti-mitochondrial activity. All the antifungals tested positive, as well as the plant extract capsaicin. Literature also suggests that capsaicin (Oyagbemi et al., 2010) has anti-mitochondrial activity. The known classic anti-mitochondrial compounds Antimycin A (Han et al., 2008) and Ethionine (Higgins et al., 1978) did display anti-mitochondrial activity. All the compounds tested did however inhibit asexual (vegetative) growth at higher concentrations (i.e. at the start of the concentration

gradient). As expected oxygen limitation inhibited mitochondrial activity while Dimethyl Sulfoxide (DMSO) and ethanol (used as solvents for some of the compounds tested) did not selectively inhibit the sexual phase and are therefore not regarded as anti-mitochondrial.

References

Included in references of Chapter 2.

Table 1: Compounds tested with the yeast bio-assay, using *Nadsonia fulvescens* as indicator organism, for specialized antifungal and anti-mitochondrial activity.

Compounds tested	Selective inhibition of asci (sexual cells)
Anti-inflammatory (8 % m/v)	
Diclofenac*	+
Diflunisal*	+
Etodolac	+
Fenbufen	+
Fenoprofen*	+
Flurbiprofen*	+
Nabumetone	+
Phenylbutazone	-
Salicylamide*	+
Sulfinpyrazone	-
Tolmetin	+
Antimalaria (8 % m/v)	
Chloroquine	-
Quinine	+

Antifungals (E-test gradient strips)

Caspofungin* (MIC reading scale: 0.002 to 32 µg/mL)	+
Fluconazole* (MIC reading scale: 0.016 to 256 µg/mL)	+
Itraconazole* (MIC reading scale: 0.002 to 32 µg/mL)	+
Ketoconazole* (MIC reading scale: 0.002 to 32 µg/mL)	+
Posaconazole* (MIC reading scale: 0.002 to 32 µg/mL)	+
Voriconazole* (MIC reading scale: 0.002 to 32 µg/mL)	+

Plant extracts (8 % m/v)

Capsaicin*	+

Others (8 % m/v)

DMSO (Solvent)	-
Ethanol	-
Antimycin A*	+
Ethionine*	+
Oxygen limitation*	+

DMSO = Dimethyl Sulfoxide; MIC = Minimum Inhibitory Concentration; * = anti-mitochondrial (Byczkowski and Korolkiewicz, 1976; Higgins et al., 1978; McDougall et al., 1983; Lageweg and Wanders, 1993; Rodriguez and Acosta, 1996; Browne et al., 1999; Somasundaram et al., 2000; Krause et al., 2003; Norman et al., 2004; Kock et al., 2007; Han et al., 2008; Lal et al., 2009; Oyagbemi et al., 2010); + = zone present; - = zone absent. All compounds tested inhibited vegetative (asexual growth) at higher concentrations i.e. at the start of concentration gradient.

Chapter 2 (cont.)

2.2. The influence of mitochondrial inhibitors on the life cycle of ascospore producing fungi: 3-D architecture and elemental composition of asci of *Nadsonia fulvescens*

Published in: SRE Vol. 5(18), 18 September 2010 (In Press). (ISI-accredited, scientific journal)

Presented on invitation at the 28th International Specialized Symposium on Yeasts: Metabolic and Bioprocess Engineering for Sustainable Development, 15 – 18 September 2010, Bangkok, Thailand.

Abstract

In this study, sexual structures of the yeast *Nadsonia fulvescens* containing mature and fluconazole-treated malformed ascospores were studied using nano scanning Auger microscopy (NanoSAM) in combination with transmission electron microscopy (TEM). This is the first application of NanoSAM to biological material. Transmission electron microscopy exposed a variety of malformed ascospores in asci treated with fluconazole. Here some ascospores produced degenerated spiky protuberances with relatively large inclusions carried inside wrinkled asci. Other ascospores contained no walls or protuberances and were enclosed within smooth spherical shaped asci. The majority of ascospores contained less dense hollow areas surrounded by cytoplasmic material. Nano scanning Auger microscopy studies on these asci corroborate the TEM results although less structural detail was obtained. Nano scanning Auger microscopy showed a decrease in element intensities during etching which assisted structural analysis of ascospore less dense hollow areas.

Key words: asci, elemental composition, fluconazole, *Nadsonia*, nano scanning Auger microscopy, transmission electron microscopy, 3-dimensional architecture.

2.2.1. Introduction

Since the first electron image with a resolution higher than that obtainable with a light microscope was obtained in 1935 (Selby, 1953), there has been continual improvements in electron microscopy (EM). Consequently, many variations of EM have been developed. These include scanning electron microscopy (SEM), electron tomography (ET) for three-dimensional (3-D) imaging, correlative microscopy that integrates the imaging of live cells and EM, transmission electron microscopy (TEM), reflection electron microscopy (REM), scanning transmission electron microscopy (STEM), low voltage electron microscopy (LVEM) and energy-dispersive X-ray spectroscopy (EDS) in combination with STEM or SEM respectively (Hochella et al., 1986; Koster and Klumperman, 2003).

The more recent combination of SEM with Auger electron spectroscopy (AES) led to the development of scanning Auger microscopy (SAM). Scanning Auger microscopy has the ability to perform semi-quantitative elemental analysis on volumes extremely smaller than those analyzed with SEM/EDS while the sample is visualized by SEM. Scanning Auger microscopy is usually used in the near-surface analysis of conductors and semi-conductors (Hochella et al., 1986). Scanning Auger microscopy has also been used in conjunction with targeted etching, where materials such as semi-conductors were etched with an Argon (Ar^+) gun. For the purpose of this study, SAM in combination with Ar^+ etching will be referred to as nano scanning Auger microscopy (NanoSAM). Yet so far, no mention has been made of the application of NanoSAM to biological material.

Previous studies show that the antifungal fluconazole inhibits mitochondrial function in *Nadsonia fulvescens* and may cause malformation of ascospores (Swart et al., 2010; Chapter 2.1.). However, detailed ultrastructural studies on malformed ascospores and associated asci have up till now not been performed. In this study NanoSAM, in combination with TEM, was applied for the first time to investigate asci and ascospores of *N. fulvescens* treated with this antifungal.

2.2.2. Materials and Methods

Yeast cells (asci) containing ascospores were prepared from the yeast *N. fulvescens* UOFS Y-0705 (obtained from the UNESCO MIRCEN yeast culture collection, University of the Free State, Bloemfontein, South Africa). To achieve this, the yeast was grown on yeast-malt (YM) agar (Wickerham, 1951) at 22 ºC, for 6 – 8 days, until sporulation was observed. The cells were then subjected to the following experimental procedures:

2.2.2.1. Fluconazole treatment

E-test strips (Davies Diagnostics, South Africa) were overlaid on agar surfaces previously covered with inocula of above yeast (Swart et al., 2010; Chapter 2.1.). Plates were incubated at 22 ºC for 6 – 8 days and viewed for the formation of inhibition as well as white and brown zones (Figure 1). Detailed cell analysis was performed by light microscopy (Zeiss Axioplan, Germany).

2.2.2.2. Scanning Electron Microscopy (SEM)

Cells were scraped from white (0.38 – 1.5 µg/mL fluconazole concentration region) and brown (< 0.38 µg/mL fluconazole concentration region) zones respectively and prepared for SEM (Figure 1). In short, cells were fixed with equal amounts of buffered 3 % (v/v; 0.1 mol/L) glutardialdehyde (Merck, Darmstadt, Germany) (Van Wyk and Wingfield, 1991). The suspension was then rinsed with the same buffer to remove excess aldehyde fixative and post-fixation was performed with 1 % (v/v) buffered osmium tetroxide (Merck, Darmstadt, Germany). The suspension was washed to remove excess osmium tetroxide. Dehydration by a graded ethanol sequence 50, 70, 95 and 100 % (x2) for 30 min per step followed, while centrifugation took place between each dehydration step. Drying was performed by using a critical point dryer, where after the specimens were mounted on stubs, coated with gold and viewed with SEM (Shimadzu SSX-550 Superscan, Tokyo, Japan) at 5 kV. Cells from the white and brown zones were treated in exactly the same manner.

2.2.2.3. Nano Scanning Auger Microscopy (NanoSAM)

Above samples were examined using a PHI 700 Nanoprobe (Japan) equipped with SAM and SEM facilities. The field emission electron gun used for the SEM and SAM analyses was set at: 2.34 A filament current; 4 kV extractor voltage and 238.1 µA extractor current. With these settings a 20 kV, 10 nA electron beam was obtained for the Auger analyses and SEM imaging. The electron beam diameter was 12 nm. The upper pressure of the electron gun unit was 8.8E-10 Torr. The pressure in the main chamber was 2.29E-10 Torr. Aperture A was used for all the measurements. The Field of View (FOV) for SEM was 8 µm and the number of frames used was 4.

The Auger point analyses were obtained by using 10 cycles per survey, 1 eV/step and 20 ms per step. The Nanoprobe was also equipped with an Ar^+ ion sputtering gun set at: 2 kV beam voltage, 2 µA ion beam current and a 1x1 mm raster area, giving a sputter rate of about 27 nm/min. The ion emission current was set at 15 mA. An alternating sputter mode with sputter intervals of 1 min and sputter time of 2 min was used without any rotation.

2.2.2.4. Transmission Electron Microscopy (TEM)

Yeast material was scraped from white (0.38 - 1.5 µg/mL fluconazole concentration region) and brown (< 0.38 µg/mL fluconazole concentration region) zones respectively and chemically fixed with 0.1 M (pH 7) sodium phosphate-buffered glutardialdehyde (3 % v/v) for 3 h and then for 1.5 h in similarly buffered osmium tetroxide (0.5 % v/v) (Van Wyk and Wingfield, 1991). Fixed cells were embedded in epoxy resin and polymerized at 70 ºC for 8 h (Spurr, 1969). An LKB III Ultratome was used to cut 60 nm sections with glass knives. Sections were stained for 10 min with Uranyl acetate (6 % m/v; saturated) (Merck, Darmstadt, Germany), followed by lead citrate (Merck) (Reynolds, 1963) for 10 min. The preparation was viewed with a Philips CM 100 TEM (Eindhoven, The Netherlands) at 60 kV and photographed as digital images.

2.2.3. Results

An inhibition (poor growth), white (cells with malformed fluconazole-inhibited asci) and brown (cells with mature asci) zone formed when yeast cells were subjected to fluconazole at different concentrations (Figure 1). The brown zone formed at low fluconazole concentrations and contained fully developed, mature asci containing spheroidal ascospores (one each) with a spiky wall surrounding inclusions referred to as lipid globules (Figure 2a; Miller and Phaff, 1998). The most susceptible part of the life cycle to fluconazole was the sexual reproductive phase. Here, no mature brown ascospores within hyaline asci were observed. Instead, some ascospores produced degenerated spiky protuberances with relatively large inclusions carried inside wrinkled asci (Figures 2b, c and d). Other ascospores again contained no walls with protuberances and were enclosed within smooth spherical shaped asci (Figures 2e, f, g and h). The majority of ascospores contained less dense hollow areas surrounded by cytoplasmic material (Figure 2i).

The ion gun was used successfully to make targeted sputtered etching depth profiles of up to 1026 nm that is about halfway into the 2.0 - 2.5 µm diameter mature (Figures 3a - f) and fluconazole-inhibited asci (Figures 3j - l). In the former, etching proceeds through shrunken cell walls of the two asci (Figure 3a) leaving bare crunched spiky appendages with irregular shape (Figure 3b). When reaching an etching depth of about 1026 nm, a solid ascospore surface was observed (Figure 3c) with remnants of the crunched spiky protuberances visible on the periphery and surrounded by the shrunken cell wall. In order to obtain an improved 3-D visualization of these spiky

protuberances, the experiment was repeated on other mature asci (Figure 3d). The outer layer of the ascus wall was etched by peeling off 27 nm (Figure 3e). As etching continued to about 1000 nm into the ascus, the ascospore as well as spiny protuberances was observed in 3-D (Figure 3f). Scanning Auger microscopy element colour maps indicated a high gold (Au) intensity (Au indicated in green, Figure 3g; corresponding to Figure 3d) as etching commenced. This is to be expected since the samples are covered with Au during preparation, to make it more electron conductive. As the outer layer of the ascus wall was etched off, carbon (C) was revealed (Au indicated in green; C indicated in blue; Figure 3h; corresponding to Figure 3e). Some remains of Au were also observed where etching has not yet taken place. As etching continued into the ascus, Au was no longer visible, yet a high intensity of C could be observed (Figure 3i; corresponding to Figure 3f).

The cell wall surrounding the fluconazole-inhibited ascus was smooth (Figure 3j) and upon further etching a second, also smooth-walled structure, with different texture became visible (Figure 3k). This 3-D structure seems to contain less dense hollow areas inside the malformed ascospore that disintegrated upon further etching (Figure 3l). This structure corresponds well to structures observed with TEM (Figure 2i). A movie showing sequential etching into fluconazole-treated asci and normal asci can be viewed in CD format at the end of the thesis.

In order to make a quantitative assessment of the element composition as etching proceed, elemental composition depth profiles of asci during sputtering were also obtained (Figure 4). A drastic decrease in Au and osmium (Os) intensities was evident when reaching an etching depth of 135 nm into asci suggesting that these

elements are associated mainly with asci outer cell walls thereby also diluting C intensities substantially (sputter time = 0 min; Figures 4b and d). The fluorine (F) content (indicates fluconazole) remained at low intensities throughout etching of the malformed asci (Figure 4d), while no F was detected in the mature asci (Figure 4b). This was to be expected since yeast cannot produce compounds containing F. Fluorine can therefore be used as a marker to detect the presence of the antifungal fluconazole in yeast cells. In both cases, trace amounts of nitrogen (N) could be observed (results not shown).

Different C/O intensity ratios were observed during etching through asci (Figure 4). The mature asci (target point 3; Figures 4a and b) were characterized by relatively high C/O ratios throughout etching while the malformed ascus (target point 2; Figures 4c and d) was characterized by a decrease in C/O ratio. These results were reproducible when repeated on target sites 1, 2 and 4 (Figure 4a). In addition, a significant decrease in C intensity occurred as etching proceeded in malformed ascospores (Figure 4d). The cell wall onto which target point 1 was projected was not considered since limited etching occurred (Figure 4c). These results correspond well with the SAM element maps of similar etched asci (Figures 3g – i). The observed pulsing (repetitive increase and decrease of elemental intensities; Figures 4b and d) is ascribed to changes in chemical structures and concentrations as etching proceed through asci inclusions.

2.2.4. Discussion

In 2007, Kock and co-workers showed that the oxygen-dependent sexual stages of yeasts are most sensitive to mitochondrial inhibitors and are therefore selectively targeted. This suggests that mitochondrial inhibitors may also serve as antifungals by inhibiting yeast spore dispersal. To further test the general validity of this hypothesis, the antifungal fluconazole (also regarded as a mitochondrial inhibitor) (Swart et al., 2010), was further studied for its ability to selectively target sexual reproduction of the yeast *N. fulvescens*. This yeast is characterized by a peculiar type of sexual reproduction where each sexual birth-sac (ascus) produces only one, rarely two, sexual spore(s) (ascospore) with spiky protuberances enclosed within the ascus (Figure 2a; Miller and Phaff, 1998). Colonies with these sexual stages are brown in colour due to melanin-stained mature asci (Miller and Phaff, 1998).

According to the results obtained (Figures 1 and 2) it is clear that the most susceptible part of the yeast life cycle was the sexual stage, in particular ascus development. This is in accordance with literature where mitochondrial inhibitors affected similar responses in other yeasts (Kock et al., 2007). Since ascospore development was impaired in various ways (Figures 2b – i), it will be interesting to determine if these are fluconazole concentration dependent. Future studies should address this possibility. We also obtained the 3-D architecture and element composition of fluconazole-inhibited ascus structure (Figure 2i) with NanoSAM and compared this to mature asci each containing a single enclosed mature ascospore (Figure 2a). Here, SEM, nano-etching with an Ar^+ sputter gun and also elemental

analysis using a nanoprobe was for the first time successfully applied in yeast biology. Nano-etching was achieved by sputtering the sample with ionized Ar^+ atoms, thereby peeling 27 nm segments from the sample with every bombardment (sputtering). This enabled the detection of the 3-D nanostructure of mature and fluconazole-inhibited asci. From the results (Figures 3a – l) we conclude that fluconazole inhibits ascospore formation especially the development of spiky protuberances and causes the formation of less dense areas inside malformed ascospores. The spiny protuberances shown in Figure 3f corroborates the ascospore morphology observed using TEM (Figure 2a), except that some shrinkage of the ascus cell wall occurred during NanoSAM preparation, probably through dehydration giving a wrinkled appearance to the ascus. Such 3-D visualization has not been reported before for any type of biological system. The ability of these malformed ascospores to germinate as well as the induction of mutations should now be assessed.

Elemental analysis was performed by focusing the nanoprobe on a specific target site on the sample, the site was then bombarded with electrons from the nanoprobe and Auger electrons released. These Auger electrons were detected via a detector and a specific energy profile was obtained. These profiles were specific for every element and therefore the unknown elements in the sample could be identified. Scanning Auger microscopy was achieved by mapping the various elements across the etched surfaces in the sample. Here the nanoprobe scanned across the sample, indicating specific elements in specific colours. A colour map of various elements was therefore obtained for each sample surface analyzed (Figures 3g – i). Although, removal of Au from the surface by Ar^+ etching could be clearly visualized (Figure 3h),

no hint of ultrastructural structures such as organelles could be observed. This may be possible if the resolution of the different colour maps could be increased in future.

In combination with elemental analyses, this method was capable of determining the elemental composition of asci including ascospores. Changes in the elemental composition as etching proceeded through asci clearly show a drastic loss in C intensity towards the inside of the ascospore in fluconazole-treated asci. This corroborates the existence of a less dense area inside these ascospores (compare Figure 4d with Figure 2i). It is interesting to note that the observed hole inside the treated ascospore (Figure 3l) was not empty but contained less dense material. Although, this could not be detected by the NanoSAM SEM mode, it was clear from the elemental analysis (Figure 4d). Therefore, elemental tracking by NanoSAM may be used to study surfaces not visible by SEM. The difference between the elemental composition of the mature and fluconazole-inhibited malformed asci can only be explained when a more detailed chemical analysis of asci is performed and the relative amounts of glutardialdehyde, chitosan, beta-glucan, melanin, mannan, etc., are known.

2.2.5. Conclusions

The authors conclude that fluconazole at concentrations of 0.38 to 1.5 µg/mL inhibits normal ascospore development in the yeast *N. fulvescens.* In most cases, these fluconazole treated asci produced malformed ascospores with internal less dense hollow areas. We found that NanoSAM in conjunction with TEM is capable of

visualizing the 3-D architecture as well as elemental intensities of malformed and normal ascospores. Changes in element intensities, as analysed by NanoSAM, may also be useful in probing less dense areas (not visible by SEM) which are concealed within structures such as malformed ascospores. This is not possible with presently used EM and other microscopy protocols. This is an advancement in 3-D ultrastructure research methodology (Sorzano et al., 2007) with obvious wide application. The application of NanoSAM to microbial ultrastructure, systematics, animal embryonic cell development, early cancer cell detection and many more should now be assessed. The influence of different cell treatment regimes for NanoSAM on elemental analysis should also be researched.

2.2.6. Acknowledgements

The authors wish to thank the South African National Research Foundation (NRF) Blue Skies Research Programme (BS2008092300002) as well as SAFOI for financial support.

2.2.7. References

Hochella MF, Harris DW, Turner AM (1986). Scanning Auger Microscopy as a high-resolution microprobe for geologic materials. Am. Mineralogist 71: 1247 – 1257.

Kock JLF, Sebolai OM, Pohl CH, Van Wyk PWJ, Lodolo EJ (2007). Oxylipin studies expose aspirin as antifungal. FEMS Yeast Res. 7: 1207 – 1217.

Koster AJ, Klumperman J (2003). Review: Electron microscopy in cell biology: integrating structure and function. Nat. Rev. Mol. Cell Biol. 4: SS6 - SS10.

Miller MW, Phaff HJ (1998). *Nadsonia* Sydow. In Kurtzman et al. (eds) The Yeast – a Taxonomic Study, 4th ed, Elsevier Science Publication BV, Amsterdam, The Netherlands, pp. 268 – 270.

Reynolds ES (1963). The use of lead citrate at high pH as an electron opaque stain in electron microscopy. J. Cell. Biol. 17: 208 – 212.

Selby CC (1953). Microscopy II. Electron Microscopy: A Review. Cancer Res. 13(11): 753 – 775.

Sorzano COS, Jonic S, Cottevieille M, Larquet E, Boisset N, Marco S (2007). 3-D electron microscopy of biological nanomachines: principles and applications. Eur. Biophys. J. 36: 995 – 1013.

Spurr AR (1969). A low viscosity epoxy resin embedding medium for electron microscopy. J. Ultrastruct. Res. 26: 1 – 43.

Swart CW, Van Wyk PWJ, Pohl CH, Kock JLF (2010). Variation in mitochondrial activity over the life cycle of *Nadsonia fulvescens*. Afr. J. Microbiol. Res. 4(16): 1727 – 1732.

Van Wyk PWJ, Wingfield MJ (1991). Ascospore ultrastructure and development of *Ophiostoma cucullatum*. Mycologia 83: 698 – 707.

Wickerham LJ (1951). Taxonomy of yeasts. Technical Bulletin No. 1029. US Department of Agriculture. Washington, D.C., USA.

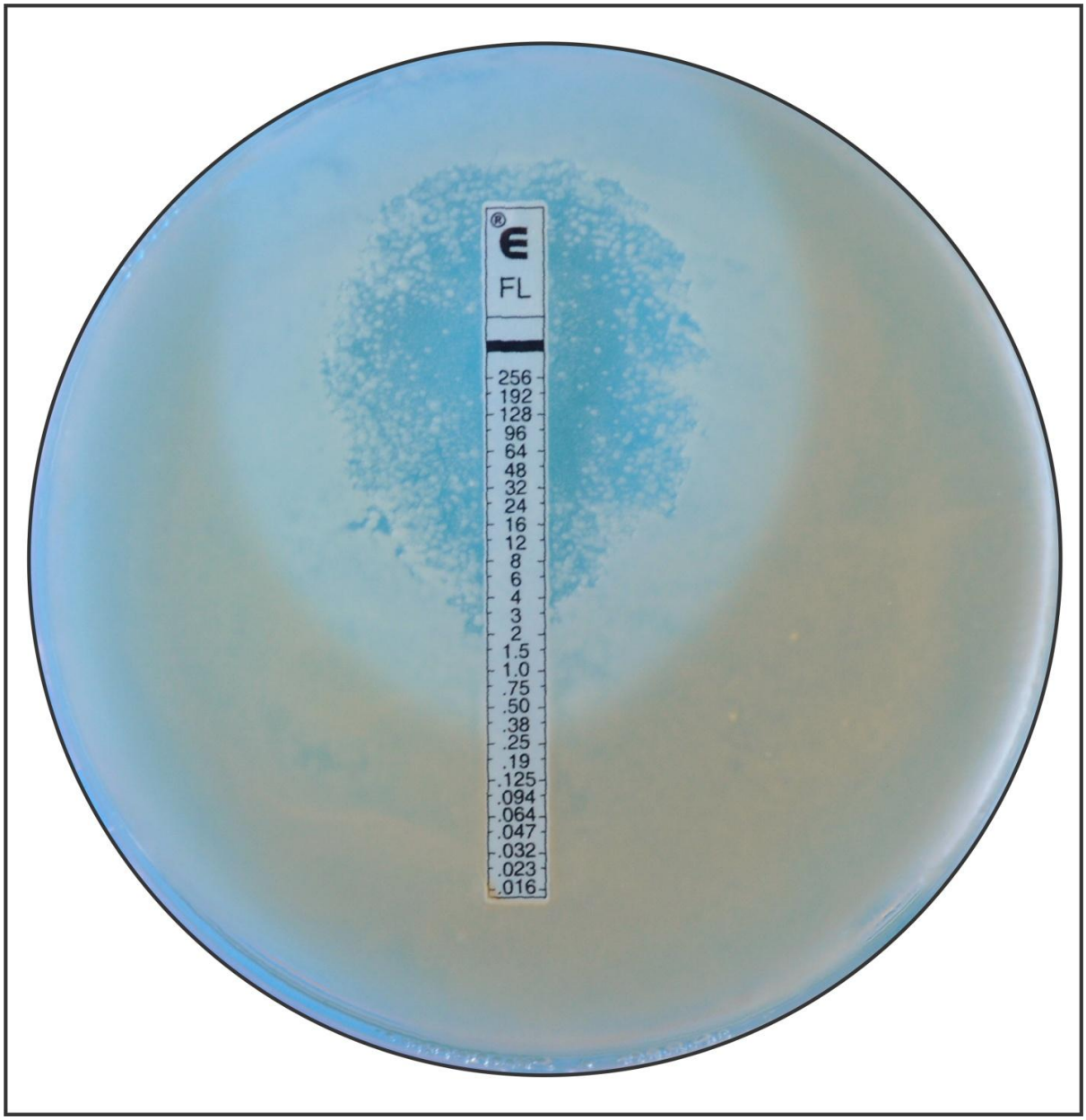

Figure 1 – An antifungal bio-assay showing inhibition of cell growth (blue zone) at high concentrations of fluconazole, inhibition of mainly ascus development (white zone) at lower concentrations and eventually no inhibition of ascus development (brown zone) at still lower concentrations. (Taken from Swart et al., 2010).

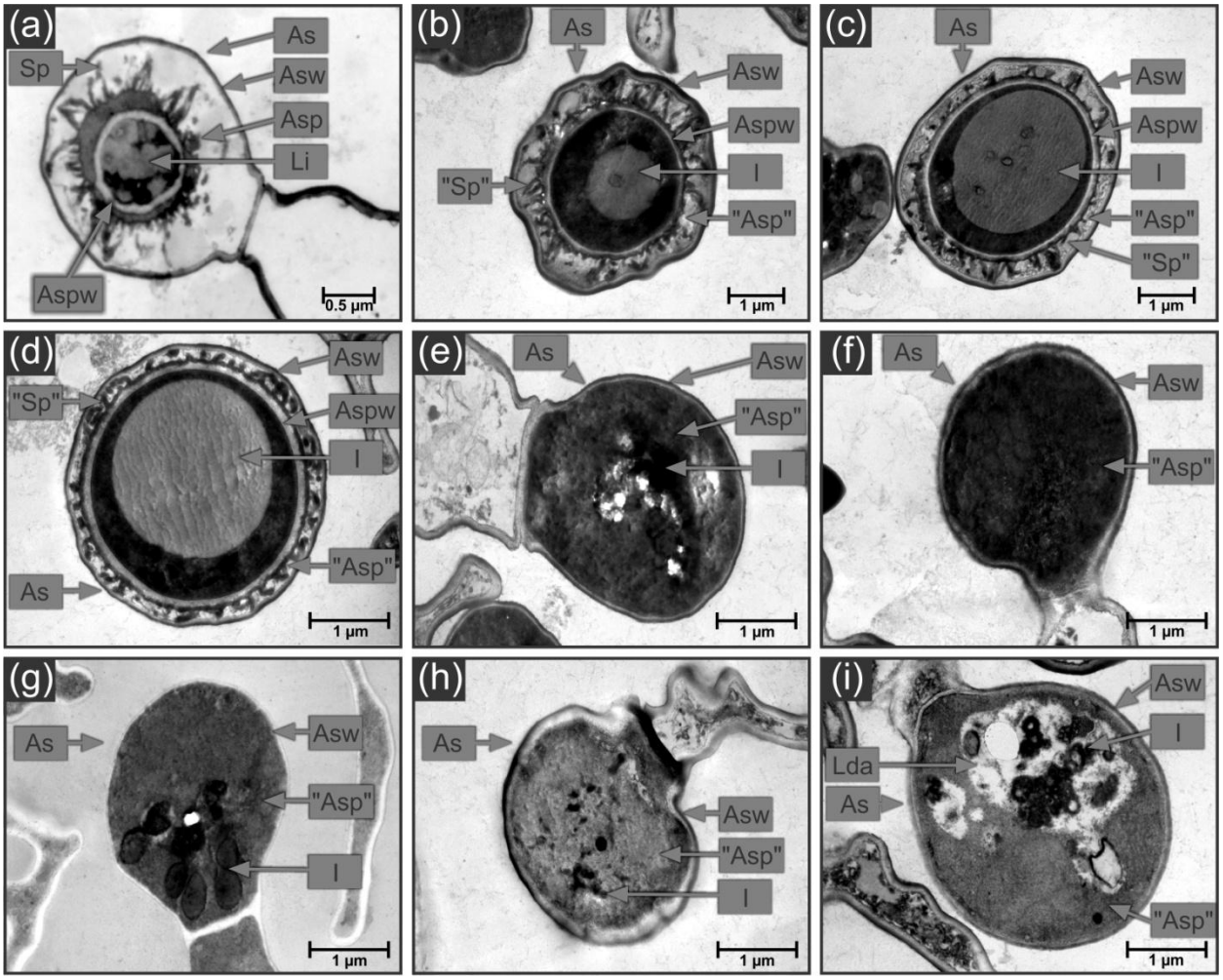

Figure 2 – Transmission electron microscopy micrographs indicating the various effects of fluconazole on ascospore development of *Nadsonia fulvescens*. (a), Ascus containing a single mature ascospore with spiky protuberances. (b - d), Ascospores that produced degenerated spiky protuberances with relatively large inclusions carried inside wrinkled asci. (e - h), Ascospores containing no walls or protuberances and enclosed within smooth spherical shaped asci. (i), Ascospore containing less dense hollow areas surrounded by cytoplasmic material. As = ascus; Asp = ascospore; “Asp” = malformed ascospore; Aspw = ascospore wall; Asw = ascus wall; I = inclusions; Lda = less dense area; Li = lipid inclusions; Sp = spiky protuberances; “Sp” = degenerated spiky protuberances.

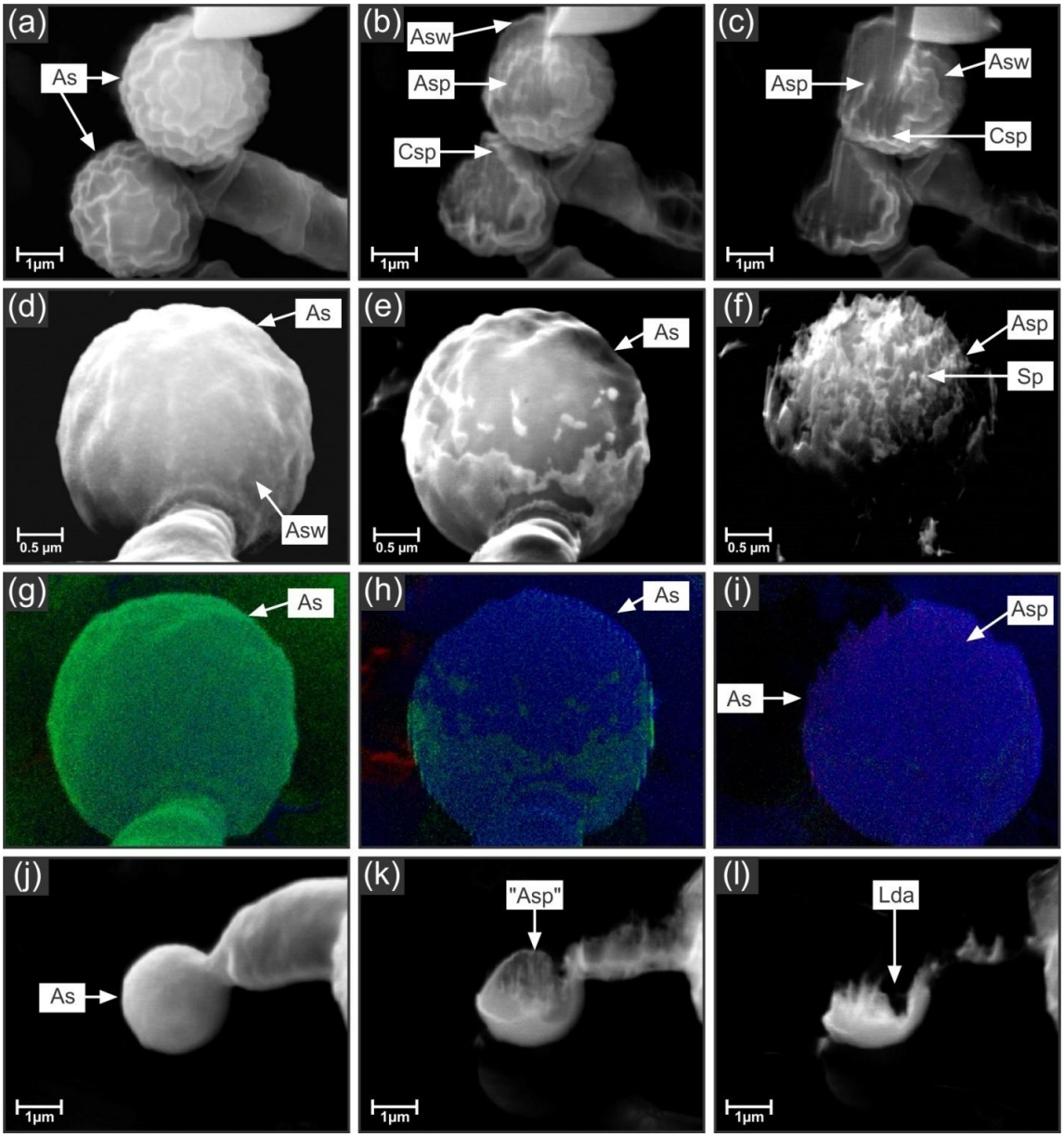

Figure 3 – Scanning electron microscopy (SEM) micrographs at different stages of sequential targeted etching into asci (As) of *Nadsonia fulvescens* developed in the presence of various concentrations of the antifungal fluconazole. (a - f), Sequential etching through spiky ascospores (Asp) within shrunken asci (As) from the brown zone. (g - i), Colour maps of the various elements present in the sample. These maps correspond to the etching micrographs (d - f). Blue – carbon (C), Green – gold (Au). (j - l), SEM micrographs at different stages of sequential targeted etching into asci (As) of *N. fulvescens* developed in the presence of higher concentrations of fluconazole indicating a less dense area (Lda) beneath the ascus wall. “Asp” = malformed ascospore; Asw = ascus wall; Csp = crunched spiky protuberances; Sp = spiky protuberance.

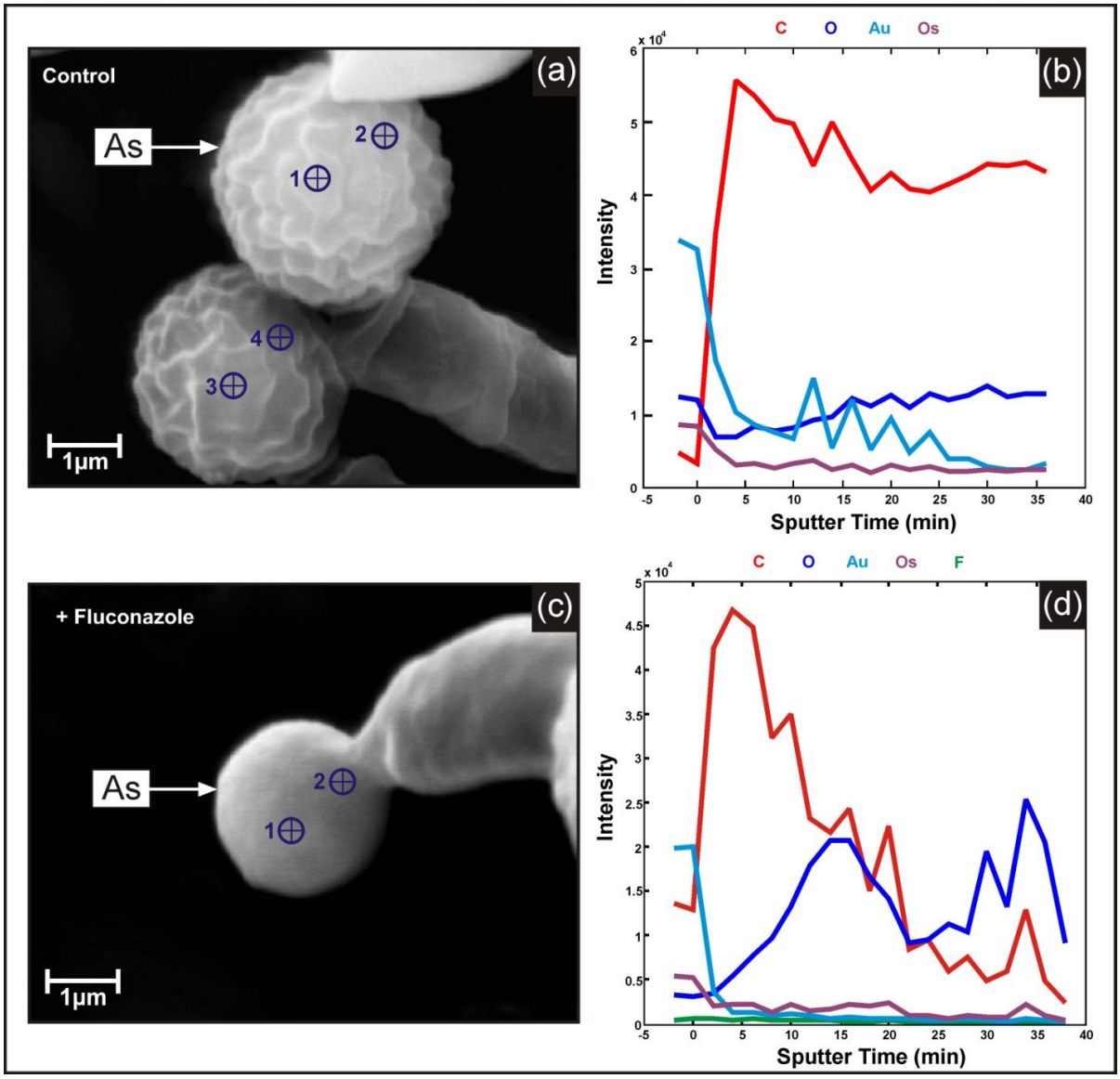

Figure 4 – Elemental analysis through asci (As) during sequential etching. (a), Scanning electron microscopy (SEM) micrographs of two asci from brown zone, each attached to a parental cell (Control). The targets for elemental analysis are indicated by crossed circles. (b), A graph showing elemental intensity over sputter time of control sample in (a) (Target 3). (c), SEM micrographs of a smooth walled fluconazole treated ascus attached to a parental cell from the white zone. The targets for elemental analysis are indicated as crossed circles. (d), A graph showing elemental intensity over sputter time of a fluconazole treated ascus from the white zone (Target 2).

Chapter 3

The influence of mitochondrial inhibitors on the life cycle of zoospore producing organisms: The oomycete *Phytophthora*

To be submitted for publication in SRE. (ISI-accredited, scientific journal)

Abstract

The Anti-mitochondrial Antifungal Hypothesis implies a link between mitochondrial activity, fungal fruiting structures and susceptibility towards mitochondrial inhibitors. Here it is shown that the oomycete, *Phytophthora nicotianae* fits the hypothesis. Fruiting structures (zoosporangia) of this oomycete showed increased beta (β)-oxidation when probing levels of 3-hydroxy fatty acids (3-OH oxylipins) with specific polyclonal antibodies. In addition, increased mitochondrial activity was also observed in the zoosporangia when the mitochondrial transmembrane potential ($\Delta\psi_m$) probe, Rhodamine 123 was added to the culture. This indicates increased mitochondrial activity in the zoosporangia when compared to the hyphae. When the anti-mitochondrial drug acetylsalicylic acid (ASA) was added to cultures of this oomycete, the zoosporangia were as expected most susceptible and were drastically inhibited in the presence of 1 mM of this compound. Similar ASA inhibition results were recorded for *P. citrophthora*. It is concluded that anti-mitochondrial compounds may find application in combating these devastating plant pathogens and that urgent further research is needed in this direction.

Key words: acetylsalicylic acid, antifungal, anti-mitochondrial, asci, *Phytophthora*, plant pathogen.

3.1. Introduction

In 2007, Kock and co-workers proposed the Acetylsalicylic acid (ASA) Antifungal Hypothesis, stating that the sexual stages in yeast life cycles have increased mitochondrial activity when compared to asexual vegetative stages. Increased mitochondrial activity was observed using different fluorescing probes to determine transmembrane potential ($\Delta\psi_m$), a polyclonal antibody to locate 3-hydroxy (OH) fatty acids [3-OH oxylipins from mitochondrial beta (β)-oxidation], as well as a monoclonal antibody (specific for prohibitin) to locate mitochondria. These results indicated that the sexual reproduction sites have increased mitochondrial activity when compared to asexual vegetative cells. This is to be expected since an increase in energy is probably needed to produce multiple ascospores inside the ascus. This phenomenon seems to be a conserved characteristic in most ascomycetous yeasts except in *Zygosaccharomyces* (Kock et al., 2007; Ncango et al., 2008; Swart et al., 2008).

Previous studies indicate the effect of mitochondrial inhibitors on the reproduction of yeasts (Kock et al., 2007; Swart et al., 2010). Here, it was observed that the sexual reproductive stage of yeasts is inhibited at relatively low concentrations by mitochondrial inhibitors, whereas asexual growth is inhibited at higher concentrations.

Based on the above mentioned studies, Kock and co-workers also investigated the possibility that this characteristic could be conserved amongst other fungi. They obtained positive results for fruiting structures (sporangia and phialide-conidia

structures) for various non-yeast fungi and fungi-like organisms including *Aspergillus*, *Mucor* and *Rhizopus*. Consequently they decided to expand the hypothesis (Leeuw et al., 2009; Ncango et al., 2010).

In this study two pathogenic species of the oomycete genus, *Phytophthora* were investigated to assess if they also fit the hypothesis. This group include the notorious destructive crop pathogens and is considered a distinct lineage of fungi-like eukaryotes that are related to organisms such as brown algae and diatoms. This group of pathogens has already caused worldwide crop losses of in access of $6.7billion (Alexopoulos, 1962; Brasier, 1992; Judelson, 1997; Haverkort et al., 2008; Haas et al., 2009).

3.2. Materials and Methods

Phytophthora species, including *P. nicotianae* and *P. citrophthora* were obtained from Dr. W.J. Botha, Agricultural Research Council – Plant Protection Research Institute (ARC-PPRI), Roodeplaat, South Africa, a specialist in oomycetous organisms.

3.2.1. Culturing

The organisms were first plated onto soft potato dextrose agar (PDA) plates (0.7 % m/v agar). From there, plugs were taken and placed in 20 mL sterile soilwater (soil extract). Round discs were cut from surface sterilised citrus leaves and placed in the soilwater to aid sporulation. The plates were then incubated at 21 ºC under near UV

and white light to aid sporulation. Following this, the cells were subjected to the following procedures:

3.2.2. Morphology studies

Cells from both the species were scraped from the leaves and the PDA agar plugs and viewed with an Olympus YX70 light microscope (Tokyo, Japan) to determine the morphological characteristics of these oomycetes.

3.2.3. Mitochondrial activity studies - mitochondrial products (3-OH oxylipins)

To determine if 3-OH oxylipins are also present and where they are mainly located, cells of *P. nicotianae* were subjected to the Oxytrack (fluorescing probe to track oxylipins) system as described by Kock et al. (1998). In short, cells from *P. nicotianae* were treated with a primary antibody specific for 3-OH oxylipins, washed with phosphate buffered saline (PBS; Oxoid, Hampshire, England) and further treated with a primary antibody-specific fluorescein isothiocyanate (FITC)-conjugated secondary antibody (Jackson Immunoresearch Laboratories, USA). Cells were washed again with PBS to remove the unbound secondary antibodies and then fixed on a microscope slide in Dabco (Sigma-Aldrich, USA) and viewed using a Nikon TE 2000, confocal laser scanning microscope (CLSM; Japan).

3.2.4. Mitochondrial activity studies - membrane potential ($\Delta\psi_m$)

To determine the mitochondrial $\Delta\psi_m$, cells of *P. nicotianae* were scraped from the citrus leaves and the PDA agar plugs and placed in a 2 mL plastic tube. Cells were then washed with PBS to get rid of agar and debris. Next, cells were treated with

Rhodamine 123 (Rh123; 31 µL per sample), a mitochondrial stain (Molecular Probes, Invitrogen Detection Technologies, Eugene, Oregon, USA), for 1 h in the dark at room temperature (21 ºC). Cells were washed again with PBS to remove excess stain and fixed on microscope slides in Dabco (Sigma-Aldrich, USA). Finally, cells were viewed with a Nikon TE 2000, CLSM.

3.2.5. Mitochondrial location

Since 3-OH oxylipins in yeasts are produced by β-oxidation in mitochondria (Kock et al., 2007), it was decided to map the distribution of these organelles in *P. nicotianae* as well. Cells were treated with a primary monoclonal antibody (Genway Biotech Inc., San Diego, USA) specific for mitochondrial prohibitin (30 µL for 1 h in the dark at room temperature) and then washed with PBS to remove unbound antibodies before further treatment with a FITC-conjugated secondary antibody (Jackson Immunoresearch Laboratories, USA), specific for the primary antibody, (30 µL for 1 h in the dark at room temperature). Cells were washed again with PBS to remove the unbound secondary antibodies. Staining was peformed in 2 mL plastic tubes in order to maintain cell structure. After washing, the cells were fixed in Dabco on a microscope slide and viewed using a Nikon TE 2000, CLSM.

3.2.6. Mitochondrial inhibition studies

The effects of ASA [a non-steroidal anti-inflammatory drug (NSAID) and anti-mitochondrial compound] on mitochondrial activity in cells of both *Phytophthora* species were assessed. The organisms were firstly plated onto PDA plates, from where plugs were taken and placed in 20 mL sterile soilwater. Round discs were cut from surface sterilised citrus leaves and placed in the soilwater to aid in sporulation.

Before incubation, ASA (8 % m/v ethanol; dissolved in 96 % ethanol) (ethanol obtained from Merck, Gauteng, South Africa) was added to the plates to a final concentration of 0.1 mM, 1 mM, 2.5 mM and 5 mM respectively. In addition, ethanol alone was tested as control (the same volume used to dissolve 5 mM of ASA). The plates were then incubated at 21 ºC under near UV and white light to aid in sporulation. Samples were taken at random from the growth surrounding the plugs and leaves and viewed with an Olympus YX70 light microscope. The number of full and empty zoosporangia were then counted in four randomly selected microscopic fields (n = 4) for each of the experimental plates (containing 0 mM, 0.1 mM, 1 mM, 2.5 mM and 5 mM ASA as well as the ethanol control) and the average and standard deviation calculated. Results were compared using the Student's *t*-test to determine if there is a significant difference between the results obtained. These experiments were done in triplicate.

3.3. Results and Discussion

Morphology studies: In *P. nicotianae*, characteristic hyphae as well as zoosporangia with zoospores could be observed with light microscopy (Figure 1a). The exit pore, where zoospores are usually released from, is clearly visible. Similar results were obtained for *P. citrophthora*.

Mitochondrial activity studies - mitochondrial products (3-OH oxylipins): Results obtained indicate an accumulation of 3-OH oxylipins situated in the exit pore of the zoosporangium (Figure 1b) from where the zoospores are released (indicated by the

intense green fluorescence) in *P. nicotianae*. A live video in CD format is attached at the end of the thesis showing a 3-dimensional (3-D) view of the 3-OH oxylipin coated fluorescing zoosporangium exit pore. This accumulation was not observed in the surrounding vegetative hyphae. The zoosporangium is empty, indicating that the zoospores have already been liberated (Figure 1b). Literature suggests that 3-OH oxylipins may act as lubricants during ascospore release through narrow bottleneck ascus openings in yeast (Kock et al., 2007). A similar phenomenon may be observed here, where the 3-OH oxylipins situated in this bottleneck or exit pore of the zoosporangium, probably act as lubricants to ensure the effective release of zoospores into the environment. On the other hand, this may also be 3-OH oxylipins that were scraped off in the narrow exit pore opening during zoospore release.

Mitochondrial activity studies - membrane potential ($\Delta\psi_m$): In *P. nicotianae*, an increase in mitochondrial $\Delta\psi_m$, indicated by the intense green fluorescence, was observed in the zoosporangium and not in the surrounding vegetative hyphae (Figure 1c). This indicates that an increase in mitochondrial activity is probably needed to produce multiple zoospores in the zoosporangium. Interestingly, the mitochondrial $\Delta\psi_m$ was very intense at the exit pore – the position where 3-OH oxylipins accumulated. Here the same trend is observed as previously reported for yeasts (Kock et al., 2007), where there was an increase in $\Delta\psi_m$ associated with the sexual phase.

Mitochondrial location: Since the results indicate an increase in mitochondrial activity i.e. increased $\Delta\psi_m$ as well as increased β-oxidation (3-OH oxylipin production) in the zoosporangium, the accumulation of mitochondria in this location was not surprising.

According to CLSM results, mitochondria are situated mostly in the zoosporangium surrounding the zoospores of *P. nicotianae* as indicated by an increase in green fluorescence (Figure 1d). In the surrounding hyphae the mitochondria are less, as indicated by very little green fluorescence (Figure 1d). This is probably due to the fact that a higher number of mitochondria (to produce necessary energy) are needed for the production of multiple zoospores inside the zoosporangium. Similar results have been obtained with various other fungi and fungi-like organisms where the fruiting structures (i.e. sexual phase, phialide-conidia complex and sporangia) showed increased mitochondria populations (Leeuw et al., 2009; Ncango et al., 2010).

Effects of acetylsalicylic acid on growth: Macroscopically, growth was visible around the plugs and leaves in the control (Figure 2a) and ethanol control plates (Figure 2b). However, a drastic decrease in growth was observed in the presence of 1 mM ASA (Figure 2c) while in the presence of 5 mM ASA (Figure 2d), no growth could be observed. These inhibitory effects can be attributed to the presence of ASA since in the ethanol control (ethanol concentration same as with 5mM ASA culture) good growth was also observed. These experiments were performed in triplicate and reproducible observations were recorded. Biomass measurement was not possible in these experiments due to the extremely small amount of growth and difficulty to separate these from agar plugs and leave discs.

Mitochondrial inhibition studies: Previous studies indicated that sites with increased mitochondrial activity (fruiting structures such as sexual stages, phialide-conidia-complex and sporangia) are more susceptible to mitochondrial inhibitors such as

ASA. It was confirmed in this study that fruiting structures i.e. zoosporangia of *Phytophthora* are also more susceptible to ASA at low concentrations, than hyphal growth (Table 1). A significant difference was observed between the number of zoosporangia in the control plates (0 mM ASA; Figure 3a) and the plate containing 0.1 mM ASA ($P < 0.001$) although good growth could be observed in both cases (Figure 3b). This indicates that the fruiting structure or zoosporangium is more sensitive towards this antifungal at low concentrations, than the vegetative hyphae. There was no significant difference between the number of zoosporangia and growth in the control (0 mM ASA) and the ethanol control (contains the same amount of ethanol needed to dissolve 5 mM of ASA) indicating that ethanol does not have an inhibitory effect on zoosporangium formation. No zoosporangia were observed in the plates containing 1 mM – 5 mM ASA. The plate containing 1 mM of ASA had impaired hyphal growth, with the hyphae being misformed and showing unusual nodules. No growth could be observed in the presence of 2.5 mM and 5 mM ASA. This pattern is also demonstrated in Figure 3 (a - d). Similar results were obtained with *P. citrophthora*.

3.4. Conclusions

The genus *Phytophthora* is a very large group of fungi-like organisms, including aquatic, amphibious and terrestrial species. The oomycetes consist of organisms that reproduce asexually by means of biflagellate zoospores. These spores are contained in zoosporangia of various types. Sexual reproduction is rare and almost always heterogametangic. Members of *Phytophthora* bear their zoosporangia

directly on the somatic hyphae and the presence of zoosporangia of different ages can be observed on the same sporangiophore at any given time (Alexopoulos, 1962; Brasier, 1992; Judelson, 1997; Schumann and D'Arcy, 2000). It is important to note that zoospores (asexual reproduction) are mainly responsible for infecting plants. Consequently, the release of zoospores from the zoosporangium could be referred to as one of the main infectious stages.

Results from this study implicate novel targets by which *Phytophthora* infections may be inhibited. These findings necessitate urgent investigations into more oomycete representatives and assessing various anti-mitochondrials including NSAIDs as anti-oomycetous compounds. Who knows, these may prove in future to be effective in field applications.

To conclude, *P. nicotianae* displays an increase in mitochondrial activity associated with the zoosporangia and zoospores. This could be observed in mitochondrial distribution studies, mitochondrial $\Delta\psi_m$ determination as well as the location of mitochondrial β-oxidation products (3-OH oxylipins). These oxylipins may play a role in the release of the zoospores from the zoosporangium exit pore by acting as a lubricant. *Phytophthora* does therefore fit the ASA Antifungal Hypothesis (i.e. fruiting structures such as zoosporangia and yeast sexual phases reacts similar to ASA; Kock et al., 2007), indicating that this phenomenon is widely conserved in the fungal domain as well as distantly related organisms. The infectious stage of both *Phytophthora* species tested in this study was found to be more sensitive towards ASA than the growth phases suggesting ASA as a possible agent to combat this notorious group of plant pathogens. Detailed biochemical studies should now be

performed on mitochondria to identify the type of mitochondrial inhibition exerted by different anti-mitochondrial drugs.

3.5. Acknowledgements

The authors wish to thank the South African National Research Foundation (NRF) Blue Skies Research Programme (BS2008092300002) as well as SAFOI for financial support.

3.6. References

Alexopoulos CJ (1962). Introductory Mycology. Second Edition. John Wiley and Sons, Inc., USA, Toppan Company, LTD., Japan.

Brasier CM (1992). Evolutionary biology of *Phytophthora*: Genetic system, sexuality and the generation of variation. Ann. Rev. Phytopath. 30: 153 – 171.

Haas BJ, Kamoun S, Zody MC et al. (2009). Genome sequence and analysis of the Irish potato famine pathogen *Phytophthora infestans*. Nature 461(17): 393 – 398.

Haverkort AJ, Boonekamp PM, Hutten R, Jacobsen E, Lotz LAP, Kessel GJT, Visser RGF, Van der Vossen EAG (2008). Societal costs of late blight in potato and prospects of durable resistance through cisgenic modification. Potato Res. 51: 47 – 57.

Judelson HS (1997). The genetics and biology of *Phytophthora infestans*: Modern approaches to a historical challenge. Fungal Genet. Biol. 22: 65 – 76.

Kock JLF, Venter P, Linke D, Schewe T, Nigam S (1998). Biological dynamics and distribution of 3-hydroxy fatty acids in the yeast *Dipodascopsis uninucleata* as investigated by immunofluorescence microscopy. Evidence for a putative regulatory role in the sexual reproductive cycle. FEBS Lett. 472: 345 – 348.

Kock JLF, Sebolai OM, Pohl CH, Van Wyk PWJ, Lodolo EJ (2007). Oxylipin studies expose aspirin as antifungal. FEMS Yeast Res. 7: 1207 – 1217.

Leeuw NJ, Swart CW, Ncango DM, Kriel WM, Pohl CH, Van Wyk PWJ, Kock JL (2009). Anti-inflammatory drugs selectively target sporangium development in *Mucor*. Can. J. Microbiol. 55(12): 1392 – 1396.

Ncango DM, Swart CW, Goldblatt ME, Pohl CH, Van Wyk PWJ, Botes PJ, Kock JLF (2008). Oxylipin and mitochondrion probes to track yeast sexual cells. Can. J. Microbiol. 54(6): 450 – 455.

Ncango DM, Swart CW, Pohl CH, Van Wyk PWJ, Kock JLF (2010). Mitochondrion activity and dispersal of *Aspergillus fumigatus* and *Rhizopus oryzae*. Afr. J. Microbiol. Res. 4(9): 830 – 835.

Schumann GL, D'Arcy CJ (2000). Late blight of potato and tomato. The Plant Health Instructor. DOI: 10.1094/PHI-I-2000-0724-01.

Swart CW, Van Wyk PWJ, Pohl CH, Kock JLF (2008). Variation in yeast mitochondrial activity associated with asci. Can. J. Microbiol. 54(7): 532 – 536.

Swart CW, Van Wyk PWJ, Pohl CH, Kock JLF (2010). Variation in mitochondrial activity over the life cycle of *Nadsonia fulvescens*. Afr. J. Microbiol. Res. 4(16): 1727 – 1732.

Table 1: The influence of acetylsalicylic acid (ASA) concentration on zoosporangium formation by *Phytophthora nicotianae*.

ASA concentration	Number of zoosporangia				Average	SD
	Field #1	Field #2	Field #3	Field #4		
0 mM	72	65	80	67	71	6.7
0.1 mM	15	4	3	2	6	6.1
1 mM	0	0	0	0	-	-
2.5 mM	0	0	0	0	-	-
5 mM	0	0	0	0	-	-
Ethanol control	65	69	64	70	67	2.9

SD = standard deviation; Fields #1 - #4 = Microscopic fields selected at random around discs and plugs.

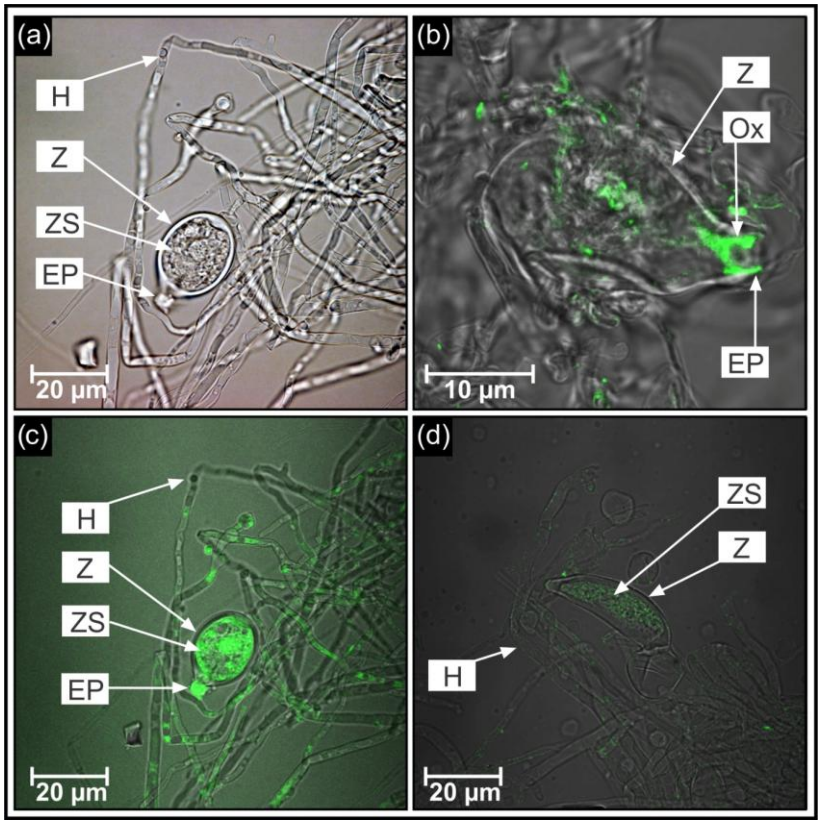

Figure 1 – (a), A light micrograph indicating vegetative hyphae (H) and a zoosporangium (Z), containing zoospores (ZS) of *Phytophthora nicotianae*. The exit pore (EP) where the zoospores are released can also be observed. (b), An empty zoosporangium (Z) surrounded by vegetative hyphae. Here, 3-hydroxy (OH) oxylipins (Ox; indicated by the green fluorescence) can be observed covering the exit pore of the zoosporangium where the zoospores are released. These compounds probably act as a lubricant to ensure the effective release of the zoospores through the narrow opening in the zoosporangium. (c), A confocal laser scanning micrograph indicating again the vegetative hyphae (H) and a zoosporangium (Z) with zoospores (ZS). Here we can see an increase in mitochondrial membrane potential ($\Delta\psi_m$; indicated by the green fluorescence), as determined by Rhodamine 123 staining, associated with the zoospores inside the zoosporangium. This drastic increase in mitochondrial activity is not observed in the surrounding hyphae. (d), A confocal laser scanning micrograph indicating an increase in the number of mitochondria (determined using a monoclonal antibody specific for prohibitin in the mitochondria; indicated by the green fluorescence) in the zoosporangium (Z) containing zoospores (ZS). This increase could not be observed in the surrounding hyphae (H).

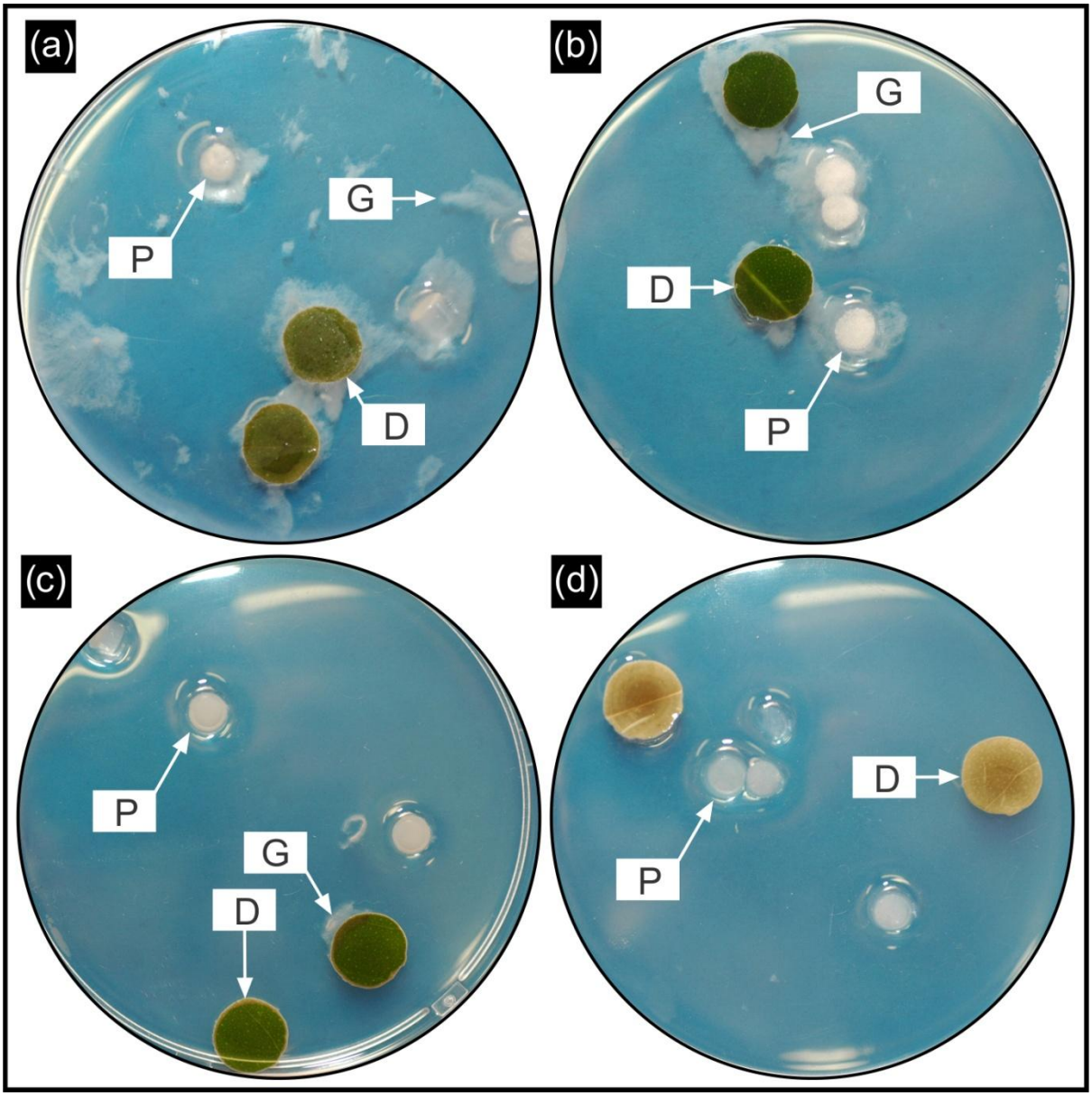

Figure 2 – Photographs of plates containing *Phytophthora nicotianae* on soft potato dextrose agar (PDA) plugs and discs of surface sterilized citrus leaves. (a), Control plate containing only the organism on plugs (P) as well as citrus discs (D). Here good growth (G) could be observed around the plugs as well as discs. (b), Ethanol control plate containing the same amount of ethanol used to dissolve 5 mM of acetylsalicylic acid (ASA). Here good growth was also observed around the plugs as well as the discs, indicating that ethanol has no inhibitory effect on the growth of this organism. (c), A plate containing 1 mM of ASA. In this case a drastic decrease in growth could be observed, with only little growth around the disc. (d), A plate containing 5 mM of ASA. Here no growth could be observed around the plugs or discs, demonstrating the effect that ASA has on the growth of this organism.

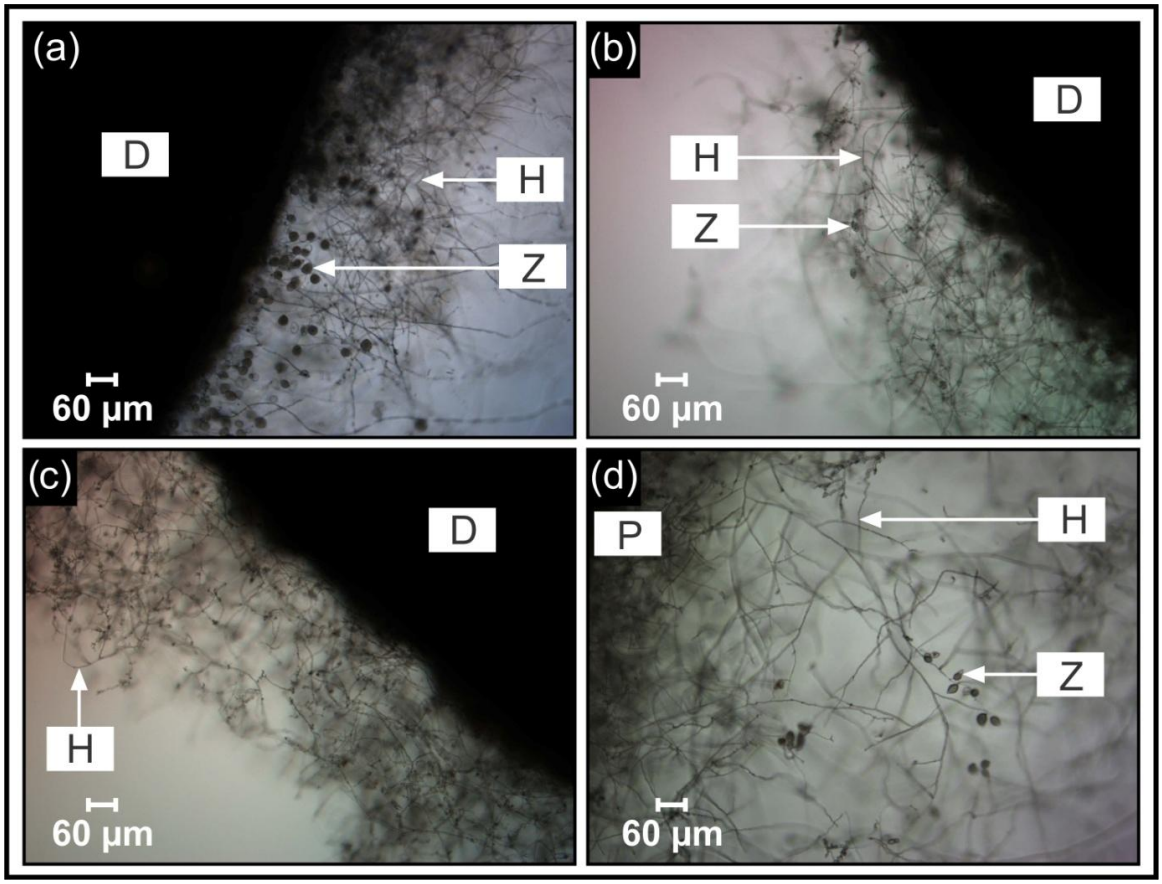

Figure 3 – (a), Light micrograph of growth of *Phytophthora nicotianae* obtained from the control plate that contains no acetylsalicylic acid (ASA). Here, good hyphal (H) growth as well as a vast number of full and empty zoosporangia (Z) could be observed. (b), A drastic decrease in zoosporangia in the plate containing 0.1 mM of ASA could be observed in this light micrograph, yet good hyphal growth was evident. (c), Light micrograph of growth obtained from the plate containing 1 mM of ASA. In this case impaired hyphal growth, with the hyphae being misformed and showing unusual nodules, could be observed. In this plate no zoosporangia could be observed, indicating that the fruiting structure has increased susceptibility towards ASA when compared to hyphae. (d), Light micrograph of growth obtained from the plate containing only ethanol. Here, hyphal growth and zoosporangium production were similar to the control, indicating that ethanol did not influence the results obtained. These results are similar to that shown in Table 1. D = leave discs; P = plugs.

Chapter 4

Main Conclusions

The main conclusions are hereby presented as synthesised from the previous chapters of this Ph.D. study. **Parts of this work are in the process of being submitted on invitation to the highly accredited journal: Expert Opinion on Drug Discovery.**

4.1. Expanding the ASA Antifungal Hypothesis

Since the discovery of acetylsalicylic acid (ASA)-sensitive oxylipins in yeast, this field of research has expanded significantly resulting in the ASA Antifungal Hypothesis (Kock et al., 2007). This hypothesis has recently been extended to also include the mould *Aspergillus* and some representatives of the Mucorales (Leeuw et al., 2009; Ncango et al., 2010). As a result of this Ph.D. study, the hypothesis now also include the notorious oomycetous pathogens of *Phytophthora*. *Nadsonia fulvescens* can also be included in this hypothesis, especially if the mother cell with attached first bud be regarded as part of the sexual phase. This phenomenon is partly similar to that found for the yeast *Pichia farinosa* (Swart et al., 2008) characterised by only mother-daughter-cell conjugation. The latter forms the ascus characterised by increased mitochondrial activity and higher susceptibility towards mitochondrial inhibitors.

Fruiting dispersal structures characterised by active cell proliferation such as found in most sexual phases in yeasts, fungi with active phialide-conidia development in *Aspergillus*, sporangia of *Mucor* as well as zoosporangia of *Phytophthora* showed increased mitochondrial activity and increased sensitivity towards various mitochondrial inhibitors. This hypothesis now suggests that mitochondrial inhibitors

including various non-steroidal anti-inflammatory drugs (NSAIDs) may be used as novel antifungals targeting mitochondrial activity and therefore dispersal fruiting structures of a wide array of fungi, fungi-like organisms and a distantly related oomycete (Figure 1).

4.2. Developing yeast bio-assays from the Hypothesis

In 2009, the ASA Antifungal Hypothesis aided in the development of an *in vivo* anti-mitochondrial yeast bio-assay, capable of screening mitochondrial inhibitors (Kock et al., 2009). The construction of this bio-assay was mainly based on studies performed on the yeast *Eremothecium ashbyii* that served as indicator organism. Since various anti-mitochondrial compounds have been tested, the hypothesis can now be named the Anti-mitochondrial Antifungal Hypothesis (Figure 1).

In this Ph.D. study a second yeast anti-mitochondrial antifungal assay, by applying the yeast *N. fulvescens* as indicator organism, was developed. In this case the sexual fruiting stage is brown coloured while the vegetative stage with immature sexual fruiting structures is white. Under normal growth conditions all colonies eventually colour brown due to the development of amber (melanin) stained sexual spores. Therefore, when applying this assay to screen compounds for anti-mitochondrial activity, the development of white yeast colonies indicates a positive outcome [Chapter 2; 2.1., Figure 3]. As observed in the *Eremothecium* bio-assay, it is also possible to test many compounds at a time to assist High Throughput Screening (HTS) by directly adding them onto many agar surfaces in small wells

followed by incubation. Even compound crystals, if water soluble, may be added directly onto agar surfaces.

When fluconazole was tested for anti-mitochondrial activity in the *Nadsonia* bio-assay [Chapter 2; 2.1., Figure 3], interesting results were obtained. Here, the most susceptible part of the *Nadsonia* bio-assay towards this azole was the brown coloured sexual fruiting stage [minimum inhibition concentration (MIC) = 0.3µg/mL] and not the growth phase (MIC = 3µg/mL). This is contrary to expectations since the target for this azole is generally accepted to be the synthesis of membrane sterols thereby inhibiting cell growth (Odds, 2003). Research concerned with exposing possible new targets and mitochondrial toxicity of this important antifungal drug should now be performed.

4.3. The value of the yeast bio-assays

The effectiveness of these yeast bio-assays were demonstrated by comparing results to that obtained for the Food and Drug Administration (FDA) Black Box Warnings (Dykens and Will, 2007). A good correlation was found between compounds that tested positive for anti-mitochondrial action, using the fungal bio-assays and those that obtained Black Box Warnings by the FDA with mitochondrial liabilities. However, some NSAIDs such as Diflunisal and Fenoprofen tested positive with the fungal anti-mitochondrial bio-assay but negative for Black Box Warning with mitochondrial toxicity. These NSAIDs however were reported to be anti-mitochondrial in other literature (Chan et al., 2005). All drugs that received Black Box

Warnings with and without mitochondrial liabilities should be tested with the fungal anti-mitochondrial antifungal bio-assays and the corresponding MICs determined.

4.4. Application of a new nanotechnology to biology

In this Ph.D. study, the successful application of nano scanning Auger microscopy (NanoSAM) to fluconazole treated fungal cells opens up a new field in biological and medical research where 3-dimensional (3-D) ultrastructure and elemental composition of all types of cells can now be determined on nano-scale while being etched in nanometre “slices” by argon (Ar^+).

With this nanotechnology, scanning electron microscopy (SEM) as well as elemental analysis is performed. The possibility now exists to map cell inclusions in 3-D mode and compare cells that have been exposed to different environmental conditions on the basis of elemental composition and structure. This nanotechnology may find application in investigating drug chemical quality as well as various cell types (include fungal, mammalian cells, etc.) subjected to compounds such as antimicrobials, anticancer drugs and others showing cell toxicity, to mention only a few. Even the distribution of anti-mitochondrial drugs within cells may be quantified.

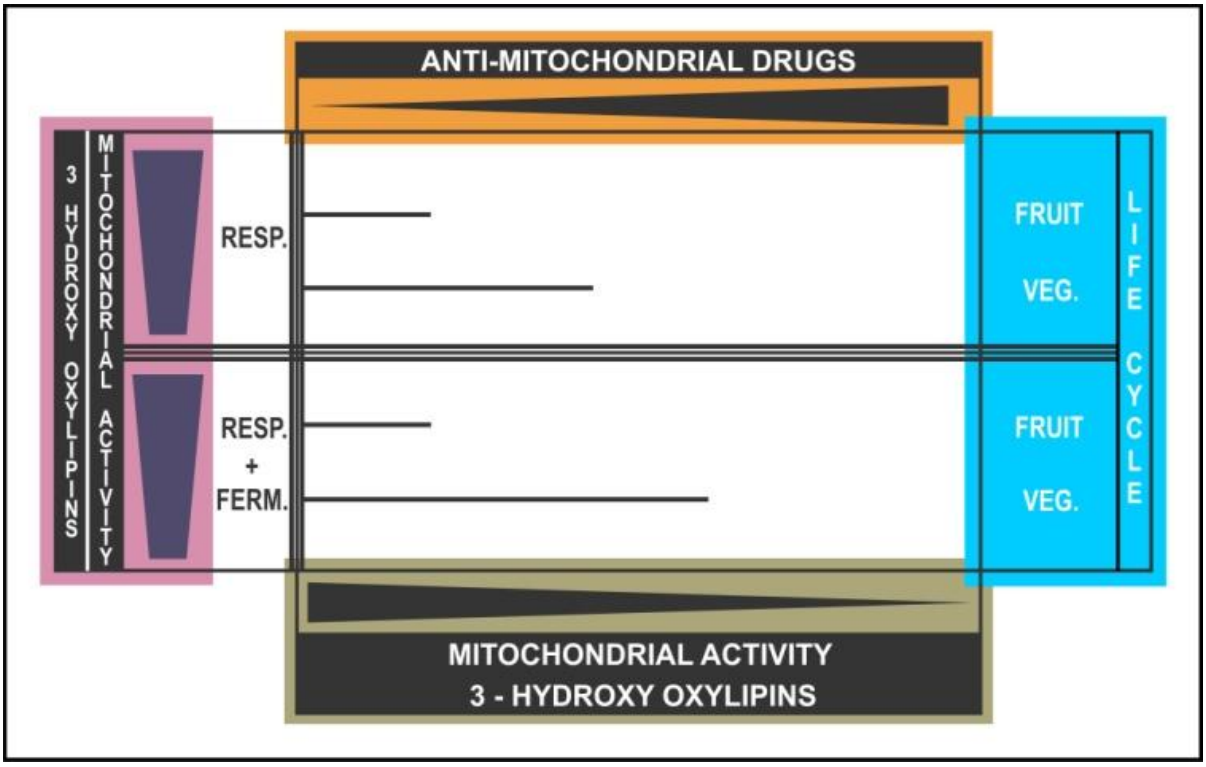

Figure 1 – A schematic representation of the expanded Anti-mitochondrial Antifungal Hypothesis. This suggests a possible link between mitochondrial 3-hydroxy (OH) oxylipin production, mitochondrial activity and anti-mitochondrial sensitivity. X-axis, top: increase in anti-mitochondrial drug concentration from left to right. X-axis, bottom: decrease in mitochondrial activity and 3-OH oxylipin levels from left to right. Y-axis, left: decrease in mitochondrial activity and 3-OH oxylipin levels from high proliferation stage (FRUIT) to low proliferation vegetative growth (VEG.) phases in both strictly aerobic fungi/fungi-like (RESP.) and fungi/fungi-like with both aerobic and fermentative pathways (RESP. + FERM.). Y-axis, right: different phases of fungal/fungi-like life cycles. Middle block: response surface showing the relative sensitivities of different fungal/fungi-like phases towards increasing levels of anti-mitochondrials. Fungi and fungi-like refers to yeasts, moulds, zygomycetes and oomycetes.

4.5. References

Chan K, Truong D, Shangari N, O'Brien PJ (2005). Drug-induced mitochondrial toxicity. Expert Opin. Drug Metab. Toxicol. 1(4): 655 – 669.

Dykens JA, Will Y (2007). The significance of mitochondrial toxicity testing in drug development. Drug. Discov. Today 12(17/18): 777 – 785.

Kock JLF, Sebolai OM, Pohl CH, Van Wyk PWJ, Lodolo EJ (2007). Oxylipin studies expose aspirin as antifungal. FEMS Yeast Res. 7: 1207 – 1217.

Kock JLF, Swart CW, Ncango DM, Kock (Jr) JLF, Munnik IA, Maartens MMJ, Pohl CH, Van Wyk PWJ (2009). Development of a yeast bio-assay to screen anti-mitochondrial drugs. Curr. Drug. Disc. Technol. 6(3): 186 – 191.

Leeuw NJ, Swart CW, Joseph M, Pohl CH, van Wyk PWJ, Coetsee E, Swart HC, Hugo A, Kock JLF (2009). Anti-inflammatory drugs selectively target sporangium development in *Mucor*. Can. J. Microbiol. 55(12): 1392 – 1396.

Ncango DM, Swart CW, Pohl CH, Van Wyk PWJ, Kock JLF (2010). Mitochondrion activity and dispersal of *Aspergillus fumigatus* and *Rhizopus oryzae*. Afr. J. Microbiol. Res. 4(9): 830 – 835.

Odds FC (2003). Antifungal agents: their diversity and increasing sophistication. Mycologist 17(2): 351 – 355.

Swart CW, Van Wyk PWJ, Pohl CH, Kock JLF (2008). Variation in yeast mitochondrial activity associated with asci. Can. J. Microbiol. 54(7): 532 – 536.

Appendix

Expanded and detailed layout of the materials and methods referred to as abbreviated in Chapters 2 and 3 due to publication restrictions. Methods 1 – 4.1 have been adapted from Strauss (2005) with permission.

1. Synthesis of 3-hydroxy (OH) oxylipins and antibodies

(Performed by research groups of Prof. S. Nigam and Prof. J.L.F. Kock)

For antibody preparation, the oxylipin 3-hydroxy-5, 8, 11, 14,-eicosatetraenoic acid (3-HETE) was chemically synthesized. Synthesis of 3*R* and 3*S* hydroxyl arachidonic acid (AA) included a convergent approach where a chiral aldehyde molecule was coupled to a Wittig salt (Bhatt et al., 1998; Groza et al., 2002). These compounds are derivatives of 2-deoxy-D-ribose and AA respectively. Rabbits were used to raise antibodies against 3-HETE as follows: The carboxyl group of 3*R*-HETE was conjugated to amino groups of bovine serum albumin (BSA) via the N-succinimidyl ester method. With the first injection, 1 mg of the latter conjugated protein was emulsified in an equal volume of Freund's complete adjuvant. The following further injections were performed with an incomplete adjuvant. Next, a female New Zealand white rabbit was subcutaneously injected in its back every second week with this emulsion. This was continued for about a further 3 months. After treatment the blood was collected from the carotid artery, left for 2 h at room temperature (21 ºC) and centrifuged at 1200 *g* for 20 min at 4 ºC. As a final step, the serum was purified by Biogenes, Berlin (Kock et al., 1998).

2. Preparation and characterization of the antibody

(Performed by research groups of Prof. S. Nigam and Prof. J.L.F. Kock)

The titer, sensitivity and specificity of above antibody were characterized (Kock et al., 1998). First a biological tracer was prepared in small amounts by the biotransformation of [^{14}C]-AA to [^{14}C]-3-HETE using the yeast *Dipodascopsis uninucleata*. Next the radio labelled [^{14}C]-3-HETE was purified using Radio High Performance Liquid Chromatography (HPLC). The antibody titer resulted in approximately 30 % labelled 3-HETE at a dilution of 1:1000 in the absence of unlabelled 3-HETE. The sensitivity (minimum detectable amount) of 3-HETE was 30 pmol. This was determined by 10 % displacement of radioactivity by unlabelled 3-HETE from the zero point. Finally the specificity of the antibody was analysed, using various structurally related compounds to determine the possible cross-reactions with the antibody. The antibody cross-reacted < 0.5 % with 5-, 12-, or 15-HETE, while significant cross reactivity was observed against other 3-hydroxy (OH) oxylipins of different chain lengths and degrees of desaturation. Free fatty acids evoked no immunoreactivity. Thus, in our studies immunoreactivity solely indicates the presence of 3-OH oxylipins.

3. Identification and analysis of 3-hydroxy (OH) oxylipins

(Performed by candidate: C.W. Swart)

Cells of *Nadsonia fulvescens* were scraped from white and brown zones respectively (white and brown zones obtained on petri dishes with the addition of mitochondrial inhibitors as discussed in Chapter 2; 2.1.). The cells were then suspended in 100 mL distilled water (dH_2O) and the pH decreased to 3.8 using 3 % formic acid (Merck, Darmstadt, Germany). Next, oxylipins were extracted and then dissolved in 2x volumes of ethyl acetate (Merck, Darmstadt, Germany). After the organic and water phases have separated, the organic phase was evaporated with N_2 gas (AFROX, Bloemfontein, South Africa). This was followed by derivatizing (methylating and silylating) of the extracts which were finally dissolved in 400 µL chloroform:hexane (4:1) (Merck, Darmstadt, Germany) mixtures. All experiments were performed in at least duplicate. Derivatized samples from the white and brown zones respectively were injected into a Finnigan Trace GC Ultra gas chromatograph (Thermo Electron Corporation, San Jose, Calif., USA) with a HP5 (60 m x 0.32 mm diameter) fused silica capillary column (0.1 µm coating thickness) coupled to a Finnigan Trace DSQ mass spectrometer (Thermo Electron Corporation, San Jose, Calif., USA). The carrier gas was helium at 1.0 mL/min. The initial oven temperature of 110 ºC was maintained for 2 min then increased to a final temperature of 280 ºC at a rate of 5 ºC/min. The gas chromatography – mass spectrometer (GC-MS) was auto-tuned for an *m/z* of 50 - 400. One µL of the sample was injected into the GC-MS at a split ratio of 1:50 at an inlet temperature of 230 ºC (Venter et al., 1997).

4. Confocal Laser Scanning Microscopy (CLSM)

(Performed by candidate: C.W. Swart)

4.1. Immunofluorescence studies (3-OH oxylipin distribution)

Immunofluorescence studies were performed on cells of *N. fulvescens* as well as *Phytophthora nicotianae* using a method described by Kock et al. (1998). In order to maintain cell structure, these experiments were performed in 2 mL plastic tubes. Cells were harvested and a very small amount of these cells obtained from the two organisms, were suspended in phosphate buffered saline (PBS; Oxoid, Hampshire, England) and centrifuged to wash the cells. These cells were then treated with 30 µL (1:2 v/v) of the primary antibody specific for 3-OH oxylipins (1 h in the dark at room temperature; 21 ºC). After adequate washing with PBS, 30 µL (1:2 v/v) of fluorescein isothiocyanate (FITC)-conjugated Affinipure Goat Anti-Rabbit IgG (Jackson Immunoresearch Laboratories, USA) was added and incubated for 1 h in the dark at room temperature (21 ºC). Next, the cells were again washed and there after mounted in Dabco (Sigma-Aldrich, USA) on a microscope slide. Dabco, a free radical scavenger, assists to sustain fluorescence. Fluorescing material was photographed using a Nikon TE 2000, confocal laser scanning microscope (CLSM; Japan).

4.2. Monoclonal antibody fluorescence studies (Mitochondrial location)

A small amount of cells from *N. fulvescens* and *P. nicotianae* were placed in 2 mL plastic tubes respectively, to retain cell structure. These cells were then treated with

a primary monoclonal antibody (Genway Biotech Inc., San Diego, USA) specific for prohibitin in the mitochondria (30 µL for 1 h in the dark at room temperature; 21 ºC). Cells were then washed with PBS to remove unbound antibodies and further treated with a FITC-conjugated secondary antibody (Jackson Immunoresearch Laboratories, USA), specific for the primary antibody (30 µL for 1 h in the dark at room temperature; 21 ºC). Cells were washed again with PBS to remove the unbound secondary antibodies. After washing, the cells were fixed in Dabco (Sigma-Aldrich, USA) on a microscope slide and viewed using a Nikon TE 2000, CLSM (Japan).

4.3. Mitochondrial membrane potential determination (fluorescing dye: Rhodamine 123)

A small amount of cells from *N. fulvescens* (obtained from the white and brown zones as discussed in Chapter 2; 2.1.) and *P. nicotianae* were collected and placed in 2 mL plastic tubes respectively, to retain cell structure. The cells were then washed with PBS to get rid of agar and debris. Next, cells were treated with Rhodamine 123 (Rh123; 31 µL per sample), a mitochondrial stain (Molecular Probes, Invitrogen Detection Technologies, Eugene, Oregon, USA), for 1 h in the dark at room temperature (21 ºC). Here after cells were washed again with PBS to remove excess stain and fixed on microscope slides in Dabco (Sigma-Aldrich, USA). Finally, cells were viewed and photographed with a CLSM (Nikon TE 2000, Japan).

5. Scanning Electron Microscopy (SEM)

(Performed by candidate: C.W. Swart)

Cells of *N. fulvescens* were scraped from white and brown zones (obtained on a petri dish when adding mitochondrial inhibitors, as discussed in Chapter 2; 2.1.) respectively and prepared for scanning electron microscopy (SEM) using the method described by Van Wyk and Wingfield (1991). The mentioned cells were fixed with equal amounts of buffered 3 % (v/v; 0.1 mol/L) glutardialdehyde (Merck, Darmstadt, Germany) in a 0.1 M sodium phosphate buffer for 3 h. The suspension was then rinsed with the same buffer to remove excess aldehyde fixative and post-fixation was performed with 1 % (v/v) buffered osmium tetroxide (Merck, Darmstadt, Germany) for 1.5 h. After fixation the suspension was washed with the above mentioned buffer to remove excess osmium tetroxide. Dehydration by a graded ethanol sequence 50 %, 70 %, 95 % and 100 % (x2) for 30 min per step followed, while centrifugation took place between each dehydration step. Drying was performed by using a critical point dryer, where after the specimens were mounted on stubs, coated with gold and viewed with SEM (Shimadzu SSX-550 Superscan, Tokyo, Japan) at 5 kV.

6. Transmission Electron Microscopy (TEM)

(Performed by candidate: C.W. Swart)

Transmission electron microscopy (TEM) was performed according to the method of Van Wyk and Wingfield (1991). Cell material for TEM was firstly chemically fixed using 3 % (v/v) glutardialdehyde (3 h) and 0.5 % (v/v) osmiumtetroxide (1.5 h) in a 0.1 M sodium phosphate buffer. Following fixation the cells were rinsed with the same buffer and dehydrated using an acetone gradient (50 %, 70 %, 95 % and 100 % x2 for 30 min per step). The material was then impregnated in epoxy resin (Spurr, 1969) and set in gelatine capsules. The cells embedded in epoxy were polymerized at 70 ºC in an oven for 8 hours. After this polymerization step, ultramicrotomy was performed with a LKB Ultratome III (Sweden). The ultra-thin sections (60 nm) were collected on 200 mesh Formvar copper coated grids. These sections were finally stained with a saturated solution of uranyl acetate (6 % m/v) for 10 min and lead citrate for 10 min (Reynolds, 1963). Transmission electron micrographs were taken with a Philips CM 100 TEM (Eindhoven, The Netherlands).

7. *Phytophthora* cultivation

(Performed by candidate: C.W. Swart)

In order to induce sporulation, *Phytophthora* was grown in soil extract in sterile petri dishes. The soil extract was prepared by adding 20 g of sand to 1 L of dH_2O. This mixture was then filtered and the filtrate autoclaved. Following this, 20 mL of the soil

extract was added to sterile petri dishes. Plugs of potato dextrose agar (PDA) containing growth were placed in the soil extract along with round discs cut from surface sterilized citrus leaves (to aid in sporulation). The cultures were incubated under white light at 22 – 25 ºC for 3 – 5 days to allow zoosporangium formation.

8. References

Bhatt RK, Falck JR, Nigam S (1998). Enantiospecific total synthesis of a novel arachidonic acid metabolite 3-hydroxy eicosatetraenoic acid. Tetrahedron Lett. 39: 249 – 252.

Groza NV, Ivanov IV, Romanov SG, Myagkova GI, Nigam S (2002). A novel synthesis of 3(*R*)-HETE, 3(*R*)HTDE and enzymatic synthesis of 3(*R*), 15(*S*)-DiHETE. Tetrahedron 58: 9859 – 9863.

Kock JLF, Venter P, Linke D, Schewe T, Nigam S (1998). Biological dynamics and distribution of 3-hydroxy fatty acids in the yeast *Dipodascopsis uninucleata* as investigated by immunofluorescence microscopy. Evidence for a putative regulatory role in the sexual reproductive cycle. FEBS Lett. 472: 345 – 348.

Reynolds ES (1963). The use of lead citrate at high pH as an electron opaque stain in electron microscopy. J. Cell. Biol. 17: 208 – 212.

Spurr AR (1969). A low viscosity epoxy resin embedding medium for electron microscopy. J. Ultrastruct. Res. 26: 1 – 43.

Strauss CJ (2005). The role of lipids in the flocculation of *Saccharomyces cerevisiae*. PhD Thesis, University of the Free State, South Africa.

Van Wyk PWJ, Wingfield MJ (1991). Ascospore ultrastructure and development of *Ophiostoma cucullatum*. Mycologia 83: 698 – 707.

Venter P, Kock JLF, Sravan Kumar G, Botha A, Coetzee DJ, Botes PJ, Bhatt RK, Falck JR, Schewe T, Nigam S (1997). Production of 3*R*-hydroxy-polyenoic fatty acids by the yeast *Dipodascopsis uninucleata*. Lipids 32(12): 1277 – 1283.

Summary

In 2007, Kock and co-workers published the Acetylsalicylic acid (ASA) Antifungal Hypothesis that indicated a definite link between oxylipin production [3-hydroxy (OH) oxylipins], mitochondrial activity [mitochondrial transmembrane potential ($\Delta\psi_m$)] and ASA sensitivity in respiring as well as non-respiring yeasts. Here an increase in mitochondrial activity was observed in the sexual phase where an increase in energy production is probably needed for multiple ascospore development. This hypothesis has since been expanded to also include various anti-mitochondrial drugs as well as the fungi and fungi-like organisms *Aspergillus*, *Rhizopus* and *Mucor*. In this study the yeast *Nadsonia fulvescens* as well as some species of the notorious plant pathogen *Phytophthora* was evaluated for their ability to fit the expanded hypothesis now called the Anti-mitochondrial Antifungal Hypothesis. The yeast *N. fulvescens* is characterized by a unique life cycle. After conjugation between the parent cell and the first bud, the zygote moves into a second bud formed at the opposite end of the parent cell. This second bud is then delimited by a septum and becomes the ascus according to literature. Usually one, rarely two spherical, brownish, spiny to warty ascospores are formed within the ascus giving rise to brown coloured colonies. In this study the parent cell with attached first bud showed increased mitochondrial activity when compared to the ascus. When anti-mitochondrial compounds were added, the mitochondrial activity was inhibited in the parent cell with attached first bud followed by the formation of less asci with ascospores (many not fully developed and white coloured). It is suggested that sufficient mitochondrial activity in the parent cell and first bud is necessary to produce enough energy for the formation of a proper ascus with brown coloured ascospore(s). If the parent cell and first bud is regarded as part of the yeast sexual phase, then *N. fulvescens* also fits the hypothesis. Further investigations were conducted to study the asci of the yeast *N.*

fulvescens containing mature and fluconazole-treated malformed ascospores using nano scanning Auger microscopy (NanoSAM) in combination with transmission electron microscopy (TEM). This is the first application of NanoSAM to biological material. Transmission electron microscopy exposed a variety of malformed ascospores in asci treated with fluconazole. Here some ascospores produced degenerated spiky protuberances with relatively large inclusions carried inside wrinkled asci. Other ascospores contained no walls or protuberances and were enclosed within smooth spherical shaped asci. The majority of ascospores contained less dense hollow areas surrounded by cytoplasmic material. Nano scanning Auger microscopy studies on these asci corroborate the TEM results although less structural detail was obtained. Nano scanning Auger microscopy showed a decrease in elemental intensities during etching which assisted structural analysis of ascospore less dense hollow areas. In this study it is shown that the oomycete, *Phytophthora nicotianae* also fits the hypothesis. Fruiting structures (zoosporangia) of this oomycete showed increased beta (β)-oxidation when probing levels of 3-OH oxylipins with specific polyclonal antibodies. In addition increased mitochondrial activity was also observed in the zoosporangia when the $\Delta\psi_m$ probe, Rhodamine 123 was added to the culture. This indicates increased mitochondrial activity in the zoosporangia when compared to the hyphae. When the anti-mitochondrial ASA was added to cultures of this oomycete, the zoosporangia were, as expected most susceptible and were drastically inhibited in the presence of 1 mM of this compound. Similar ASA inhibition results were recorded for *P. citrophthora*. Anti-mitochondrial compounds may now find application in combating these devastating plant pathogens and urgent further research is needed in this direction.

Key words

Asci, ascospore, elemental composition, fluconazole, life cycle, mitochondria, mitochondrial inhibitors, *Nadsonia fulvescens*, nano scanning Auger microscopy, *Phytophthora*, plant pathogen, sexual phase, transmission electron microscopy, 3-dimensional architecture.

Opsomming

In 2007 publiseer Kock en mede-werkers die Asetielsalisielsuur (ASS) Antifungale Hipotese wat ‘n definitiewe verband voorstel tussen oksilipienproduksie [3-hidroksie (OH) oksilipiene], mitochondriale aktiwiteit [mitochondriale transmembraan potensiaal ($\Delta\psi_m$)] en ASS sensitiwiteit in respirerende sowel as nie-respirerende giste. Tydens die bogenoemde studie is ‘n toename in mitochondriale aktiwiteit waargeneem in die geslagtelike (seksuele) fase waar ‘n toename in energie produksie moontlik nodig is vir die vorming van veelvoudige askospore. Hierdie hipotese is sedertdien uitgebrei om verskeie anti-mitochondriale middels asook fungi en fungi-agtige organismes soos byvoorbeeld *Aspergillus*, *Rhizopus* en *Mucor* in te sluit. In hierdie studie is die gis *Nadsonia fulvescens* sowel as sekere spesies van die bekende plant patogeen *Phytophthora* getoets vir hul vermoë om in te pas by die uitgebreide hipotese, nou genoem die Anti-mitochondriale Antifungale Hipotese. Die gis *N. fulvescens* word gekarakteriseer deur ‘n unieke lewenssiklus. Na konjugasie tussen die moedersel en die eerste botsel, beweeg die sigoot na ‘n tweede botsel wat vorm aan die teenoorgestelde kant van die moedersel. Hierdie tweede botsel word afgesper deur ‘n septum en vorm die askus volgens literatuur. Gewoonlik word een, in rare gevalle twee, bruin, stekelagtige tot vratagtige askospore gevorm binne die askus wat lei tot die vorming van bruin kolonies. In hierdie studie toon die moedersel met aangehegde eerste botsel ‘n verhoging in mitochondriale aktiwiteit in vergelyking met die askus. Byvoeging van anti-mitochondriale middels het die mitochondriale aktiwiteit in die moedersel met eerste botsel ge-inhibeer, gevolg deur die vorming van minder aski met askospore (baie nie volledig ontwikkeld nie en wit in kleur). Daar word voorgestel dat verhoogde mitochondriale aktiwiteit nodig is in die moedersel en eerste botsel om genoeg energie te produseer vir die vorming van volwasse aski met bruin gekleurde askospore. Indien die moedersel tesame met die

eerste botsel beskou word as deel van die gis se geslagtelike voortplantingsfase, dan pas *N. fulvescens* in die hipotese. Verdere studies is ook gedoen om die aski van die gis *N. fulvescens* met volwasse en fluconazole-behandelde askospore te bestudeer met nano skanderings Auger-mikroskopie (NanoSAM) in kombinasie met transmissie-elektronmikroskopie (TEM). Hierdie is die eerste toepassing van NanoSAM op biologiese materiaal. Transmissie-elektronmikroskopie het ‘n verskeidenheid van misvormde askospore in aski wat behandel is met fluconazole ontbloot. Sommige askospore het misvormde stekelagtige uitsteeksels getoon met relatief groot insluitsels in die geplooide askus. Ander askospore het geen wande of uitsteeksels gehad nie en is waargeneem in gladde, sferiese aski. Die meerderheid askospore het minder digte areas bevat, wat omring word deur sitoplasmiese materiaal. Nano skanderings Auger-mikroskopie studies op hierdie aski stem ooreen met die TEM resultate alhoewel minder strukturele besonderhede waargeneem is. Nano skanderings Auger-mikroskopie het ‘n afname in element intensiteit ontbloot tydens etsing wat gehelp het met die strukturele analise van die minder digte areas in die aski. In die studie is ook aangetoon dat die oomiseet, *Phytophthora nicotianae* wel inpas by die hipotese. Vrugliggame (zoosporangia) van hierdie oomiseet het ‘n toename in beta (β)-oksidasie getoon met ‘n merker vir 3-OH oksilipiene (spesifieke poliklonale teenliggame). Verder is verhoogde mitochondriale aktiwiteit waargeneem in die zoosporangia wanneer die $\Delta\psi_m$ merker, Rhodamien 123 by die kultuur gevoeg is. Dit wys daarop dat daar verhoogde aktiwiteit in die zoosporangia voorkom wanneer dit vergelyk word met vegetatiewe hifes. Wanneer die anti-mitochondriale middel ASS by kulture van hierdie oomiseet gevoeg is, is bevind dat die zoosporangia meer sensitief is as die hifes. ‘n Aansienlike vermindering in zoosporangium vorming is waargeneem in die teenwoordigheid van 1 mM ASS.

Soortgelyke ASS-inhibisie studie resultate is waargeneem vir *P. citrophthora*. Anti-mitochondriale middels kan moontlik nou aangewend word om hierdie plant patogene te bekamp en dringende verdere studies is nodig in hierdie verband.

Sleutelwoorde

Aski, askospore, elementsamestelling, fluconazole, geslagtelike fase, lewenssiklus, mitochondria, mitochondriale inhibitore, *Nadsonia fulvescens*, nano skanderings Auger-mikroskopie, *Phytophthora*, plantpatogeen, transmissie-elektronmikroskopie, 3-dimensionele argitektuur.

Supplementary Movies

Please turn to the back of the thesis to find attached CD.

[Contact swartcw@ufs.ac.za if not operational on your computer model]

Procedure:

1. **Insert CD.**
2. **Choose "Open folder to view files".**
3. **A selection of videos will appear.**
4. **Double-click on a specific movie to start playing.**

Menu

Chapter 2.1.

Movie 1 – A rotating 3-dimensional (3-D) image [confocal laser scanning microscopy (CLSM) model] of a parent cell with an attached first bud observed in *Nadsonia fulvescens* - the first step towards ascus formation. Cells were probed with fluorescing antibodies specific for 3-hydroxy (OH) oxylipins. The green fluorescence indicates the location of 3-OH oxylipins that mainly accumulate in the parent cell where these compounds probably act as lubricants to ensure nucleus movement between the parent cell and first bud to eventually form the zygote (Chapter 2; 2.1.; Figure 1a; pp. 58). Intact cytoplasm in parent cell with attached first bud, is indicated by red auto fluorescence. The model was constructed from real time CLSM analysis using the program Imaris 3.1 (2001), Bitplane, Zùrich.

Movie 2 – A rotating 3-D image (CLSM; model) of an older parent cell with attached first bud, as well as a second bud (ascus) that contains a mature ascospore observed in *N. fulvescens*. The parent cell and attached first bud have already

released its content therefore we only observe small amounts of green fluorescence (indicating 3-OH oxylipins) and small amounts of red fluorescence (cytoplasm) in the parent cell with attached first bud. No accumulation of 3-OH oxylipins was observed in the ascus (indicated mainly by red auto fluorescence). The green and red fluorescence surrounding the parent cell and attached first bud indicate the 3-OH oxylipins and cytoplasm that have been liberated (Chapter 2; 2.1.; Figure 1c; pp. 58). The model was constructed from real time CLSM analysis using the program Imaris 3.1 (2001), Bitplane, Zùrich.

Chapter 2.2.

Movie 3 – A video clip showing, for the first time in Biology, sequential nano-etching [obtained with the use of nano scanning Auger microscopy (NanoSAM)] through normal, mature asci of *N. fulvescens*. As etching commences, two wrinkled asci (due to the dehydration steps of NanoSAM preparation) can be observed attached to two parent cells respectively. As etching continues, the ascus wall is etched away in nanometer thick slices, revealing the crunched spiny protuberances situated around the ascospore. When etching reaches a depth of about 1026 nm into the ascus, a solid ascospore structure can be observed surrounded by the crunched spiny protuberances (Chapter 2; 2.2.; Figure 3a – c; pp. 83). During nano-etching (sputtering), elemental analysis is performed on the surface of the sample after each 27 nm nano-slice (Chapter 2; 2.2.; Figure 4b; pp. 84).

Movie 4 – A video clip showing sequential nano-etching (obtained with the use of NanoSAM) through fluconazole-inhibited, malformed asci of *N. fulvescens*. As etching commences, a smooth-walled ascus could be observed attached to a parent cell. As etching proceeds the ascus wall is etched away in nanometer thick slices, revealing a spherical structure without any spiny protuberances. Upon further etching this spherical structure disintegrated, indicating less dense areas in the ascospore that was inhibited by fluconazole. This indicates the effect that fluconazole has on ascospore development in this yeast (Chapter 2; 2.2.; Figure 3j – l; pp. 83).

Strikingly, fluconazole distribution throughout the ascus could be followed by tracking fluorine (F; component of fluconazole) with elemental analysis performed on the surface of the sample after each 27 nm nano-slice (Chapter 2; 2.2.; 4d; pp. 84)

Chapter 3

Movie 5 – A video clip showing a Z-stack (obtained with CLSM) of an empty zoosporangium (have already liberated the zoospores) surrounded by hyphal growth as observed in *Phytophthora nicotianae*. Cells were probed with antibodies specific for 3-OH oxylipins. The green fluorescence observed in the exit pore indicates an accumulation of 3-OH oxylipins. Here the 3-OH oxylipins could act as lubricant to aid in the dispersal of zoospores through the narrow opening of the exit pore (Chapter 3; Figure 1b; pp. 100). ***Vertical z-axis – right hand side*** shows front view of the exit pore indicating 3-OH oxylipins lining its inner surface.